UNIVERSITY OF OKLAHOMA

GRADUATE COLLEGE

KINETIC STUDIES OF SACCHAROPINE REDUCTASE FROM *Saccharomyces cerevisiae*

A DISSERTATION

SUBMITTED TO THE GRADUATE FACULTY

In partial fulfillment of the requirement for the

Degree of

DOCTOR OF PHILOSOPHY

By

ASHWANI KUMAR VASHISHTHA
Norman, Oklahoma
2009

KINETIC STUDIES OF SACCHAROPINE REDUCTASE FROM
Saccharomyces cerevisiae

A DISSERTATION APPROVED FOR THE
DEPARTMENT OF CHEMISTRY AND BIOCHEMISTRY

BY

_____

Dr. Paul F. Cook, Chair

_____

Dr. Ann H. West

_____

Dr. George B. Richter-Addo

_____

Dr. Helen I. Zgurskaya

_____

Dr. Roger G. Harrison Jr.

To my Parents

ACKNOWLEDGEMENTS

I would like to express my sincere gratitude and deepest appreciation to my major advisor Dr. Paul Fabyan Cook, for being very kind and supportive throughout my graduate carrer. Dr. Paul Cook always stressed on independent thinking, was always open to new ideas and suggestions and always encouraged me to try out new things. Without his guidance and support, it would not have been possible to finish this project. I really appreciate his patience during preparation of the manuscripts and for stimulating a positive attitude towards research. I am glad to have an advisor like him who made my graduate studies a pleasant experience and I would miss his guidance and support in future.

I would also like to thank Dr. Ann H. West for invaluable discussions, comments and suggestions for improvement during the lysine group meetings and annual evaluation meetings and for serving as my graduate committee chair during my proposal defense. I would like to thank my other committee members, Dr. George B. Richter-Addo, Dr. Helen I. Zgurskaya, Dr. Roger G. Harrison Jr. for their valuable comments and suggestions in my proposal defense and annual evaluation meetings, and for their continued support, participation and encouragement during my graduate research.

I would like to sincerely thank Dr. William Karsten “Bill”, Dr. Lillian Chooback and Dr. Babak Andi for their help, guidance and training in learning and carrying out the experiments.

I would like to extend my thanks to all members of Dr. Cook's and Dr. West's laboratory, Lei Li, Hengyu Xu, Mamar Baizid, Wael Rabeh, Jinghua Qian, Hui Tian, Deniz Aktas, Kostyantyn Bobyk, Devi Ekanayake, Chaonan Hsu, Vidya Kumar, Hui Tan, Dr. Fabiola Janiak, Alla Kaserer, and Rong Guan who made the lab a great environment. I also would like to sincerely thank my friends in the department, Ganesh Krishnamoorthy, Vishakha Devroy, Shweta Deshpande, Simone McMill, Dipti Barman, Girija Dhamdhere, Shekar Mekala, Rahul Kadam, Sachin Chavan, James Robinson, Bikash Mondal for being friendly and supportive through these years.

I would like to appreciate efforts of my host family (Dale and Lisa Robinett), and my friends Lloyd Powers, Keith Catto, Jim, Marjorie Canon, Tom Hoot, Mary Allen, Wm. Paul Patterson and Will Decker who have been with me in difficult times and have provided their love and blessings all these years.

I would like to express my heart felt appreciation ans sincere thanks to my parents Mr. S. P. Sharma and Mrs. Urmila Sharma for their priceless love, prayers, motivation and encouragement which has constantly helped me to do the best and achieve goals. I would like to express my thanks to my brother Amit Sharma and my sister Priyanka Sharma for their love and encouragement. At Last, I would like to express my appreciation to Dr. Kanwal Kumar, Dr. B. K. Puri, Dr. Chadrashekar Rao and Mr. Siddharth Kak for their endless encourgement and kind support.

TABLE OF CONTENTS

LIST OF TABLES

LIST OF FIGURES

ABSTRACT

Saccharopine reductase (SR) (EC 1.5.1.10) is the penultimate enzyme in the α-aminoadipate pathway encoded by the *LYS9* gene in *Saccharomyces cerevisiae.* Saccharopine reductase (SR) catalyzes the condensation of L-α-aminoadipate-δ-semialdehyde (AASA) with L-glutamate to form an imine which is subsequently reduced by NADPH to give saccharopine. Kinetic studies were carried out for histidine-tagged saccharopine reductase from *Saccharomyces cerevisiae* at pH 7.0, suggesting a sequential mechanism with ordered addition of NADPH to the free enzyme followed by AASA, which adds in rapid equilibrium prior to L-glutamate in the forward reaction direction. In the reverse reaction direction, NADP adds to enzyme prior to saccharopine. Product inhibition by NADP is competitive vs. NADPH and noncompetitive vs. AASA and L-glutamate consistent with addition of the dinucleotide prior to the aldehyde; saccharopine is noncompetitive vs. NADPH, AASA and L-glutamate. In the direction of saccharopine oxidation, NADPH is competitive vs. NADP and noncompetitive vs. saccharopine, L-glutamate is noncompetitive vs. both NADP and saccharopine, while AASA is noncompetitive vs. saccharopine and uncompetitive vs. NADP. The sequential mechanism is also corroborated by dead-end inhibition studies using analogs of AASA, L-glutamate, and saccharopine. 2-amino-6-heptenoic acid was chosen as a dead-end analog of AASA and is competitive vs. AASA, uncompetitive vs. NADPH, and noncompetitive vs. L-glutamate. Ketoglutarate (α-Kg) served as a dead-end analog

of L-glutamate and is competitive vs. L-glutamate and uncompetitive vs. L-AASA and NADPH. In the direction of saccharopine oxidation, N-oxalylglycine, L-pipecolic acid, L-leucine, α-ketoglutarate, glyoxylic acid and L-ornithine were used as dead-end analogs of saccharopine and showed competitive inhibition vs. saccharopine and uncompetitive inhibition vs. NADP. All data are consistent with the proposed ordered mechanism. The equilibrium constant for the reaction was measured at pH 7.0 by monitoring the change in absorbance of NADPH when all reactants were present; K_{eq} is 200 M^{-1}. The value is in good agreement with the value determined using the Haldane relationship.

An acid-base chemical mechanism has been proposed for SR on the basis of pH rate profiles and solvent deuterium kinetic isotope effects. A finite solvent isotope effect is observed indicating that proton(s) are in flight in the rate limiting step(s) and likely the same step is limiting under both limiting and saturating substrate concentrations. A concave upward proton inventory suggests that more than one proton is transferred in a single transition state, likely a conformation change required to open the site and release products. Two groups are involved in the acid-base chemistry of the reaction. One of these groups catalyzes the steps involved in forming the imine between the α-amine of glutamate and the aldehyde of AASA. The group, which has a pK_a of about 8, is observed in the pH-rate profiles for V_1 and V_1/K_{Glu}, and must be protonated for optimal activity. It is also observed in the V_2 and V_2/K_{Sacc} pH-rate profiles, and is required unprotonated. The second group, which has

a pK_a of 5.6, accepts a proton from the α-amine of glutamate so that it can act as a nucleophile in forming a carbinolamine upon attack of the carbonyl of AASA.

Site directed mutagenesis has been carried out to elucidate the role of D125, C154 and Y99 residues in the reaction catalyzed by SR. Kinetic parameters for single and double mutants show a sharp decrease in k_{cat} for the mutants suggesting that these residues are important for the reaction. pH-rate profiles for D125A, C154S, Y99F, D125A-Y99F and D125A-C154S mutants indicate that these residues do not play the role of general acid-base catalyst in the reaction and further studies are required to determine the identity of the general acid-base catalyst. A possible candidate for the general acid-base catalyst is the primary amine of saccharopine and chemical modification needs to be carried out to determine its role in the reaction.

Substrate specificity studies have been carried out using analogues of saccharopine and nicotinamide adenine dinucleotide. Alternative substrates have been used for NADPH in the forward reaction direction at pH 7.0. Inhibition studies using analogues of the dinucleotide show that most of the binding energy comes from the ADP of NADP. Replacement of the carbonyl group of nicotinamide ring with a thio group results in poor binding indicating that the bulky and considerably less electronegative sulphur results in steric hindrance and prevention of hydrogen bonding in the active site of SR, as shown by the high $appK_m$ value. The 2' phosphate group plays a significant role in binding which is indicated by the sharp decrease in the V/K value when NADH is employed as an alternative substrate in the forward

reaction direction. Dead end analogues of saccharopine suggest that the carboxylate groups need to be flexible and orientation of the carboxylate groups is crucial to binding of saccharopine to SR.

CHAPTER 1

Introduction

1-1. Amino acid biosynthesis

Most living organisms use 20 different amino acids in order to synthesize proteins. Amino acid biosynthesis can be divided into the following six major families: 1) the aspartate family for the biosynthesis of Asp, Asn, Lys, Met, Thr, Ile; 2) the aromatic amino acid family for the biosynthesis of Phe, Tyr and Trp; 3) the glutamate family for the biosynthesis of Arg, Glu, Gln and Pro; 4) the biosynthesis of histidine; 5) the pyruvate family for the biosynthesis of Ala, Ile, Leu and Val; and 6) the serine family for the biosynthesis of Cys, Gly and Ser (*1*). The α-aminoadipate pathway is a member of the glutamate family of amino acid biosynthesis (*7*, *8*). The biosynthetic pathways for lysine will be considered briefly below.

1-2. Lysine biosynthesis

L-lysine is an essential amino acid for humans and animals and can only be obtained from protein in the diet. Two completely different routes for the biosynthesis of the essential amino acid L-lysine have evolved in nature: the α-aminoadipate (AAA) pathway in phycomycetes, euglenoids, yeasts and higher fungi such as basidiomycetes (*8* , *9*), and the diaminopimelate (DAP) pathway in bacteria, plants and lower fungi such as the mucorales and blastocladiales (*2*, *22*). Other amino acids have similar synthetic pathways in fungi and bacteria (*3*).

1-2-1. Diaminopimelate pathway of L-lysine biosynthesis

In plants and bacteria the diaminopimelic acid pathway is used for the synthesis of lysine and consists of seven enzyme-catalyzed reactions (Fig. 1-1) (*8*). The diaminopimelate pathway found in most plants, bacteria and lower fungi belongs to the aspartate family of amino acid biosynthetic pathway which also leads to the synthesis of asparagine, methionine, threonine and isoleucine (*27*). The DAP pathway has also been studied in *E. coli* (*28*). In addition to the lysine required for protein biosynthesis, the DAP pathway is the source of the diaminopimelate (DAP) and lysine that is incorporated into bacterial cell wall peptidoglycans. The DAP pathway begins with the phosphorylation of aspartate by aspartokinase to give aspartyl-β-phosphate (1; E.C. 2.7.2.4), followed by an NADPH dependent reduction to give aspartic-β-semialdehyde catalyzed by aspartate semialdehyde dehydrogenase (2; E.C. 1.2.1.11). In the next step aspartic-β-semialdehyde undergoes aldol condensation with pyruvate to give 2, 3-dihydrodipicolinate catalyzed by dihydrodipicolinate synthase (3; E.C. 4.2.1.52), which upon reduction by NADPH gives Δ́ piperidine-2, 6-dicarboxylate catalyzed by dihydrodipicolinate reductase (4; E.C. 1.3.1.26). The ring is opened in the next step by succinylation with succinyl-CoA to give N-succinyl α-amino-ε-ketopimelate catalyzed by tetrahydrodipicolinate acyltransferase (5; E.C. 2.3.1.117). In the next step, the acyl group is removed after transamination using glutamate to produce L, L-diamino pimelate brought about by N-succinyl-α-amino-ε-ketopimelate-glutamate aminotransaminase (6; E.C. 2.6.1.17). The step involving removal of the acyl group is catalyzed by N-acyldiaminopimelate

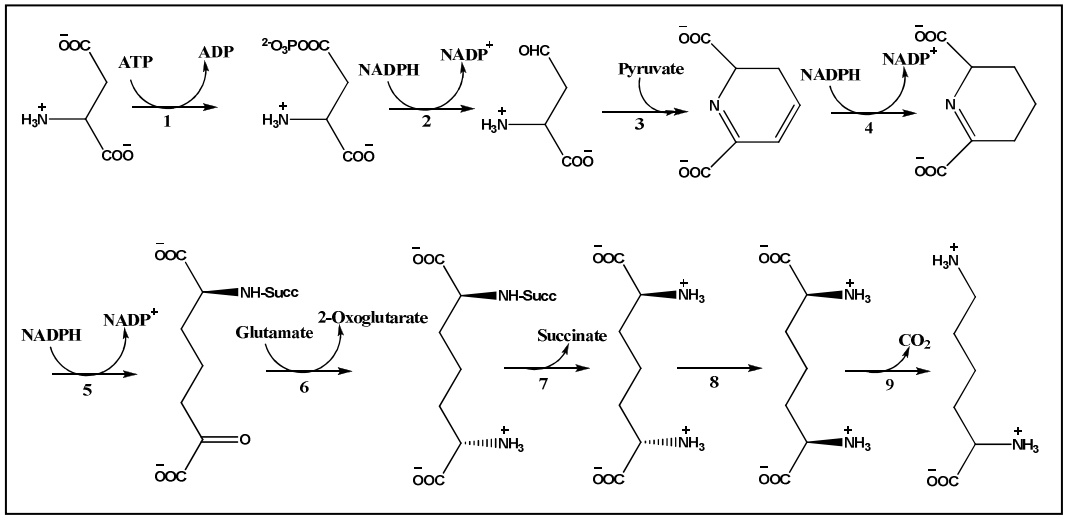

Fig. 1-1: The Diaminopimelic acid pathway in bacteria and the enzymes in the pathway are: (1) Aspartate kinase (E.C. 2.7.2.4), (2) Aspartate semialdehyde dehydrogenase (E.C. 1.2.1.11), (3) Dihydrodipicolinate synthase (E.C. 4.2.1.52), (4) Dihydrodipicolinate reductase (E.C. 1.3.1.26), (5) Tetrahydrodipicolinate acyltransferase (E.C. 2.3.1.117), (6) N-succinyl-α-amino-ε-ketopimelate-glutamate aminotransaminase (E.C. 2.6.1.17), (7) N-acyldiaminopimelate deacylase (E.C. 3.5.1.18), (8) Diaminopimelate epimerase (E.C. 5.1.1.7), (9) Diaminopimelate decarboxylase (E. C. 4.1.1.20).

deacylase (7; E.C. 3.5.1.18). This is followed by the racemization of L, L-diaminopimelate to the meso compound catalyzed by diaminopimelate epimerase, which on decarboxylation yields the final product L-lysine catalyzed by diaminopimelate decarboxylase.

1-2-2. α-aminoadipate (AAA) pathway of L-lysine biosynthesis

The AAA pathway has been reported in *Saccharomyces cerevisiae* (*10*), *Schizosaccharomyces pombe* (*11*), *Penicillinum chrysogenum* (*12*), *Neurospora crassa* (*13*), *Magnoporthe grisea* which is a plant pathogen (*1*), and human pathogenic fungi including *Candida albicans* (*14*), *Aspergillus fumigatus* (*15*) and *Cryptococcus neoformans* (*15*). The *Saccharomyces cerevisiae* genome has been

completely sequenced (*16-18*). Extensive genetic, enzymatic, regulatory, and cloning studies of the lysine biosynthetic pathway are now being carried out in *S. cerevisiae* and *N. crassa* (*14*, *26*). Some cloning and molecular studies have also been carried out in *C. albicans* **(***19-21*, *32*).

The AAA lysine biosynthetic pathway is also used by bacteria for lysine biosynthesis and Kobashi *et al*. has reported a modified AAA pathway in the bacterium, *T. thermophilus*, which is an extreme thermophile (*4*). The pathways

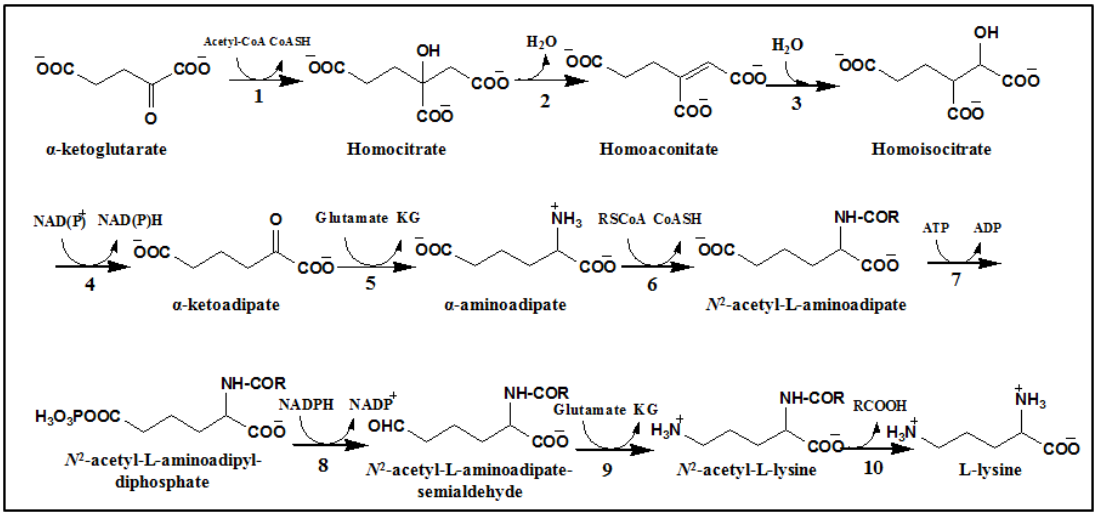

Fig. 1-2: Proposed lysine AAA biosynthetic pathway in *Thermus thermophilus*

leading to the formation of α-aminoadipic acid (AAA) are same in fungi and bacteria, and the steps leading to the formation of L-lysine in *Thermus thermophilus* are shown in Fig. 1-2 (*3*). Miyazaki *et al*. showed that in *Thermus thermophilus*, the enzymes involved in the conversion of α-ketoglutarate to AAA are homologous to the corresponding genes of fungi and that the pathway from AAA to lysine is dissimilar. In *T. thermophilus*, AAA is condensed with acetyl CoA to produce N^2-

acetyl-L-aminoadipate. The following step involves the phosphorylation to give N^2-acetyl-L-aminoadipyl-diphosphate which upon reduction by NADPH gives N^2-acetyl-L-aminoadipate semialdehyde. The next step involves the transamination by glutamate to give N^2-acetyl-L-lysine. In the last step, acetyl group is removed resulting in the formation of lysine.

Besides *T. thermophilus*, a gene cluster for lysine biosynthesis via AAA has also been reported in *Pyrococcus horikoshii* which is similar to the gene clusters for the leucine and arginine biosynthetic pathways (*5*). Four of the genes involved in the AAA pathway of *P. horikoshii* also participate in the leucine biosynthetic pathway.

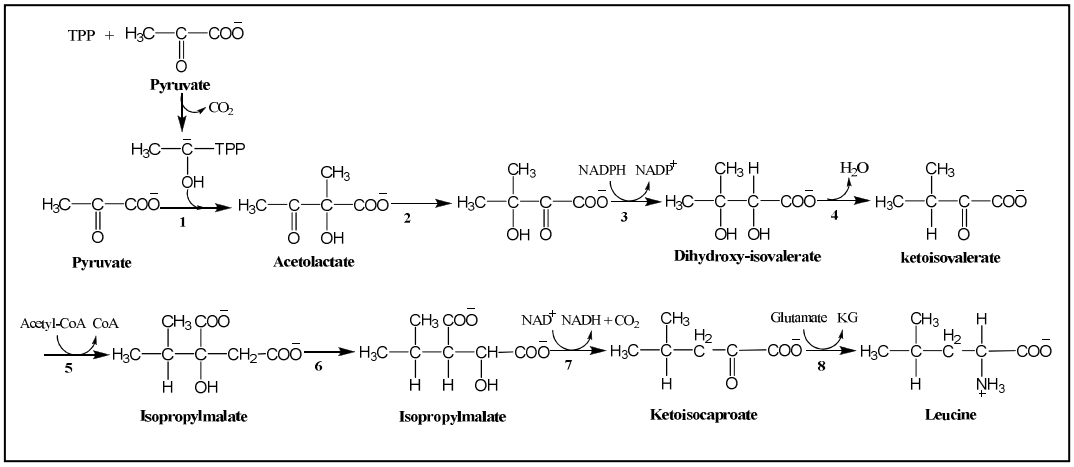

Fig. 1-3: The Leucine biosynthesis pathway. The enzymes involved are (1) Acetolactate synthase, (2) Acetolactate mutase, (3) Reductase, (4) Dihydroxy acid dehydratase, (5) α-isopropylmalate synthase, (6) α-isopropylmalate dehydratase, (7) Isopropylmalate dehydrogenase, (8) Leucine aminotransferase.

P. horikoshii, has existed on the earth for a long time, and it has been suggested that the biosynthetic pathways for lysine, and leucine may be related to each other and they might have been evolved from common ancestors, with broad substrate

specificity (*5*). The leucine biosynthetic pathway has been shown in Fig. 1-3.

The lysine biosynthetic pathway in yeast is shown in Fig. 1-4. In *S. cerevisiae* (*1*, *7*, *13*) and *S. lipolytica* (*12*) eight gene loci have been shown to be present for the enzymes of the AAA pathway using complementation and recombination analyses.

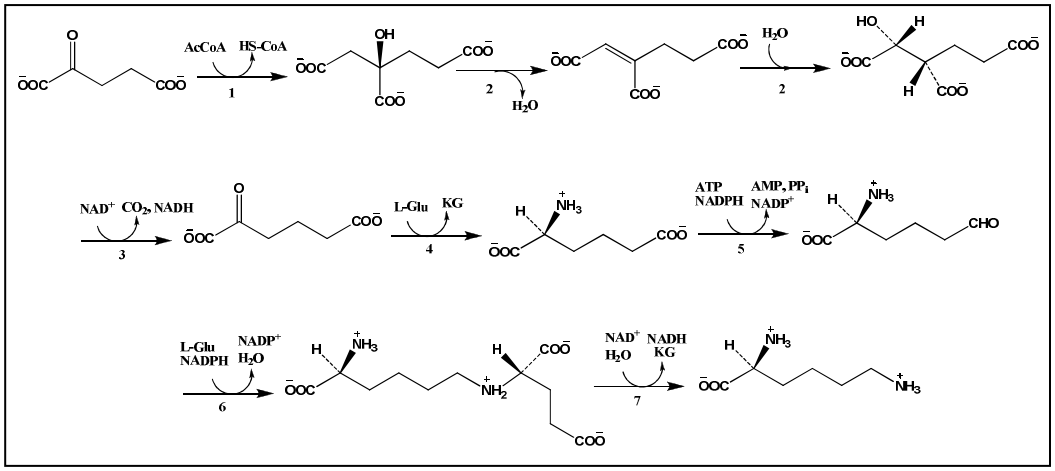

Fig. 1-4: The α-aminoadipate pathway in yeast. The pathway enzymes are (1) Homocitrate synthase (E.C. 4.1.3.21), (2) Homoaconitase (E.C. 4.2.1.36), (3) Homoisocitrate dehydrogenase (E.C. 1.1.1.87), (4) α-aminoadpate aminotransferase (E.C. 2.6.1.39), (5) α-aminoadipate reductase (E.C. 1.2.1.31), (6) Saccharopine reductase (E.C. 1.5.1.10), (7) Saccharopine dehydrogenase (L-Lys forming, E.C. 1.2.1.31).

The first step in the pathway involves the condensation of α-ketoglutarate and acetylCoA followed by the hydrolysis of the resulting homocitryl CoA to produce homocitrate, catalyzed by homocitrate synthase (*19*). Homocitrate is then converted to homoisocitrate by homoaconitase (*20*). Homoisocitrate then undergoes oxidative decarboxylation to give α-ketoadipate, catalyzed by homoisocitrate dehydrogenase (*21*). The next step involves transamination with L-glutamate to give L-α-aminoadipate catalyzed by α-aminoadipate aminotransferase (*18*). The first half of the pathway occurs in the mitochondrion (homocitrate synthase and aminotransferase

are present in mitochondrion and the cytoplasm) (*19*). The second half of the pathway occurs in the cytoplasm where α-aminoadipate reductase catalyzes the ATP and NADPH-dependent reduction of the δ-carboxylate to α-aminoadipic acid-δ-semialdehyde. Once the semialdehyde is formed, it is condensed with L-glutamate to give an imine, which is then reduced by NAD(P)H to L-saccharopine catalyzed by saccharopine reductase. L-Saccharopine is then oxidatively deaminated by saccharopine dehydrogenase (L-lysine forming) to give L-lysine.

A plausible reason for the pathway to be distributed into the mitochondria and cytosol is that the compartmentalization could provide a better overall regulation. Also, one of the reasons for the distribution could be the availability of the cofactors: NAD(P)H and ATP, allosteric regulators, or the proper environment to give the active site residues the correct protonation states so that they can catalyze reactions in the pathway.

Lys9 mutants, which lack saccharopine reductase activity, accumulate aminoadipate semialdehyde, confirming its participation in the AAA pathway for lysine biosynthesis (*23*). In *N. crassa*, lysine-requiring mutants have been used to show that saccharopine is a precursor of lysine (*25*). The last two enzymes in the pathway have very little sequence homology at the amino acid level, but both enzymes are fungal specific and catalyze the oxidation of saccharopine at adjacent bonds. SR and SDH use $NADP^+$ and NAD^+, respectively, as coenzymes so that a high NADPH to NADH ratio may favor the forward reaction direction, synthesis of L-lysine from aminoadipate semialdehyde, while, a low ratio would favor the reverse

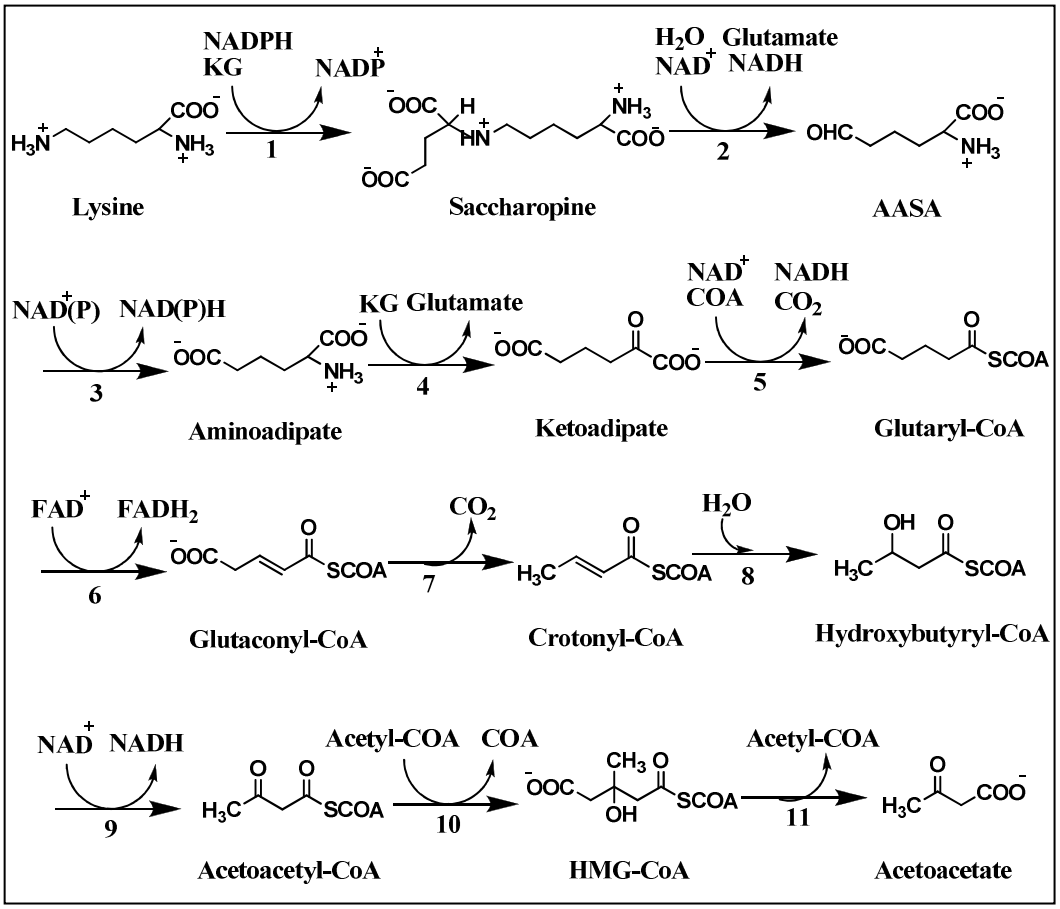

Fig. 1-5. Lysine degradation pathway in mammalian liver. The enzymes of the lysine degradation pathway in mammalian liver are as follows: (1) saccharopine dehydrogenase ($NADP^+$, lysine forming), (2) saccharopine dehydrogenase (NAD^+, glutamate forming), (3) aminoadipate semialdehyde dehydrogenase, (4) aminoadipate aminotransferase, (5) α-keto acid dehydrogenase, (6) glutaryl-CoA dehydrogenase, (7) decarboxylase, (8) enoyl-CoA hydratase, (9) β-hydroxyacyl-CoA dehydrogenase, (10) HMG-CoA synthase, (11) HMG-CoA lyase. Steps 1 and 2 are included in a bifunctional enzyme (*53*).

reaction direction, degradation of lysine. In humans and animals, L-lysine degradation is favored whereas, in fungi L-lysine formation is favored; lysine synthesis does not occur in these organisms. The lysine degradative pathway in mammalian liver is shown in Fig. 1-5.

1-2-3. Significance of the α-aminoadipate pathway

Fungal infections are life threatening for those individuals who are immuno-compromised: those with AIDS, those undergoing chemotherapy, and those who have undergone a transplant. Opportunistic pathogens such as *Candida albicans, Aspergillus fumigatus and Cryptococcus neoformans* cause candidiasis, aspergillosis, and cryptococcosis respectively (*29*). *Candida albicans* causes oral candidiasis and may also produce infections in the fingernails and toenails, and lesions in the gastrointestinal tract. *Cryptococcus neoformans* is responsible for meningitis, a central nervous system infection prevalent in the immunocompromised host. *Aspergillus fumigatus* mainly affects the lungs, but can also cause diseases of the skin, ear and central nervous system. The enzymes involved in the lysine biosynthetic pathway are present in *C. albicans, C. neoformans, and A. fumigatus*.

The presence of five enzymes of the pathway, namely, homocitrate synthase, homoisocitrate dehydrogenase, α-aminoadipate reductase, saccharopine reductase, and saccharopine dehydrogenase have been shown in all of these organisms (*5*). *Candida albicans* shows higher levels of homocitrate synthase, homoisocitrate dehydrogenase, and α-aminoadipate reductase compared to *C. neoformans,* and *A. fumigatus*; high enzyme activity in *C. albicans* may allow the detection of this organism in clinical specimens (*5*). Lysine auxotrophs of *C. albicans* have been reported by several investigators (*30, 31, 33*). *Candida albicans* use lysine and α-aminoadipate as sole nitrogen sourcess (*34*), whereas, *S. cerevisiae* cannot use these amino acids as they are growth inhibitory (*35*). This property of *C. albicans* may also

be exploited for its detection in specimens.

The diagnosis of fungal infections is time consuming and cumbersome (*37*). The first step in the diagnosis involves the examination of those organs that are readily accessible, notably the skin, eyes, nose, and throat. The most important diagnostic tools for fungal infection are: detection of fungal antigens such as cryptococcal antigen, detection of genomic fungal DNA, and staining using India ink and calcoflour white. It has been reported that the lysine biosynthetic pathway is required for fungal growth and pathogenicity *in vivo* (*38*). The various antifungal drugs currently available include the azoles, e.g. fluconazole and itraconazole, and amphotericin B (*29*). All of these antifungal drugs have some side effects which include nausea, vomiting and diarrhoea. Hence, it is important to develop new antifungal drugs which would be more effective in treating the fungal infections and would also be less toxic. Since the α-aminoadipate pathway and the enzymes involved in this pathway are unique to fungi, transition state analog(s) may be developed to inhibit fungal growth by blocking the synthesis of lysine. The uniqueness of the AAA pathway and the fact that it is present only in fungi may also be exploited for the rapid detection of fungal pathogens using its unique enzymes and cloned genes as molecular probes for identification (*5*). Hence, a detailed study of the pathway and its enzymes is crucial to gain knowledge of the metabolism and molecular genetics of the pathogenic fungi.

1-2-4. Regulation of the α-aminoadipate pathway

The pathway is highly regulated at both the genetic and enzymatic levels and the regulation is described below (*23*).

1-2-4-1. Regulation at the genetic level

The AAA pathway is regulated by the control of amino acid biosynthesis as well as transcriptional activation by the co-inducers, α-aminoadipate-δ-semialdehyde (AASA) is a co-inducer for the transcription of the genes of the pathway (*40*). The transcription of the genes of the lysine biosynthetic pathway is brought about by the protein encoded by the *LYS14* gene (*LYS14p*) in the presence of its coinducer AASA. The synthesis of saccharopine reductase is also affected by the induction mechanism, which functions at the transcription level, together with the general regulation. *LYS14* protein plays the role of a positive factor requiring activation by AAS which renders the protein capable of stimulating the expression of various *LYS* genes (*40*). Hence the *LYS14* protein plays a regulatory role in the expression of the *LYS* genes.

In *S. cerevisiae,* two genes, *LYS9* (coding for saccharopine reductase) and *LYS14* (which encodes the protein that activates the lysine genes) are required for the production of saccharopine in *S. cerevisiae* (*44*, *54*). An intact *LYS14* is necessary for the synthesis of *LYS9* mRNA. Mutant yeast strains that lack these genes show a tendency to accumulate AASA and show a significant reduction in saccharopine reductase activity; sacchaorpine reductase activity is absent in *LYS9*-strains and is significantly reduced in the *LYS14*-strains. These results clearly indicate that the

LYS14 gene plays an important role in the biosynthesis of saccharopine reductase, and thus, two distinct genes, representing two different gene loci, are required for the biosynthesis of saccharopine reductase (*58*). Bhattacharjee *et al.* reported that SR is composed of a single polypeptide chain indicating that the enzyme is a product of a single gene, *LYS9*, also indicating that *LYS14* likely plays a nonstructural role (*59*). This result is supported by complementation and recombination experiments, which established that *LYS9* and *LYS14* are distinct loci (*58*). In *S. cerevisiae*, SR is repressed by lysine (*60*). The *LYS9*-strain accumulates AAS and is derepressed for the lysine biosynthetic enzymes homocitrate synthase, α-aminoadipate reductase and saccharopine dehydrogenase. The specific activity of these enzymes is 3-4 fold higher than in the wild type strain (*40*). The *LYS2-LYS9*- double mutant which lacks the α-aminoadipate reductase and saccharopine reductase activity does not exhibit derepression, suggesting α-aminoadipate reductase is required for depression. Similarly, *LYS2*- and *LYS5*-mutants lack aminoadipate reductase and *LYS1*-mutants lack saccharopine dehydrogenase (*44*).

The first enzyme in the pathway, HCS is highly regulated. L-Lysine, the final product inhibits HCS by feedback inhibition (*61*). In addition to homocitrate synthase, five other enzymes in the pathway, homoaconitase, homoisocitrate dehydrogenase, α-aminoadipate reductase, saccharopine reductase, and saccharopine dehydrogenase are repressed by lysine when the cells are grown in a medium containing lysine, with the maximum repression reported for homoisocitrate dehydrogenase, saccharopine reductase, and α-aminoadipate reductase (*53*).

Enzymes of the second half of the pathway respond differently to the general control of amino acids than those of the first half of the pathway, and during starvation conditions, enzymes under general control are depressed (*56*).

In *S. cerevisiae*, hydroxylysine acts as a short term growth inhibitor, but the inhibition is overcome after a short growth-inhibitory period, and cells grow rapidly and produce lysine (*4*). Cells are not able to use hydroxylysine as a nutrient, and hydroxylysine inhibit the pathway in cells resulting in the inhibition of the growth of the organism (*65*). N-formyllysine gives a comparable effect. The enzymes of AAA pathway show a non-coordinate effect of hydroxylysine, with the level of saccharopine reductase, but not of α-aminoadipic acid reductase or saccharopine dehydrogenase, being reduced significantly (*4*).

1-2-4-2. Enzymatic regulation

The first enzyme of the pathway, homocitrate synthease (HCS) is highly regulated. Lysine, which is the end product of the pathway can feedback inhibit HCS. Lysine inhibition has been reported in *P. chrysogenum*, *T. thermophilus* and *S. cerevisiae* (*50*, *48*, *61*). In *P. chrysogenum*, the lysine inhibition is partial (*50*), while in *S. cerevisiae*, the inhibition is linear to 5 mM. Also, in *P. chrysogenum*, lysine inhibition is pH dependent with no inhibition observed from pH 6.6 to 7.0 and a K_i of 8 μM is reported at pH 8.0 (*50*). In *S. cerevisiae*, the competitive inhibiton by lysine vs KG suggests that they compete for the active site of HCS. However, the dissociation constant of KG from the E:KG binary complex is independent of the

presence of lysine suggesting that lysine likely binds to an allosteric site (*61*). From kinetic data the K_i for lysine is 550 μM, while from fluorescence titration studies the value is 40 μM. The difference in the K_i values for lysine has been explained on the basis of the existence of HCS in two conformations with lysine binding with high affinity to the inactive form and KG which is the substrate binds to the active form of HCS (*61*).

The monovalent cation Na^+ binds to the free enzyme form. The effect of Na^+ depends on the concentration of acetyl CoA. At high acetyl CoA, Na^+ acts as an activator, but at low acetyl CoA, Na^+ acts as an activator at low concentrations and is a linear inhibitor at high concentrations (*61*). It has been proposed that Na^+ inhibition occurs as a result of Na^+ binding to the acetyl CoA site, while the activation is a result of sodium binding to a site other than the active site on the free enzyme.

1-3. Saccharopine reductase

Saccharopine reductase (SR) [saccharopine dehydrogenase (L-glutamate forming), EC 1.5.1.10] catalyzes the condensation of L-α-aminoadipate-δ-semialdehyde with L-glutamate to form an imine which is subsequently reduced by NADPH to give saccharopine (*23*).

1-3-1. Expression, purification, and characterization

Saccharopine reductase from *S. cerevisiae* consists of a single 50,000 Da

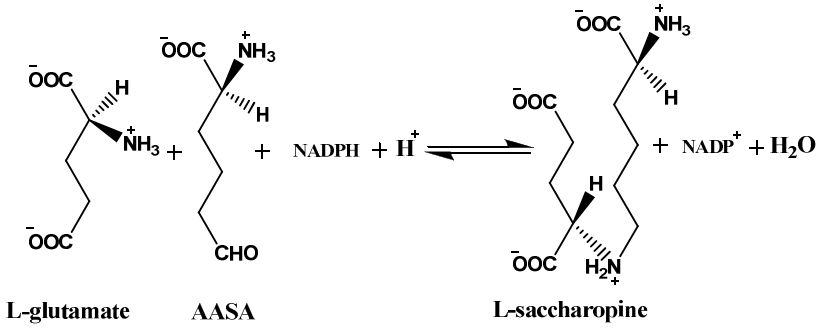

polypeptide chain, on the basis of SDS PAGE (*61*). The enzyme is stable in Tris, pH 8.0, 1 mM PMSF, 10 mM 2-mercaptoethanol and 5 mM EDTA for several weeks when stored at -70 °C. Using gel filtration chromatography, the molecular weight of the enzyme was found to be 67,000 Da (*61*), which is close to the value reported using sucrose density gradient centrifugation (*62*). A M.W. of 70,000-90,000 Da was shown under native conditions, suggesting a dimeric structure for SR (*63*). SR from *Magnoporthe grisea,* a plant pathogen, shows a M.W. of 84,000 from gel-filtration chromatography suggesting a dimeric structure, in agreement with structural studies (*19*, *64*).

In *S. cerevisiae,* the pH optimum for SR in the direction of saccharopine formation is 7.0 (*61*), while it is 9.5-9.75 in the direction of L-α-aminoadipic acid-δ-semialdehyde formation (*61-62*). Enzyme activity decreases significantly if the pH is varied by more than one unit from the optimum pH, and no activity is observed at 8 > pH > 10.5 (*59*). The enzyme is stable at temperatures below 34 °C and becomes denatured above this temperature; no activity was detected above 46 °C (*61*).

The apparent K_m values for L-saccharopine, $NADP^+$ and NAD^+ are 2.3 mM, 22 µM and 54 µM, respectively (*61-62*), with NADPH reported as a better substrate

than NADH in the physiologic reaction direction (*13*, *62*). Since one of the substrates in the physiologic reaction direction, α-aminoadipate-δ-semialdehyde is not commercially available, the enzyme is typically assayed in the direction of formation of the semialdehyde (*2*).

Metal chelators such as 2, 2´-bipyridine and 1, 10-phenanthroline inhibit the enzyme, while carbonyl reagents such as hydroxylamine, and semicarbazide have no effect on enzyme activity (*61*). Enzyme is completely inactivated in the presence of $HgCl_2$ suggesting that a sulfhydryl group might be important for enzyme activity (*61*); similar results have been reported using *p*-hydroxymercuribenzoate as an inhibitor (*13*, *61*). The loss of activity was attributed to binding to Cys155 (*27*).

1-3-2. Structure of saccharopine reductase

The crystal structures of saccharopine reductase from *M. grisea* and *S. cerevisiae* have been solved (*27*, *30*). *Magnoporthe grisea* is a plant pathogen and is responsible for large losses in the rice crop annually due to the blast disease in which the fungus invades the plant's vascular system blocking the transport of nutrients and water from the roots and produce lesions on aerial plant parts (*19*, *66*). The structure of the apo form of SR and substrate bound ternary complex, E:NADPH:saccharopine were solved to 2.0 and 2.1 Å, respectively.

The structure was found to be homodimeric for both the apo form and the ternary complex with each subunit binding one NADPH and one saccharopine molecule (*27*). A ribbon diagram of the enzyme from *S .cerevisiae* is shown in Fig.

1-6.

SR is a homodimer with each subunit consisting of 3 domains. Domain I is a variant of the dinucleotide-binding Rossmann fold, consisting of a central parallel seven stranded β sheets packed against three helices on one side and four on the other. The dinucleotide, $NADP^+$ or NADPH, binds at the carboxyl terminal of the β sheet (*67*). Domain II is an α/β fold known as the saccharopine reductase fold, and is

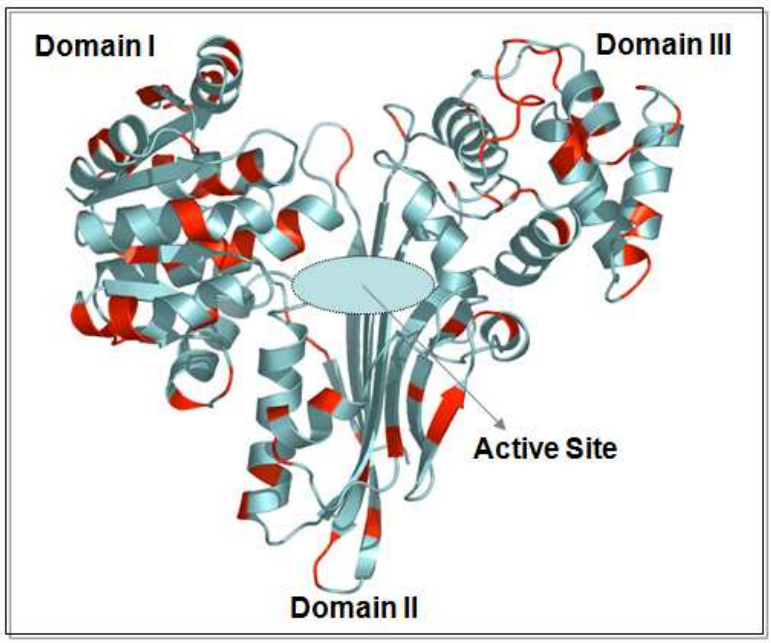

Fig. 1-6: Structure of SR from *S. cerevisiae*. The red regions represent the non-conserved amino acids relative to the structure from *M. grisea*

involved in substrate binding. Domain III is all helical and apparently moves upon substrate binding. The active site is located in a deep cleft between Domain I and Domain II (*27*). The dimer interface contains 45% polar and 55% non-polar residues, and is formed by domains I and II.

SR from *Magnoporthe grisea* shows 63% sequence identity and 78% sequence homology to the enzyme from *S. cerevisiae* (*30*). Superimposition of the structure of SR from *Magnoporthe grisea* and *S. cerevisiae* shows that all the residues in the active site are completely conserved. A close up view of the active site is shown in Fig. 1-7 and 1-8.

Upon ligand binding, a conformational change is induced that includes a rotation of Domain III by 17.7° and a translation of -0.93 Å compared to the structure of the apo enzyme. This conformational change makes the active site less accessible to solvent, protecting reactive intermediates. Once the cofactor, NAD(P)H binds to the Rossmann fold, the nicotinamide ring lies deeply buried in the cleft and is prevented from solvent attack in the relatively hydrophobic interior of the cleft. NAD(P)H is held in place in the active site by several main chain hydrogen bonds. The reaction is stereospecific, and hydride transfer is from the A-side (*pro*-R). The other substrate, saccharopine, is held in the active site by a combination of hydrogen bonding, ionic and hydrophobic interactions (*27*). Thr245, Arg224, Tyr100, Ser99, Asp126, Asp130 and Cys155 are present in the active site and are involved in hydrogen bonding and ionic interactions with saccharopine and stabilize the substrate in the active site (*27*), Fig. 1-7. In addition to the residues shown in Fig. 1-8, the nicotinamide ring is stabilized by hydrophobic interactions with Val399 and Trp174, hydroxyl group of nicotinamide mononucleotide ribose is stabilized by interactions with the main chain oxygen of Ile76. The pyrophosphate group forms hydrogen bonds with the backbone NH of Val14, Phe13 and Ser175 (*27*). The

adenine ring lies in a pocket formed by Arg 34, Val56, Ile76, Pro77, and Phe80. NADPH also forms hydrogen bonds with amide backbone nitrogen of Ser11, Thr35, and Arg34 resulting in stabilization in the active site (*27*). The 2' phosphate group is hydrogen bonded to guanidium group of Arg 34 residue. It is not obvious what

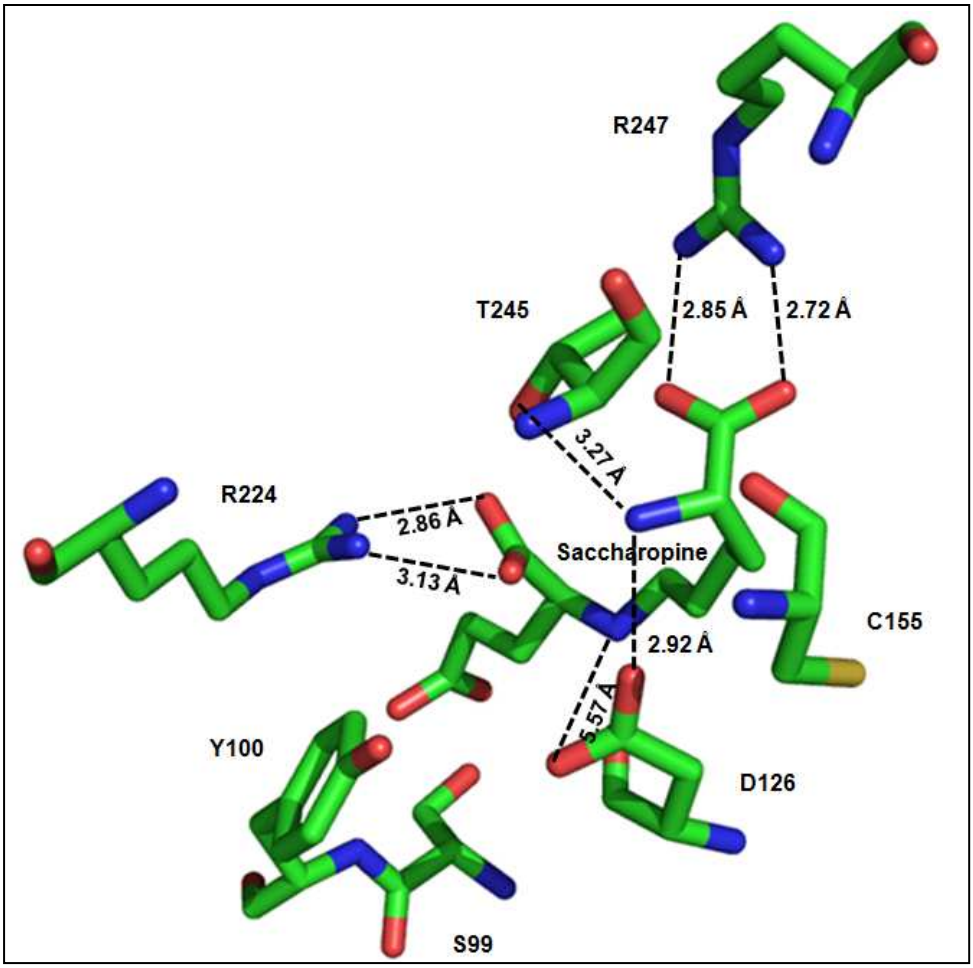

Fig. 1-7: Close-up view of the active site of saccharopine reductase from *M. grisea* (PDB code 1E5Q). Residues that interact with saccharopine and their hydrogen-bonding distances are shown. The following color scheme is used: C, green, O, red, N, blue; and P, orange. This figure was generated using the PyMOL molecular visualization program (website: http:// pymol.Sourcefor ge.net/).

residues in the active site could serve as acid base catalysts for proton transfers that

must occur in the formation of saccharopine. In addition, there is an absence of helix dipoles that might stabilize negative charges expected in the transition state. It was thus proposed that the enzyme provides its major rate enhancement by proximity and orientation effects (*27*).

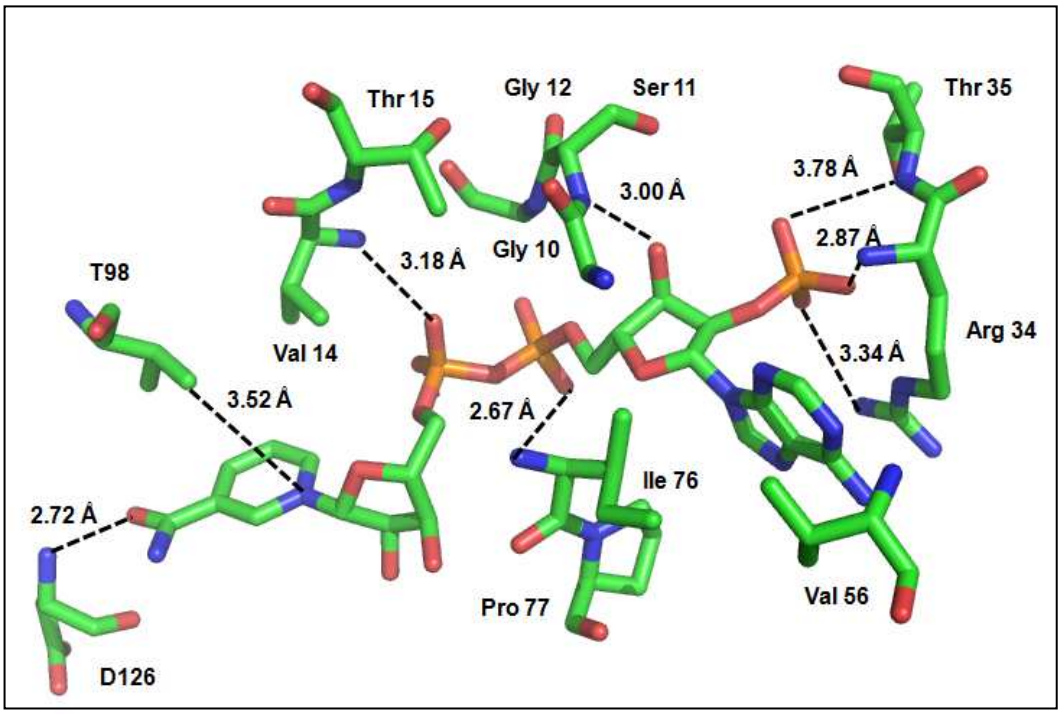

Fig. 1-8: Close-up view of the saccharopine reductase from *M. grisea* (PDB code 1E5Q) binding site for NADP(H). Residues that interact with the cofactor and their hydrogen-bonding distances are shown. The following color scheme is used: C, green, O, red, N, blue; and P, orange. This figure was generated using the PyMOL molecular visualization program (website: http:// pymol.Sourcefor ge.net/).

1-4. Summary

This dissertation describes the determination of the kinetic and chemical mechanisms of saccharopine reductase from *S. cerevisiae*. In the second chapter, we describe the determination of the kinetic mechanism of SR via initial rate studies,

product inhibition studies, dead end inhibition studies, and isotope effect studies. The determination of chemical mechanism of the reaction catalyzed by SR is discussed for the first time in chapter three using pH rate profiles, solvent isotope effect studies, and proton inventory study. Site directed mutagenesis is employed to determine the groups involved in binding and catalysis in the reaction using initial velocity studies, pH-rate profile studies, and solvent isotope effect studies. Alternate substrates and analogues of sacharopine, AASA, glutamate, and nicotinamide adenine dinucleotide have been used to probe the binding of substrates in the active site.

References

1. Umbarger, H. E. (1978) Amino acid biosynthesis and its regulation. *Annl. Rev. Biochem 47*, 532-606.

2. Zabriskie, T. M. and Jackson, M. D. (2000) Lysine biosynthesis and metabolism in fungi. *Nat. Prod. Rep. 17*, 85-97.

3. Miyazaki, J., Kobashi, N., Nishiyama, M., and Yamane, H. (2001) Functional and evolutionary relationship between arginine biosynthesis and prokaryotic lysine biosynthesis through α-aminoadipate *J. Bacteriol. 183*, 5067–5073.

4. Altschul, S. F., Madden, T. L., Schaffer, A. A., Zhang, J., Zhang, Z., Miller, W. and Lipman, D. J. (1997) Gapped BLAST and PSI-BLAST: a new generation of protein database search programs. *Nucleic Acid Res. 25*, 3389–3402.

5. Nishida, H., Nishiyama, M., Kobashi, N., Kosuge, T., Hoshino, T., and Yamane, H. (1999) A prokaryotic gene cluster involved in synthesis of lysine through the aminoadipate pathway: a key to the evolution of amino acid biosynthesis. *Genome Res. 9*, 1175-1183.

6. Lejohn, H. J. (1971) Enzyme regulation, lysine pathways and cell wall structures as indicators of major lines of evolution of fungi. *Nature* (London) 231, 164-168.

7. Bhattacharjee, J. K. (1985) α-aminoadipate pathway for the biosynthesis of lysine in lower eukaryotes. *Crit. Rev. Microbiol. 12*, 131-151.

8. Vogel, H. J. (1960) Two modes lysine synthesis among lower fungi: evolutionary significance. *Biochim. Biophys. Acta. 41*, 172-174.

9. Ye, Z. H. and Bhattacharjee, J. K. (1988) Lysine biosynthesis pathway and biochemical blocks of lysine auxotrophs of *Schizosaccharomyces pombe*. *J. Bacteriol. 170*, 5968-5970.

10. Broquist, H. P. (1971) Lysine biosynthesis (yeast). *Methods Enzymol. 17*, 112-129.

11. Garrad, R. C. and Bhattacharjee, J. K. (1992) Lysine biosynthesis in selected pathogenic fungi: characterization of lysine auxotrophs and the cloned *LYS1* gene of *Candida albicans*. *J. Bacteriol. 174*, 7379-7384.

12. Andi, B., West, A. H., and Cook, P. F. (2004) Stabilization and characterization of histidine-tagged homocitrate synthase from *Saccharomyces cerevisiae*. *Biochim. Biophys. Arch. 421,* 243-254.

13. Jacq, C., Alt-Morbe, J., Andre, B., Arnold, W., Bahr, A., Ballesta, J. P.,Bargues, M., Baron, L., Becker, A., Biteau, N., Blocker, H., Blugeon, C., Boskovic, J., Brandt, P., Bruckner, M., Buitrago, M. J., Coster, F., Delaveau, T., del Ray, F., Dujon, B., Eide, L. G., Garcia-Cantalejo, J. M., Goffeau, A., Gomez-Peris, A., Zaccaria, P., and al, e. (1997) The nucleotide sequence of *Saccharomyces cerevisiae* chromosome IV. *Nature 387*, 75-78.

14. Philippsen, P., Kleine, K., Pohlmann, R., Dusterhoft, A., Hamberg, K., Hegemann, J. H., Obermaier, B., Urrestarazu, L. A., Aert, R., Albermann, K., Altmann, R., Andre, B., Baladron, V., Ballesta, J. P., Becam, A. M., Beinhauer, J., Boskovic, J., Buitrago, M. J., Bussereau, F., Coster, F., Crouzet, M., D'Andelo, M., Dal Pero, F., De Antoni, A., Hani, J. and al, e. (1997) The nucleotide sequence of *Saccharomyces cerevisiae* chromosome XIV and its evolutionary implications. *Nature 387*, 93-98.

15. Tettelin, H., Agostoni Carbone, M. L., Albermann, K., Albers, M., Arroyo, J., Backes, U., Barreiros, T., Bertani, I., Bjourson, A. J., Bruckner, M., Bruschi, C. V., Carignani, G., Castagnoli, L., Cerdan, E., Clemente, M. L., Coblenz, A., Coglievina, M., Coissac, E., Defoor, E., Del Bino, S., Delius, H., Delneri,

D., de Wergifosse, P., Dujon, B., Kleine, K. and al, e. (1997) The nucleotide sequence of *Saccharomyces cerevisiae* chromosome VII. *Nature 387*, 81-84.

16. Irvin, S. D. and Bhattacharjee, J. K. (1985) General and specific controls of lysine biosynthesis in *Saccharoyces cerevisiae*. *Curr. Gent. 9*, 341-344.

17. Karsten, W. E. and Cook, P. F. (2000) Pyridine nucleotide-dependent β-hydroxyacid oxidative decarboxylases: an overview. *Protein and Peptide Letters 7*, 281-286.

18. Ye, Z. H., Garrad, R. C., Winston, M. K., and Bhattacharjee, J. K. (1991) Use of alpha-aminoadipate and lysine as sole nitrogen source by *Schizosaccharomyces pombe* and selected pathogenic fungi. *J. Basic Microbiol. 31*, 149-56.

19. Kunzel, G., Bode, H., Schmidt, I., Samsonova, A., and Birmbaum, D. (1987) Identification of a *lys2* mutant of *C. maltosa* by means of transformation. *Curr. Genet. 11*, 385-391.

20. Kurtz, M. B., Kirsch, D. R. (1986) Integrative transformation of *Candida albicans*, using a cloned *Candida ADE2* gene. *Mol. Cell. Biol. 6*, 142-149.

21. Magee, B. B., Koltin, Y., Gorman, J. A., and Magee, P. T. (1988) Assignment of cloned genes to the seven electrophoretically separated *Candida albicans* chromosomes. *Mol. Cell. Biol. 8*, 4721-4728.

22. Vogel, H. J. (1961) Lysine synthesis and phytogeny of lower fungi: some chytrids versus *Hyphochytrium*. *Nature 189*, 1026–1027.

23. Jones, E. E. and Broquist, H. P. (1965) Saccharopine, an Intermediate of the Aminoadipic Acid Pathway of Lysine Biosynthesis. II. Studies in *Saccharomyces Cerevisiae*. *J. Biol. Chem. 240*, 2531-2536.

24. Trupin, J. S. and Broquist, H. P. (1965) Saccharopine, an intermediate of the aminoadipic acid pathway of lysine biosynthesis. I. Studies in *Neurospora Crassa*. *J. Biol. Chem. 240*, 2524-2530.

25. Trupin, J. S., and Broquist, H. P., (1963) Lysine biosynthesis in *Neurospora crassa*. *Federation Proc. 22*, 243.

26. Perkins, D. D., and M. Bjorkman. (1982) *Neurospora crassa* genetic maps. *Neurospora Newsl. 29*, 31-34.

27. Johansson, E., Steffens, J. J., Lindqvist, Y., and Schneider, G. (2000) Crystal

structure of saccharopine reductase from *Magnaporthe grisea*, an enzyme of the α-aminoadipate pathway of lysine biosynthesis. *Structure 8*, 1037-1047.

28. Gilvarg, C., (1960) Biosynthesis of diaminopimelic acid. *Federation Proc. 19*, 948.

29. Musial, C. E., Cockeril, F. R., and Roberts, G. D. (1988) Fungal infections of the immonocompromised host: clinical and aboratory aspects. *Clin. Microbiol. Rev. 1*, 349-364.

30. Andi B., Cook P. F., West, A. H., (2006), Crystal structure of the his-tagged saccharopine reductase from Saccharomyces cerevisiae at 1.7-Å resolution. *Cell Biochem Biophys. 46*, 17-26.

31. Poulter, R. (1990) The genetics of *Candida albicans*. *CRC Press*, Boca Raton, Fia. 75-124.

32. Scherer, S., and Magee, P. T. (1990) Genetics of *Candida albicans*. *Microbiol. Rev. 54*, 226-241.

33. Sarachek, A., D. D. Rhoads, and R. H. Schwarzhoff (1981) Hybridization of *Candida albicans* thorugh fusion of protoplasts. *Arch. Microbiol. 129*, 1-8.

34. Ye, Z. H., Garrad, R. C., Winston, M. K., and Bhattacharjee, J. K. (1991) Use of alpha-aminoadipate and lysine as sole nitrogen source by *Schizosaccharomyces pombe* and selected pathogenic fungi. *J. Basic Microbiol. 31*, 149-156.

35. Winston, M. K., and Bhattacharjee, J. K. (1982) Growth inhibition by α-aminoadipate and reversal of the effect by specific amino acid supplements in *Saccharomyces cerevisiae*. *J. Bacteriol*. *152*, 874-879.

36. Carson, N. A., Scally, B. G., Neill, D. W., and Carre, I. J. (1968) Saccharopinuria: a new inborn error of lysine metabolism. *Nature* (London) *218*, 679.

37. Garrad, R. C. and Bhattacharjee, J. K. (1992) Lysine biosynthesis in selected pathogenic fungi: characterization of lysine auxotrophs and the cloned *LYS1* gene of *Candida albicans*. *J. Bacteriol*. *174*, 7379-7384.

38. Liebmann, B., Muhleisen, T. W., Muller, M., Hetcht, M., Weidner, G., Braun, A., Brock, M., and Brakhage, A. (2004) Deletion of *Aspergillus fumigatus* lysine biosynthesis gene *lysF* encoding homoaconitase leads to attenuated virulence in a low-dose mouse infection model of invasive

aspergillosis. *Arch. Microbiol. 181*, 378-383.

39. Vogel, H. J. (1960) Two modes lysine synthesis among lower fungi: evolutionary significance. *Biochim. Biophys. Acta. 41*, 172-174.

40. Ramos, F., Dubois, E., and Pirard, A. (1988) Control of enzyme synthesis in the lysine biosynthetic pathway of *Saccharomyces cerevisiae.* Evidence for a regulatory role of gene *LYS14. Eur. J. Biochem. 171*, 171-176.

41. Ramos, F., Verhasselt, P., Feller, A., Peters, P., Watch, A., Dugois, E., and Volckaert, G. (1996) Identification of a gene encoding a homocitrate synthase isoenzyme of *Saccharomyces cerevisiae*. *Yeast 12*, 1315-1320.

42. Tucci, A. F. and Ceci, L. N., (1972) Homocitrate synthase from yeast. *Arch. Biochem. Biophys. 153*, 742-750.

43. Feller, A., Ramos, F., Piérard, A., and Bubois, E. (1999) In *Saccharomyces cerevisiae,* feedback inhibition of homocitrate synthase isoenzymes by lysine modulates the activation of *LYS* gene expression by Lys14p. *Eur. J. Biochem. 261*, 163-170.

44. Borell, C. W., Urrestarazu, L.A., and Bhattacharjee, J. K. (1984) Two unlinked lysine genes (*LYS9* and *LYS14*) are required for the synthesis of saccharopine reductase in *Saccharomyces cerevisiae*. *J. Bacteriol. 159*, 429-432.

45. Hawthorne, D. C., and R. K. Mortimer (1963) Super suppressors in yeast. *Genetics 48*, 617-620.

46. Fjellstedt, T. A. and Ogur, M. (1970) Effects of Supersuppressor Genes on Enzymes Controlling Lysine Biosynthesis in *Saccharomyces J. Bacteriol. 101*, 108-117.

47. Banuelos, O., Casqueiro, J., Gutierrez, S., and Martin, J. F. (2000) Overexpression of the *lys1* gene in *Penicillium chrysogenum*: homocitrate synthase levels, α-aminoadipic acid pool and penicillin production. *Appl. Microbiol. Biotechnol. 54*, 69-77.

48. Wulandari, A. P., Miyazaki, J., Kobashi, N., Nishiyama, M., Hoshino, T., and Yamane, H. (2002) Characterization of bacterial homocitrate synthase involved in lysine biosynthesis. *FEBS Lett. 522*, 35-40.

49. Andi, B., West. A. H., and Cook P. F. (2005) Regulatory mechanism of histidine-tagged homocitrate synthase from Saccharomyces cerevisiae. I.

Kinetic studies. *J. Biol. Chem. 280*, 31624-32.

50. Jaklitsch, W. M. and Kubicek, C. P. (1990) Homocitrate synthase from *Penicillium chrysogenum*. Localization, purification of the cytosolic isoenzyme, and sensitivity to lysine. *Biochem. J.* 269, 247-253.

51. Somerson, N. L., Demain, A. L., and Nunheimer, T. D. (1961) Reversal of lysine inhibition of penicillin production by α-aminoadipic acid. *Arch. Biochem. Biophys. 93*, 238-241.

52. Friedrich, C. G. and Demain, A. L. (1977) Homocitrate synthase as the crucial site of the lysine effect on penicillin biosynthesis. *J. Antibiot. 30*, 760-761.

53. Nishida, H. and Nishiyama, M. (2000) What is characteristic of fungal lysine synthesis through the α-aminoadipate pathway? *J. Mol. Evol.* 51, 299-302.

54. Borell, C. W., Urrestarazu, A. L., and Bhattacharjee, J. K. (1984) Two unlinked lysine genes (LYS9 and LYS14) are required for the synthesis of saccharopine reductase in *Saccharomyces cerevisiae*. *J. Bacteriol. 159*, 429-432.

55. Carsiotis M., and Jones, R. F. (1974) Cross-pathway regulation: tryptophan-mediated control of histidine and arginine biosynthetic enzymes in *Neurospora crassa*. *J. Bacteriol. 119*, 889-892.

56. Demain, A. L., and Masurekar, P. S. (1974) Lysine inhibition of in vivo homocitrate synthesis in *Penicillium chrysogenum*. *J. Gen. Microbiol 82*, 143-151.

57. Jones, E. W., and Fink, G. R. (1982) Regulation of amino acid and nucleotide synthesis in yeast, in molecular biology of the yeast *Saccharomyces*, metabolism and gene regulation cold spring harbor laboratory, cold spring harbor, NY, pp. 181-299.

58. Rife, J. E., & Cleland, W. W. (1980) Evolutionary and structural relationship among dehydrogenases, *Biochemistry 19*, 2328-2333.

59. Storts, D. R. and Bhattacharjee, J. K. (1987) Purification and properties of saccharopine dehydrogenase (glutamate forming) in the *Saccharomyces cerevisiae* lysine biosynthetic pathway, *J. Bacteriol. 169*, 416-418.

60. Betterton H., Fjeustedt, T., Matsuda, M., Ogur, M., and Tate, R. (1968) Localization of the homocitrate pathway, *Biochim Biophys Acta 170*, 459-

461.

61. Andi, B., West. A. H., and Cook P. F. (2005) Regulatory mechanism of histidine-tagged homocitrate synthase from *Saccharomyces cerevisiae*: I. Kinetic studies. *J. Biol. Chem.* 280, 31624-31632.

62. Jones, E. E., Broquist, H. P. (1966) Saccharopine, an intermediate of the aminoadipic acid pathway of lysine biosynthesis. III. Aminoadipic semialdehyde-glutamate reductase. *J. Biol. Chem. 241*, 3430-3434.

63. Bhattacharjee, J. K. (1992) Evolution of α-aminoadipate pathway for the synthesis of lysine in fungi, in handbook of Evolution of Metabolic Function, (Mortlock, R. P. ed.), CRC Press, Boca Raton, Fla, pp 47-80.

64. Johansson, E., Steffens, J. J., Emptage, M., Lindqvist, Y., and Schneider, G. (2000) Cloning, expression, purification and crystallization of saccharopine reductase from *Magnoporthe grisea*. *Acta Crytallogr. D Biol. Crytallogr. 56*, 662-664.

65. Gilboe, D. P., Friede, J. D., and Henderson, L. M. (1968) Effect of hydroxylysine on the biosynthesis of lysine in *Streptococcus faecalis*. *J. Bacteriol. 95*, 856-863.

66. Talbot, N. J. (1995) Having a blast: exploring the pathogenicity of *Magnaporthe grisea*. *Trends Microbiol. 3*, 9-16.

67. Rossmann, M. G., Liljas, A., Branden, C. I., and Banaszak, L. J. (1975) Evolutionary and structural relationship among dehydrogenases. *Enzymes 11*, 51-102.

CHAPTER 2

Overall kinetic mechanism of saccharopine reductase

2-1. Introduction

The biosynthesis of L-lysine occurs via the α-aminoadipate (AAA) pathway in euglenoids and higher fungi such as basidiomycetes (*1*). The α-aminoadipate pathway is a member of the glutamate family of amino acid biosynthetic pathways (*2*). The AAA pathway has been reported in *Saccharomyces cerevisiae* (*3*), *Schizosaccharomyces pombe* (*4*), *Penicillium chrysogenum* (*5*), *Neurospora crassa* (*6*), *Magnoporthe grisea* which is a plant pathogen (*7*), and human pathogenic fungi including *Candida albicans* (*8*), *Aspergillus fumigatus* (*9*) and *Cryptococcus neoformans* (*8*).

Saccharopine reductase (SR) [saccharopine dehydrogenase (L-glutamate forming), EC 1.5.1.10] catalyzes the condensation of L-α-aminoadipate-δ-semialdehyde with L-glutamate to give an imine, which is reduced by NADPH to give saccharopine (*7*).

Crystal structures of saccharopine reductase from *S. cerevisiae* and *M. grisea* have been reported (*7*, *10*). Structures of the *M. grisea* apo form and ternary, E-NADPH-saccharopine, complex of SR were solved to 2.0 and 2.1 Å, respectively. The enzyme is a homodimer with a molecular weight of ~50, 000 and contains one binding site for substrates per subunit. The amino acid sequence of SR is highly

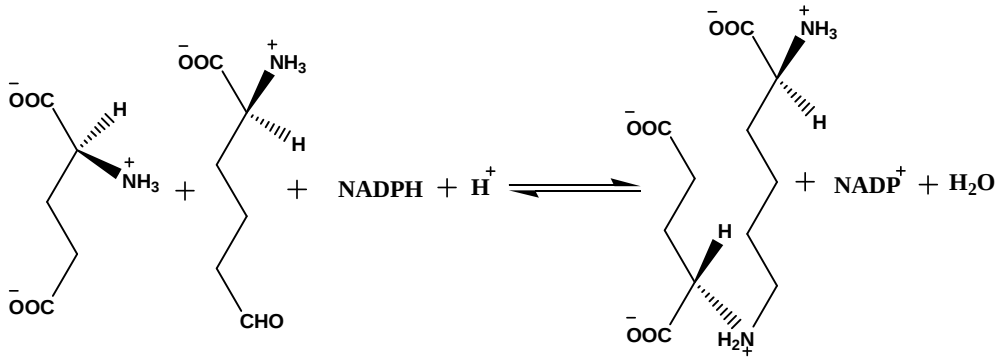

conserved in *C. albicans, A. fumigatus*, *C. neoformans*, and *S. cerevisiae*, and thus, SR is a potential target for antifungals. In preparation for the development of mechanism-based inhibitors, the kinetic and chemical mechanisms of the enzyme must be known. The pH optimum of SR from *S. cerevisiae* in the direction of saccharopine formation is 7.0 (*11*), while it is 9.5-9.75 in the direction of semialdehyde formation (11, 12). Apparent K_m values for L-saccharopine, NADP and NAD are 2.32 mM, 22 µM and 54 µM, respectively (*11*), with NADPH a better substrate than NADH in the physiologic reaction direction (*12*).

Thus far, no information is available on the kinetic mechanism of SR. In this chapter, we present a detailed steady-state kinetic analysis of the saccharopine reductase reaction in both reaction directions. On the basis of initial velocity studies in the absence and presence of product and dead-end inhibitors, an ordered kinetic mechanism is proposed for SR. This is the first report of the kinetic mechanism of a saccharopine reductase.

2-2. Materials and Methods

2-2-1. Chemicals

L-Saccharopine, L-pipecolic acid, glyoxylic acid, ornithine, L-glutamic acid, L-lysine, L-leucine, α-ketoglutarate, oxaloacetate, 5-bromopentene, ethylacetamido-cyanoacetate, sodium metal and chloramphenicol were from Sigma. *β*-NADPH[1], *β*-NADP, and LB broth were purchased from USB. The Ni-NTA agarose affinity resin was from Qiagen. Isopropyl-*β*-D-1-thiogalactopyranoside was from Invitrogen, while ampicillin was from Fisher Biotechnologies, and ethanol-d_6 (99 atom % D) was purchased from Cambridge Isotope Laboratories, Inc. AG MP-1 and Bio-Gel P-2 resins were from Bio-Rad, and HEPES was obtained from Research Organics. *N*-Oxalylglycine was from Frontier Scientific. All chemicals were of the highest grade available and were used as purchased.

2-2-2. Synthesis of α–aminoadipic acid-δ-semialdehyde

The semialdehyde was synthesized using a modification of the method of Rodwell *et al.* (*13*). All of the equipment used for the synthesis were rinsed with acetone and dried overnight. To ethylacetamidocyanoacetate in ethanol, sodium metal was added, and bromopentane was added dropwise over a period of 1 hour. The mixture was refluxed for 1 hour at 75 °C. The mixture was cooled to room temperature and the ethanol was removed *in vacuo* using a Buchi rotatory evaporator at 60 °C. 1 % NaOH was added to the residue and the mixture was refluxed at 102 °C for 15 hours, cooled, the pH was adjusted to 1.8 using 12 N HCl, followed by

concentration by rotatory evaporation at 90 °C. The residue was dissolved in a minimum amount of water and pH was adjusted to 5.0 with pyridine, followed by addition of absolute ethanol. The crude solution was rotatory evaporated, dissolved in a minimum amount of water and recrystallized using activated charcoal in hot water to obtain the HCl salt of 2-amino-6-heptenoic acid. Ozonolysis of the 2-amino-6-heptenoic acid in water was then carried out using an OREC Model V5-0 ozonator. The resulting aldehyde solution was purged with N_2 to remove excess ozone in the mixture. NMR spectra were obtained on a Varian Mercury VX-300 MHz spectrometer with a Varian 4-nuclei autoswitchable PFG probe. ^{1}H NMR spectra were collected in D_2O using the PRESAT pulse sequence supplied by Varian, Inc. The spectra were collected with a sweep width of 4803.1 Hz, eight transients, and an acquisition time of 3.411 s and processed with 108K data points resulting in a 1.0 Hz digital resolution. Chemical shifts were assigned for all peaks and are as follows: δ 9.7 [s, 1H, C(6)-H], δ 3.6 [t, 1H, C(2)-H], δ 1.78 [m, 2H, C(3)-H_2], δ 1.64 [t, 2H, C(5)-H_2], δ 1.38 [p, 2H, C(4)-H_2].

The % yield of semialdehyde was 95 % for the ozonolysis step on the basis of the concentration of semialdehyde measured using end point assay using SR and monitoring the change in absorbance of NADPH at 340 nm. A resonance for the hydrated form of the aldehyde was not observed, suggesting it lies under one of the resonances. The end-point assay exhibited a rapid utilization of 65 % of the aldehyde followed by a much slower utilization of the remaining 35 %. Thus, 35 % of the semialdehyde is present in the hydrated (or diol) form and 65 % in the aldehyde

form. The α-amino group of the semialdehyde is protonated at pH 7.0, and none of the cyclic imine was observed. The overall yield based on the starting material was 15 %.

2-2-3. Synthesis of A-Side NADPD

The A-Side NADPD was prepared using the method described by Viola *et al*. (*14*). The reaction mixture contained 5.6 mM NADP, 2.8 mM ethanol-$d_{6,}$ 100 units each of alcohol dehydrogenase (*T. brockii)*, and yeast aldehyde dehydrogenase. The reaction was carried out in 10 mL of 6 mM Ches, pH 9.0 and 25 °C. The reaction was allowed to proceed overnight and the formation of NADPD was monitored by following the absorbance at 340 nm. The pH was constantly adjusted using KOH since the pH drops as the reaction proceeds. The reaction was terminated on the following day by adding a few drops of $CHCl_3$ to the reaction mixture with shaking, followed by separation of the aqueous layer from the organic layer. The aqueous layer was adjusted to pH 10.0 with KOH, and loaded onto an AG-MP column equilibrated with 0.2 M LiCl (pH 10.0); fractions were eluted using 0.5 M LiCl (pH 10.0). The ratio of absorbance at 260 and 340 nm was 2.4 ± 0.05 for the pooled NADPD fractions compared to a value of 2.15 ± 0.05 reported preveiously (*14*). The purified A-side NADPD was then concentrated using rotatory evaporation at 50 °C to about 6 mL and the solution was loaded onto a Bio-Gel P-2 column equilibrated with 50 mM KH_2PO_4. The NADPD was eluted using the same buffers and used without further treatment.

2-2-4. Cell growth and protein expression

The gene from *S. cerevisiae* encoding for SR (*LYS9*) was cloned into the pET-16b vector (*12*). The vector containing the insert was transformed into BL21*(DE-3) RIL *E. coli* cells using heat shock at 42 °C, followed by growth on ampicillin plates. Colonies were picked and cells were grown overnight at 37 °C in LB media containing 100 μg/mL ampicillin and 25 μg/mL chloramphenicol. The cells were induced using 1mM IPTG at an A_{600} of 0.7-0.9, and allowed to grow overnight. After centrifugation at 4000*g*, the harvested cells were suspended in 100 mM Tris-HCl, pH 7.5 with 300 mM KCl.

For protein purification, PMSF (1 mM) was added to the cell suspension followed by cell disruption using a MISONIX Sonicator XL. Sonication was carried out on ice for 1 min using a pulse on time of 15 s followed by a 30 s rest period. The cell debris was removed by centrifugation at 20,400*g* for 15 min, and the supernatant was loaded onto a Ni- NTA column, washed with 30 mM imidazole, and then eluted using buffer containing 400 mM imidazole at pH 7.5. The enzyme elutes efficiently using 400 mM imidazole and is about 98 % pure on the basis of SDS PAGE.

2-2-5. Enzyme assay

The SR reaction was followed by monitoring the appearance or disappearance of NADPH at 340 nm ($\varepsilon_{340,}$ 6220 $M^{-1}cm^{-1}$) using a Beckman DU-640 spectrophotometer. All assays were carried out at 25 °C. A typical assay in 500 μL contained 100 mM HEPES, pH 7.0, and appropriate concentrations of substrates.

Reaction was initiated by adding 10 μL of appropriately diluted enzyme in 100 mM HEPES, pH 7.0. All enzyme dilutions were made fresh for each set of experiments.

2-2-6. Initial velocity studies

Studies were carried out in the forward and reverse reaction direction at pH 7.0. The rate of reaction in the direction of saccharopine formation was measured as a function of the concentration of NADPH (5-50 μM), at different fixed concentrations of L-glutamate (5-50 mM), and a fixed concentration of L-AASA (5 mM). The experiment was then repeated at different concentrations of AASA (7.14-12.5 mM). In the direction of AASA formation, initial rate data were collected as a function of NADP (0.02-0.5 mM) at different fixed saccharopine concentrations (0.1-10 mM).

2-2-7. Inhibition studies

Product inhibition studies were carried out by measuring the initial velocity with fixed substrates equal to their respective K_m values, and varying the concentration of the other substrate around its K_m value (0.5-5 K_m) at different fixed concentrations of the inhibitor including zero. First, an estimate of the inhibition constant of an inhibitor was obtained by measuring the initial rate as a function of the inhibitor concentration with all substrates fixed at their respective K_m values. The appK_i was then calculated from a plot of 1/υ vs. I with the appK_i the value equal to the abscissa intercept divided by 2.

2-2-8. Primary Substrate Deuterium Kinetic Isotope Effects

Isotope effects were measured using NADPD as the deuterated substrate. $^{D}V_1$ and $^{D}(V_1/K_{Glutamate})$ were obtained by measuring the initial rate as a function of L-glutamate concentration with NADPH(D) and α-AASA maintained at $10K_m$ and $5K_m$, respectively. Similarly, $^{D}(V_1/K_{NADPH})$ was obtained by varying NADPH(D) with glutamate and AASA fixed at saturation. All isotope effects were measured in triplicate and the S. E. M. is reported.

2-2-9. Data Processing

All data were plotted in double reciprocal form to assess the quality of the data and to determine the correct rate equation for data fitting. Initial velocity data were then fitted to the appropriate equation using Enzfitter program from BIOSOFT, Cambridge, U.K. Initial velocity data in the direction of saccharopine formation were fitted to eqs 1 and 2, while data in the direction of AASA formation were fitted to eq. 3. Data adhering to linear competitive, uncompetitive, and noncompetitive inhibition were fitted to eqs 4-6.

$$\upsilon = \frac{V_1\mathbf{ABC}}{\text{constant} + (\text{coef}\mathbf{A})\mathbf{A} + (\text{coef}\mathbf{B})\mathbf{B} + (\text{coef}\mathbf{C})\mathbf{C} + K_c\mathbf{AB} + K_b\mathbf{AC} + K_a\mathbf{BC} + \mathbf{ABC}} \quad (1)$$

$$\upsilon = \frac{V_1\mathbf{ABC}}{K_{ia}K_{ib}K_c + K_{ib}K_c\mathbf{A} + K_c\mathbf{AB} + K_a\mathbf{BC} + \mathbf{ABC}} \quad (2)$$

$$\upsilon = \frac{V_2\mathbf{AB}}{K_{ia}K_b + K_b\mathbf{A} + K_a\mathbf{B} + \mathbf{AB}} \quad (3)$$

$$\upsilon = \frac{appV\mathbf{A}}{K_a\left(1+\frac{\mathbf{I}}{K_{is}}\right)+\mathbf{A}} \tag{4}$$

$$\upsilon = \frac{appV\mathbf{A}}{K_a+\mathbf{A}\left(1+\frac{\mathbf{I}}{K_{ii}}\right)} \tag{5}$$

$$\upsilon = \frac{appV\mathbf{A}}{K_a\left(1+\frac{\mathbf{I}}{K_{is}}\right)+\mathbf{A}\left(1+\frac{\mathbf{I}}{K_{ii}}\right)} \tag{6}$$

In eqs 1-6, υ represents the measured initial velocity, app$V$ is the maximum rate, obtained with fixed substrate equal to K_m, V_1 and V_2 are the maximum rates in forward and reverse reaction directions, **A**, **B** and **C** are substrate concentrations, K_a, K_b and K_c are Michaelis constants for substrates A, B and C**,** respectively, **I** is the inhibitor concentration, K_{ia} and K_{ib} are the dissociation constants for EA and EB complexes, and K_{ii} and K_{is} are the intercept and slope inhibition constants respectively. In eq. 1, the constant and coefficient terms are products of kinetic constants, and are mechanism dependent.

2-2-10. Direct Determination of K_{eq}

In order to determine the equilibrium constant, the concentrations of saccharopine, L-AASA, NADP and NADPH were fixed at 1 mM, 5 mM, 0.5 mM, and 0.1 mM, respectively, and the concentration of L-glutamate was varied in separate reactions from 0.2-8 mM at pH 7.0. Sufficient enzyme was added to each

reaction mixture to bring the reaction rapidly to equilibrium. The absorbance was recorded before and after adding the enzyme and a plot of ΔAbs vs. glutamate was constructed. The concentration of L-glutamate that gave ΔAbs of zero was then used to calculate K_{eq} using eq. 7.

$$K_{eq} = \frac{[\text{NADP}][\text{saccharopine}]}{[\text{NADPH}][\text{L-glutamate}][\text{AASA}]} \quad (7)$$

2-3. Results

2-3-1. Initial velocity studies

In the direction of saccharopine formation, the double reciprocal plots obtained as described in Methods all intersect to the left of the ordinate. A fit of the data to eq 1 indicated the coef B, coef C, and K_b terms were indeterminate. Data were then fitted to eq. 2, which suggest a kinetic mechanism with ordered addition of A followed by rapid equilibrium addition of B, followed by addition of C. Values of kinetic parameters are given in Table 1. Initial velocity patterns were also generated in the direction of semialdehyde formation by varying the concentration of saccharopine at different fixed concentrations of NADP. An intersecting pattern was obtained. The data were fitted to eq 3 and estimates of kinetic parameters are summarized in Table 2-1.

2-3-2. Product inhibition studies

In order to obtain additional quantitative information on kinetic mechanism

Table 2-1. Summary of Kinetic Parameters for SR at pH 7.0

forward reaction		reverse reaction	
V_1/E_t (s^{-1})	8 ± 1	V_2/E_t (s^{-1})	1.06 ± 0.02
$V_1/K_{NADPH}E_t$ ($M^{-1}s^{-1}$)	(7.3 ± 1.8) x 10^5	$V_2/K_{NADP}E_t$ ($M^{-1}s^{-1}$)	(5.67 ± 0.01) x 10^3
$V_1/K_{Glu}E_t$ ($M^{-1}s^{-1}$)	(2.9 ± 0.7) x 10^2	$V_2/K_{Sacc}E_t$ ($M^{-1}s^{-1}$)	(1.6 ± 0.3) x 10^2
K_{NADPH} (μM)	11.4 ± 2.6	K_{NADP} (mM)	0.187 ± 0.006
K_{Glu} (mM)	28 ± 6	K_{Sacc} (mM)	6.6 ± 0.2
K_{iAASA} (mM)	4.4 ± 1.7	K_{iNADP} (mM)	0.020 ± 0.004
K_{iNADPH} (μM)	4.4 ± 2.1		

and test the mechanism proposed from initial velocity studies in the absence of inhibitors, product inhibition patterns were obtained for all products in both reaction directions. Product inhibition by NADPH vs. NADP is competitive, consistent with addition of the oxidized and reduced cofactor to free enzyme. AASA is uncompetitive vs. NADP and noncompetitive vs. saccharopine. All other patterns are noncompetitive, and are consistent with the proposed ordered mechanism, Table 2-2.

2-3-3. Dead end inhibition studies

To further test the proposed kinetic mechanism and obtain information on the reactant binding determinants, dead end inhibition experiments were also carried out. All patterns are consistent with the ordered mechanism, Table 2-3. The structures of dead and inhibitors used are shown in Fig. 2-1.

2-3-4. Determination of K_{eq}

The equilibrium constant for the reaction catalyzed by saccharopine dehydrogenase was determined at pH 7.0 by determining the concentration of L-glutamate that gave no change in absorbance at fixed concentration of all of the other substrates. The calculated K_{eq} value is 200 M^{-1}, in good agreement with 500 M^{-1}, the value determined using the Haldane relationship, eq 8.

$$K_{eq} = \frac{(V / K_{Glu})(K_{iNADP})}{(V / K_{Sacc})(K_{iNADPH})(K_{iAASA})} \tag{8}$$

2-3-5. Primary Substrate Deuterium Kinetic Isotope Effects

Isotope effect studies were carried out at pH 7.0 using A-side NADPD as the deuterated substrate. The isotope effects measured are all small: $^{D}V_1$ = 1.2 ± 0.1, $^{D}(V_1/K_{\text{glutamate}})$ = 0.870 ± 0.035, $^{D}(V_1/K_{\text{NADPH}})$ = 0.98 ± 0.04. Values of $^{D}V_1$ and $^{D}(V_1/K_{\text{NADPH}})$ are near unity, while the values of $^{D}(V_1/K_{\text{glutamate}})$ is inverse.

2-4. Discussion

2-4-1. Initial Velocity Studies

In the direction of saccharopine formation, intersecting patterns were obtained using a fixed nonsaturating concentration of α-AASA and varying NADPH/L-glutamate Intersecting patterns were also obtained in the direction of saccharopine oxidation. Data are consistent with a sequential mechanism.

The initial velocity data in the direction of saccharopine formation obtained as a function of the concentration of NADPH (5-50 μM), at different fixed concentrations of L-glutamate (5-50 mM), and a fixed concentration of L- AASA-(5 mM) were fitted to eq 1 for a fully random terreactant mechanism, the fitted parameters showed that coef B, coef C, and K_b terms in the denominator of equation 1 were not defined. Data suggest that the EB (E-AASA) and EC (E-L-glutamate) binary complexes are not present. The absence of the K_{AASA} term in eq 2 indicates that the binding of AASA must be in equilibrium, which suggests it binds after NADPH and before glutamate. Data were then fitted to eq 2 for an ordered mechanism with AASA adding in rapid equilibrium, and all kinetic parameters were well defined, Table 1. On the basis of initial velocity studies in the absence of inhibitors, the mechanism is sequential with an apparent requirement for NADPH bound prior to AASA or glutamate. The maximum rate in the physiological reaction direction is 8-times higher than that in the non-physiological reaction direction.

Table 2-2. Product Inhibition Data for SR

Varied Substrate	Fixed substrate	Inhibitor	K_{is} (mM)	K_{ii} (mM)	Inhibition Observed	Pattern Predicted[a]
NADPH	L-glutamate (K_m)[b] L-AASA ($2K_{ib}$)	NADP	0.015 ± 0.002	N/A	C	C
L-AASA	NADPH (K_m) L-glutamate (K_m)	NADP	0.055 ± 0.012	0.042 ± 0.004	NC	NC
L-glutamate	NADPH (K_m) L-AASA ($2K_{ib}$)	NADP	0.038 ± 0.004	0.09 ± 0.01	NC	NC
NADPH	L-glutamate (K_m) L-AASA ($2K_{ib}$)	Saccharopine	2.0 ± 0.4	1.6 ± 0.1	NC	NC
L-AASA	NADPH (K_m) L-glutamate (K_m)	Saccharopine	0.55 ± 0.07	22 ± 12	NC	NC
L-glutamate	NADPH (K_m) L-AASA ($2K_{ib}$)	Saccharopine	1.9 ± 0.3	1.00 ± 0.07	NC	NC

NADP	saccharopine (K_m)	NADPH	0.07 ± 0.01	N/A	C	C
saccharopine	NADP (K_m)	NADPH	0.008 ± 0.001	0.020 ± 0.003	NC	NC
NADP	saccharopine (K_m)	L-glutamic acid	0.14 ± 0.01	139 ± 10	NC	NC
saccharopine	NADP (K_m)	L-glutamic acid	5.7 ± 0.2	86 ± 10	NC	NC
NADP	saccharopine (K_m)	L-AASA			UC	UC
saccharopine	NADP (K_m)	L-AASA			NC	NC

[a] Patterns predicted for an ordered kinetic mechanism.
[b] Concentration of the fixed substrate.
[c] AASA shows weak inhibition. Qualitatively, the inhibition pattern for AASA vs. saccharopine is noncompetitive suggesting there may be some randomness in addition of AASA and glutamate.

Table 2-3. Summary of Dead End Inhibition Data for SR

Varied Substrate	Fixed substrate	Inhibitor	K_{is} (mM)[a]	K_{ii} (mM)[a]	Inhibition Observed	Pattern Predicted	Enzyme form[b]
NADPH	L-glutamate (K_m) L-AASA ($2K_{ib}$)	α-Kg	N/A	7.0 ± 0.4 (1.4 ± 0.1)	UC	UC	E-NADPH-AASA
L-AASA	NADPH (K_m) L-glutamate (K_m)	α-Kg	N/A	9.4 ± 0.5 (4.6 ± 0.2)	UC	UC	E-NADPH-AASA
L-glutamate	NADPH (K_m) L-AASA ($2K_{ib}$)	α-Kg	8.2 ± 0.4 (4.0 ± 0.3)	N/A	C	C	E-NADPH-AASA
NADPH	L-glutamate (K_m) L-AASA ($2K_{ib}$)	aminohept-enoic acid	N/A	336 ± 41 (67 ± 8)	UC	UC	E-NADPH
L-AASA	NADPH (K_m) L-glutamate (K_m)	aminohept-enoic acid	65 ± 7 (47 ± 5)	N/A	C	C	E-NADPH
L-glutamate	NADPH (K_m) L-AASA ($2K_{ib}$)	aminohept-enoic acid	325 ± 134 (96 ± 38)	250 ± 36 (50 ± 7)	NC	NC	E-NADPH

NADP	saccharopine (K_m)	NOG	N/A	10.0 ± 0.4 (5.0 ± 0.2)	UC	UC	E-NADP
saccharopine	NADP (K_m)	NOG	7.0 ± 0.8 (6.0 ± 0.7)	N/A	C	C	E-NADP
NADP	saccharopine (K_m)	L-pipecolic acid	N/A	87 ± 6 (43 ± 3)	UC	UC	E-NADP
saccharopine	NADP (K_m)	L-pipecolic acid	38 ± 7 (34 ± 6)	N/A	C	C	E-NADP
NADP	saccharopine (K_m)	L-leucine	N/A	38 ± 2 (19 ± 1)	UC	UC	E-NADP
saccharopine	NADP (K_m)	L-leucine	17 ± 2 (15 ± 2)	N/A	C	C	E-NADP
NADP	saccharopine (K_m)	α-Kg	N/A	14.4 ± 0.5 (7.0 ± 0.3)	UC	UC	E-NADP

saccharopine	NADP (K_m)	α-Kg	11.1 ± 0.6 (10.0 ± 0.5)	N/A	C	C	E-NADP
NADP	saccharopine (K_m)	Glyoxylic acid	N/A	14.2 ± 0.7 (7.0 ± 0.4)	UC	UC	E-NADP
saccharopine	NADP (K_m)	Glyoxylic acid	8.7 ± 0.6 (8.0 ± 0.6)	N/A	C	C	E-NADP
NADP	saccharopine (K_m)	L-Ornithine	N/A	13.7 ± 0.4 (7.0 ± 0.2)	UC	UC	E-NADP
saccharopine	NADP (K_m)	L-Ornithine	11.6 ± 1.2 (10 ± 1)	N/A	C	C	E-NADP

[a] The values in parentheses are the corrected values for the fixed substrate where applicable.
[b] Enzyme form to which the inhibitor binds.

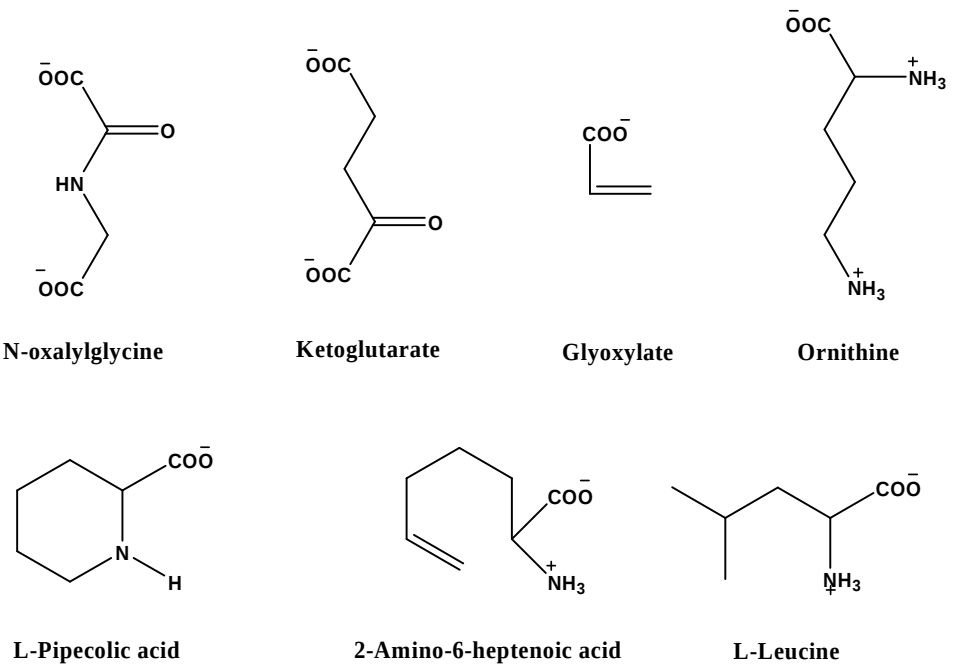

Fig. 2-1. Structures of Saccharopine, glutamate and AASA analogs tested in the saccharopine reductase reaction.

2-4-2. Product Inhibition Studies

Inhibition studies can be used to further define the kinetic mechanism of an enzyme catalyzed reaction. They provide information regarding the various enzyme forms to which substrates bind and thus the order of addition of substrates. In the direction of saccharopine formation, product inhibition studies were carried out using NADP, and saccharopine as product inhibitors. NADP is competitive vs. NADPH and noncompetitive vs. α–AASA and L-glutamate, while saccharopine exhibited noncompetitive inhibition against all the three reactants, NADPH, α–AASA and L-glutamate. In the direction of saccharopine oxidation, NADPH is competitive vs.

NADP and noncompetitive vs. saccharopine. L-Glutamate exhibited noncompetitive inhibition vs. both NADP and saccharopine, while α–AASA showed noncompetitive inhibition vs. saccharopine and uncompetitive inhibition vs. NADP. Data suggest that in the direction of saccharopine formation, AASA binds to the E-NADPH binary complex in rapid equilibrium fashion followed by the addition of L-glutamate, while in the direction of saccharopine oxidation, NADP is the first substrate to be added followed by saccharopine, which adds to the E-NADP binary complex.

2-4-3. Dead-end Inhibition Studies

In the direction of saccharopine formation, dead end inhibition patterns were obtained using analogs of L-glutamate, and α–AASA. 2-amino-6-heptenoic acid was competitive vs. AASA, uncompetitive vs. NADPH and noncompetitive vs. L-glutamate, showing that 2-amino-6-heptenoic acid (and by analogy AASA) binds to E-NADPH. α-Ketoglutarate was chosen as the dead-end analog of L-glutamate and exhibited competitive inhibition vs. L-glutamate and uncompetitive inhibition vs. AASA and NADPH consistent with binding of L-glutamate to the E-NADPH-AASA ternary complex. In the direction of oxidation of saccharopine, dead-end analogs of saccharopine are competitive vs. saccharopine and uncompetitive inhibition vs. NADP in agreement with binding of the analogs to E-NADP. Product and dead-end inhibition data are consistent with an overall ordered kinetic mechanism for SR, as shown by the agreement between the observed inhibition patterns and those predicted for an ordered mechanism, Tables 2-2 and 2-3. The proposed mechanism is

depicted in Scheme 2-1.

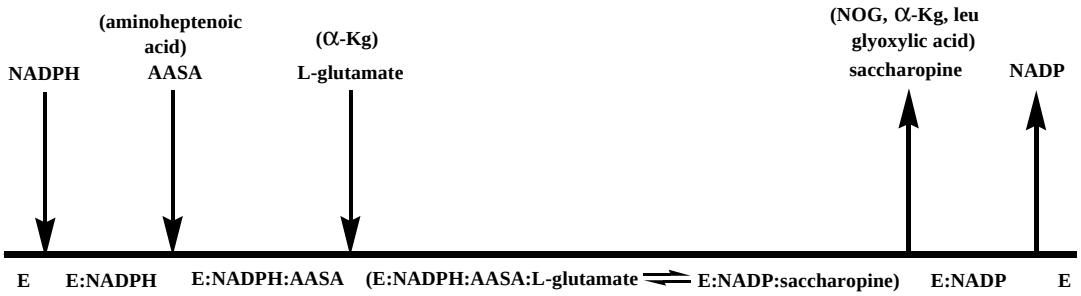

Scheme 2-1. Proposed Kinetic Mechanism for SR. Dead end analogs of the substrates are shown in parentheses

2-4-4. Calculation of true dead-end inhibition constants

Inhibition constants obtained in product and dead-end inhibition studies are apparent values since the fixed substrate(s) are present at a concentration equal to their K_m value. In the case of dead-end inhibitors, true inhibition constant values can be estimated by correcting for the presence of the fixed reactant. The true K_i value will thus be independent of the substrate varied, as long as it results from combination to the same enzyme form(s). The rate equation for the SR kinetic mechanism in the direction of saccharopine formation is given in eq. 2. Each term in the denominator of eq. 2 reflects an enzyme form. The $K_{ia}K_{ib}K_c$ and K_aBC terms represent free enzyme, while $K_{ib}K_c$A, K_cAB, and ABC terms represent the E-NADPH, E-NADPH-AASA, and the central and product complexes present at steady state, respectively.

The equation for correction of the appK_i values can easily be derived and the overall strategy is illustrated by an example below. If a competitive dead end inhibitor of substrate B (L-AASA in the terreactant direction) is used, the presence of

the inhibitor modifies the enzyme form(s) to which B binds, i.e., the $K_{ib}K_c$A term in eq. 2, by a factor of (1 + **I**/K_i) to give eq. 9, where K_i is the intrinsic dissociation constant for the inhibitor.

$$\upsilon = \frac{V\mathbf{ABC}}{K_{ia}K_{ib}K_c + K_a\mathbf{BC} + (K_{ib}K_c)\left(1+\frac{\boldsymbol{I}}{K_i}\right)\mathbf{A} + K_c\mathbf{AB} + \mathbf{ABC}} \tag{9}$$

The double reciprocal form factoring out (1/B) gives eq. 10

$$\frac{1}{\upsilon} = \left[\left(\frac{K_{ia}K_{ib}K_c}{V\mathbf{AC}} + \frac{K_{ib}K_c}{V\mathbf{C}}\right) + \left(\frac{K_{ib}K_c}{V\mathbf{C}}\right)\left(\frac{\boldsymbol{I}}{K_i}\right)\right]\left(\frac{1}{\mathbf{B}}\right) + \left(\frac{K_a}{V\mathbf{A}} + \frac{K_c}{V\mathbf{C}} + \frac{1}{V}\right) \tag{10}$$

The expression for the slope term in eq. 10 is given by eq. 11.

$$Slope = \left(\frac{K_{ia}K_{ib}K_c}{V\mathbf{AC}} + \frac{K_{ib}K_c}{V\mathbf{C}}\right) + \left(\frac{K_{ib}K_c}{VK_i\mathbf{C}}\right)\boldsymbol{I} \tag{11}$$

Setting the slope equal to zero and solving for I (appK_i) gives eq. 12.

$$appK_i = -K_i\left(1+\frac{K_{ia}}{\mathbf{A}}\right) \tag{12}$$

Thus, the intrinsic K_i is calculated using known values of appK_i, K_{ia} and A. A similar treatment gives eq. 13 when 1/A is factored out of eq. 10,

$$\frac{1}{\upsilon} = \left(\frac{K_{ia}K_{ib}K_c}{V\mathbf{BC}} + \frac{K_a}{V}\right)\left(\frac{1}{\mathbf{A}}\right) + \frac{K_{ib}K_c}{V\mathbf{BC}}\left(1+\frac{\boldsymbol{I}}{K_i}\right) + \frac{K_c}{V\mathbf{C}} + \frac{1}{V} \tag{13}$$

$$appK_{ii} = K_i\left(1+\left(\frac{\mathbf{B}}{K_{ib}}\right)\left(1+\frac{\mathbf{C}}{K_c}\right)\right) \tag{14}$$

Using this kind of analysis, estimates of intrinsic K_i values are calculated, and these are shown in parentheses in Table 3. Binding of a dead-end analog to a given enzyme form, whatever substrate is varied, should give the same K_i when the appK_i is corrected for the presence of the fixed reactant(s) The agreement in the intrinsic K_i values for dead-end analogs estimated under different conditions is consistent with the proposed ordered mechanism.

2-4-5. Primary kinetic deuterium isotope effects

The values of primary deuterium isotope effects obtained by direct comparison of V and V/K values in the direction of formation of saccharopine are small, suggesting that the hydride transfer step is not slow in the overall reaction. In an ordered mechanism, the isotope effects on the V/K of all but the final substrate to add to enzyme, in either reaction direction is unity. In agreement with the proposed ordered mechanism, $^{D}(V/K_{NADPH})$ is within error 1. The inverse isotope effect observed for $^{D}(V/K_{glutamate})$ suggests the hydride transfer step is close to equilibrium in the steady state. The equilibrium isotope effect for reduction of an imine reflects the difference in fractionation factor for deuterium at C4 of NADPD and C6 of saccharopine. The value of $^{D}K_{eq}$ was estimated as 0.87 from glutamate and alanine dehydrogenases (16), and this is equal to $^{D}(V/K_{glutamate})$. Thus, (a) step(s) after reduction of the imine limits the overall reaction, likely the conformational change to open the active site to release saccharopine. Data further suggest the deuterium isotope effect on V is unity and not a small finite value, since a finite isotope effect

other than unity should be inverse as observed for ${}^{D}(V/K_{glutamate})$.

2-4-6. Comparison of kinetic mechanism of SR with similar enzymes

Enzymes that catalyze the pyridine nucleotide dependent oxidative deamination of an amino acid fall into two classes, those that function with primary amines and those that function with secondary amines. The best studied examples of the primary amine dehydrogenases are glutamate (*15-19*) and alanine (*16*, *20*, *21*) dehydrogenases, while saccharopine dehydrogenase is the only secondary amine dehydrogenase (*22-24*) that was characterized with respect to its kinetic mechanism prior to this study.

The primary amine dehydrogenases catalyze a reversible oxidative deamination of an amino acid to give ammonia and an α-keto acid with NAD(P) serving as the oxidant. The kinetic mechanism of glutamate dehydrogenase (GDH) from bovine liver has been best studied, and has a random kinetic mechanism on the basis of steady state and pre-steady state studies and isotope effects (*15-19*). On the other hand the kinetic mechanism of alanine dehydrogenase from thermophilic *Bacillus sphaericus*, and *Bacillus subtilis*, is ordered (*20*, *21*).

Kinetic mechanisms of other amine dehydrogenases have also been reported. Leucine dehydrogenase from *Natronobacterium magaddi* (*25*), a halophilic thermophile, *Bacillus licheniformis* TSN9 (*26*), and *Bacillus stearothermophilus* (*27*) also have a sequential ordered kinetic mechanism. Phenylalanine dehydrogenase from *Thermoactinomyces* (*28*), *Rhodococcus maris* (*29*), and *Rhodococcus sp.* (*30*),

diaminopimelate dehydrogenase from *Bacillus sphaericus* (*31*), and valine dehydrogenase (which is specific for branched chain amino acid substrates) from *Streptomyces cinnamonensis* (*32*) all show a sequential ordered mechanism, with the exception of the valine dehydrogenase from *Alcaligenes faecalis* (*33*), which apparently has a random mechanism. Thus, although most of the enzymes from this class exhibit an ordered mechanism there is no consensus.

The kinetic mechanism of saccharopine dehydrogenase (L-Lysine forming) from *Saccharomyces cerevisiae*, catalyzes the final step in the lysine biosynthetic pathway in yeast and catalyzes the reversible oxidative deamination of saccharopine to generate α-Kg and lysine using NAD as an oxidant (*1*). The last two enzymes in the pathway, saccharopine reductase and saccharopine dehydrogenase bind the same substrate, saccharopine, and catalyze oxidation of adjacent bonds in the secondary amine. SR and SDH have little or no similarity in their primary, secondary, and tertiary structure, with the exception of the Rossman fold which binds the dinucleotide (*10*, *34*). The kinetic mechanism of the two enzymes is very similar, with ordered addition of NAD(P) and saccharopine and release of the reduced dinucleotide last. The addition of L-AASA and glutamate are ordered in the case of SR, while addition of α-Kg and lysine is random for SDH (*22*, *24* and this study).

2-5. Acknowledgements

We thank Dr. William E. Karsten and Dr. Babak Andi for cloning the gene encoding SR from *S. cerevisiae*.

References

1. Xu, H., Andi, B., Qian, J., West, A. H., and Cook, P. F. (2006) The α-aminoadipate pathway for lysine biosynthesis in fungi, *Cell Biochem. Biophys. 46*, 43-64.

2. Nishida, H., Nishiyama, M., Kobashi, N., Kosuge, T., Hoshino, T., and Yamane, H. (1999) A prokaryotic gene cluster involved in synthesis of lysine through the aminoadipate pathway: A key to the evolution of amino acid biosynthesis, *Genome Res. 9*, 1175-1183.

3. Broquist, H. P. (1971) Lysine biosynthesis (yeast), *Methods Enzymol. 17*, 112-129.

4. Ye, Z. H., and Bhattacharjee, J. K. (1988) Lysine biosynthesis pathway and biochemical blocks of lysine auxotrophs of *Schizosaccharomyces pombe, J. Bacteriol. 170*, 5968-5970.

5. Jaklitsch, W. M., and Kubicek, C. P. (1990) Homocitrate synthase from *Penicillium chrysogenum*. Localization, purification of the cytosolic isoenzyme, and sensitivity to lysine, *J. Biochem. 269*, 247-253.

6. Trupin, J. S., and Broquist, H. P. (1965) Saccharopine, an intermediate of the aminoadipic acid pathway of lysine biosynthesis. I. Studies in *Neurospora crassa, J. Biol. Chem. 240*, 2524-2530.

7. Johansson, E., Steffens, J. J., Lindqvist, Y., and Schneider, G. (2000) Crystal structure of saccharopine reductase from *Magnaporthe grisea*, an enzyme of the α-aminoadipate pathway of lysine biosynthesis, *Structure 8*, 1037-1047.

8. Garrad, R. C. and Bhattacharjee, J. K. (1992) Lysine biosynthesis in selected pathogenic fungi: characterization of lysine auxotrophs and the cloned *LYS1* gene of *Candida albicans*, *J. Bacteriol. 174*, 7379-7384.

9. Palmer, D. R., Balogh H., Ma, G., Zhou, X., Marko, M., and Kaminskyj, S. G. (2004) Synthesis and antifungal properties of compounds which target the alpha-aminoadipate pathway, *Pharmazie 59*, 93–98.

10. Andi, B., Cook, P. F., and West, A. H. (2006) Crystal structure of his-tagged saccharopine reductase from *Saccharomyces cereviciae* at 1.7Å resolution, *Arch. Biochim. Biophys. 46*, 243-254.

11. Storts, D. R., and Bhattacharjee, J. K. (1987) Purification and properties of saccharopine dehydrogenase (glutamate forming) in *Saccharomyces cerevisiae* lysine biosynthetic pathway, *J. Bacteriol. 169*, 416-418.

12. Jones, E. E., and Broquist, H. P., (1966) Saccharopine, an intermediate of the aminoadipic acid pathway of lysine biosynthesis. III. Aminoadipic semialdehyde-glutamate reductase, *J. Biol. Chem. 241*, 3430-3434.

13. Rodwell, V. W. (1971) δ-1-Piperdine-6-carboxylic acid and α-aminoadipic acid δ-semialdehyde, *Methods Enzymol. 17*, 188-199.

14. Viola, R. E., Cook, P. F., and Cleland, W. W. (1979) Stereoselective preparation of deuterated reduced nicotinamide adenine nucleotides and substrates by enzymatic synthesis, *Anal. Biochem. 96*, 334-340.

15. Cook, P. F., (1982) Kinetic studies to determine the mechanism of regulation of bovine liver glutamate dehydrogense by nucleotide efectors, *Biochemistry 21***,** 113-116.

16. Weiss, P. M., Chen, C. Y., Cleland, W. W. and Cook, P. F. (1988) Use of primary deuterium and ^{15}N isotope effects to deduce the relative rates of steps in the mechanisms of alanine and glutamate dehydrognases, *Biochemistry 27***,** 4814-4822.

17. Frieden, Carl, F. (1959) Glutamic dehydrogenase. The order of substrate addition in the enzymatic reaction, *J. Biol. Chem. 234*, 2891-2896.

18. Engel, P. C., and Dalziel, K. (1970) Kinetic studies of glutamate dehydrogenase. The reductive amination of 2-oxoglutarate, *Biochem. J. 118*, 409-419.

19. Colen, A. H., Prough, R. A., and Fisher, H. F. (1972) The mechanism of the glutamate dehydrogenase reaction. Evidence for random and rapid binding of substrate and coenzyme in the burst phase, *J. Biol. Chem. 247*, 7905-7909.

20. Ohshima, T., Sakane, M., Yamazaki, T., and Soda, K (1990) Thermostable alanine dehydrogenase from thermophilic *Bacillus sphaericus* DSM 462. Purification, characterization and kinetic mechanism, *Eur. J. Biochem. 191*, 715-720.

21. Grimshaw, C. E., and Cleland, W. W. (1981) Kinetic mechanism of *Bacillus subtilis* L-alanine dehydrogenase, *Biochemistry 20***,** 5650-5655.

22. Fujioka, M., and Nakatani, Y. (1970) A kinetic study of the saccharopine dehydrogenase reaction, *Eur. J. Biochem. 16*, 180-186.

23. Fujioka, M., and Nakatani, Y. (1972) Saccharopine dehydrogenase, interaction with substrate analogues, *Eur. J. Biochem. 25*, 301-307.

24. Xu, H., West, A. H., and Cook, P. F. (2006) Overall kinetic mechanism of saccharopine dehydrogenase from *Saccharomyces cerevisiae*, *Biochemistry 45*, 12156-12166.

25. Katoh, R., Ngata, S., Ozawa, A., Ohshima T., Kamekura, M., and Misono, H., (2003) Purification and characterization of leucine dehydrogenase from an alkaliphilic halophile *Natronobacterium magadii* MS-3, *Journal of Molecular Catalysis B*: *Enzymatic 23*, 231–238.

26. Nagata, S., Bakthavatsalam, S., Galkin, A. G., Asada, H., Sakai, S., Esaki, N., Soda, K., Ohshima, T., Nagasaki, S., and Misono, H. (1995) Gene cloning, purification, and characterization of thermostable and halophilic leucine dehydrogenase from a halophilic thermophile, *Bacillus licheniformi* TSN9, *Appl. Microbiol. Biotechnol. 44*, 432-438.

27. Ohshima, T., Misono, H., and Soda, K. (1978) Properties of crystalline leucine dehydrogenase from *Bacillus sphaericus*, *J. Biol. Chem. 253*, 5719-5725.

28. Ohshima, T., Takada, H., Yoshimura, T., Esaki, N., and Soda, K. (1991) Distribution, purification, and characterization of thermostable phenylalanine dehydrogenase from *Thermophilic actinomycetes*, *J. Bacteriol. 173*, 3943-3948.

29. Misono, H., Yonezawa, J., Nagata, S., and Nagasaki, S. (1989) Purification and characterization of a dimeric phenylalanine dehydrogenase from *Rhodococcus maris* K-18, *J. Bacteriol. 171*, 30-36.

30. Brunhuber, N. M. W , Thoden, J. B., Blanchard, J. S., and Vanhooke, J. L. (2000) *Rhodococcus* L-phenylalanine dehydrogenase: kinetics, mechanism, and structural basis for catalytic specifity, *Biochemistry 39*, 9174-9187.

31. Misono, H., and Soda, K., (1980) Properties of *meso*-α, ε-diaminopimelate D-dehydrogenase from *Bacillus sphaericus*, *J. Biol. Chem. 255*, *10599-10605*.

32. Priestley, N. D., and Robinson, J. A. (1989) Purification and catalytic properties of L-valine dehydrogenase from *Streptomyces cinnamonensis*, *Biochem. J. 261*, 853-861.

33. Ohshima, T. and Soda, K. (1993) Valine dehydrogenase from a non-spore-forming bacterium, *Alcaligenes faecalis*: purification and characterization, *Biochim. Biophys. Acta 1162*, 221-226.

34. Andi, B., Xu, H., Cook, P. F., and West, A. H. (2007) Crystal structures of ligand-bound saccharopine dehydrogenase from *Saccharomyces cerevisiae*, *Biochemistry 46*, 12512-12521.

CHAPTER 3

Chemical mechanism of saccharopine reductase

3-1. Introduction

L-Lysine is biosynthesized by the α-aminoadipate (AAA[1]) pathway in euglenoids and higher fungi such as basidiomycetes, and it is thus a potential target for the development of new antifungals (*1*). The presence of the AAA pathway has been reported in *Saccharomyces cerevisiae* (*2*), *Schizosaccharomyces pombe* (*3*), *Penicillium chrysogenum* (*4*), *Neurospora crassa* (*5*), and *Magnoporthe grisea*, which is a plant pathogen (*6*), and human pathogenic fungi including *Candida albicans* (*7*), *Aspergillus fumigatus* (*8*) and *Cryptococcus neoformans* (*7*). The amino acid sequence of saccharopine reductase (SR) is highly conserved in *S. cerevisiae*, *A. fumigatus*, *C. albicans* and *C. neoformans*. In order to develop mechanism-based inhibitors that may serve as lead compounds for new antifungal drugs, the kinetic and chemical mechanisms of the enzyme must be known.

The reductase (saccharopine dehydrogenase (L-glutamate forming), EC 1.5.1.10) catalyzes the penultimate step in the AAA pathway in yeast, the condensation of L-α-aminoadipate-δ-semialdehyde with L-glutamate to give an imine which is reduced by NADPH to give saccharopine (*6*).

Histidine-tagged SR from *Saccharomyces cerevisiae* has been overexpressed

in *Escherichia coli* and purified to about 98% using a Ni-NTA resin (*9*). An ordered kinetic mechanism has been proposed for SR on the basis of initial velocity studies in the absence and presence of product and dead-end inhibitors (*10*). The reduced dinucleotide substrate binds to enzyme first followed by L-α-aminoadipate-δ-semialdehyde (AASA), which adds in rapid equilibrium prior to L-glutamate; saccharopine is released prior to NADP. The pH optimum of SR from *S. cerevisiae* in the physiological reaction direction is 7.0 (*11*), while it is 9.5-9.75 in the direction of semialdehyde formation (*11, 12*).

Recently, a chemical mechanism was proposed for saccharopine dehydrogenase (L-lysine forming) from *Saccharomyces cerevisiae*, an enzyme that catalyzes a chemical reaction identical to that of the reductase, oxidative deamination of saccharopine, but at an adjacent bond (*16*). The structures of the two enzymes are dissimilar (*5, 9, 34*), and it is thus of interest to determine the chemical mechanism of SR, which has a different regiochemistry compared to SDH. In this chapter, we present a detailed analysis of the pH dependence of the kinetic parameters and solvent kinetic deuterium isotope effects of the saccharopine reductase. This is the first report of an acid-base chemical mechanism of a saccharopine reductase.

3-2. Materials and Methods

3-2-1. Chemicals and Enzymes

L-Saccharopine and L-glutamic acid were from Sigma. β-NADPH and β-NADP were purchased from USB. Mes, Mops, Ches and Hepes were obtained from

Research Organics. Deuterium oxide (99 atom % D) was purchased from Cambridge Isotope Laboratories, Inc. All other chemicals were of the highest grade available and were used as purchased.

Cell growth, expression, and SR purification were carried out as reported previously (*10*).

3-2-2. Enzyme assay

The SR reaction was monitored by the appearance or disappearance of NADPH at 340 nm (ε_{340}, 6220 $M^{-1}cm^{-1}$) using a Beckman DU-640 spectrophotometer. All assays were carried out in 500 μL total volume containing 200 mM buffer, and appropriate concentrations of substrates. The reaction was initiated by adding 10 μL of appropriately diluted enzyme, and all enzyme dilutions were made fresh for each set of experiments. All assays were carried out at 25 °C.

3-2-3. Initial Velocity Studies at pH 9.0

In order to determine whether the kinetic mechanism changes with pH, initial rate studies were carried out in the direction of formation of L-glutamate at pH 9.0. Initial rate data were collected as a function of NADP (0.02-0.5 mM) at different fixed concentrations of saccharopine (0.1-20 mM).

3-2-4. Inhibition Studies

Product and dead-end inhibition studies were carried out at pH 9.0 by

measuring the initial velocity with fixed substrates equal to their respective K_m values and varying the concentration of one substrate around its K_m value (0.5-5 K_m) at different fixed concentrations of the inhibitor including zero. First, an estimate of the inhibition constant of an inhibitor was obtained by measuring the initial rate as a function of the inhibitor concentration with all substrates fixed at their respective K_m values. The apparent K_i was then calculated from a plot of 1/υ vs. I with the apparent K_i value equal to the abscissa intercept. Product inhibition patterns were obtained using NADPH as a product inhibitor vs. NADP and saccharopine. Glyoxylate was chosen as a dead-end analog of saccharopine and dead-end inhibition patterns were obtained for glyoxylate vs. saccharopine and NADP.

3-2-5. pH Studies

The pH dependence of V and V/K for all reactants in both reaction directions was obtained by measuring the initial rate as a function of one reactant with all others maintained at saturation ($\geq 10K_m$ unless otherwise specified). The pH was maintained using the following buffers for the pH range indicated at a final concentration of 200 mM: Mes, 5.0-6.5; Mops, 6.5-7.5; Hepes, 7.5-8.5; Ches, 8.0-10.5. The pH was measured before and after the reaction and no significant change in pH was detected. In order to ensure that no effects of buffer were observed, data were obtained at the same pH when buffers were changed; no effects were observed. The enzyme is stable when incubated for at least 15 min over the pH range 5.0 to 10.5.

3-2-6. Solvent Deuterium Kinetic Isotope Effects

Initially, the pH and pD dependence of the kinetic parameters was measured and the isotope effect was estimated as the ratio of the pH(D) independent values. Solvent kinetic deuterium isotope effects were then measured by direct comparison of initial rates in H_2O and D_2O in the pH(D) independent range of the pH(D)-rate profiles (8.5-9.5). $^{D2O}V_2$ and $^{D2O}(V_2/K_{Sacc})$ were obtained by measuring the rate as a function of saccharopine with NADP maintained at saturation ($10K_m$). All substrates and buffers were initially dissolved in a small amount of D_2O and lyophilized to dryness. The dried substrates and buffers were then re-dissolved in D_2O to give the desired concentrations. The buffers were titrated to the desired pD using DCl or NaOD. The pD value was obtained by adding 0.4 to the pH meter reading (*13, 17*).

3-2-7. Proton Inventory

In the direction of glutamate formation, finite solvent deuterium kinetic isotope effects were observed, and proton inventory experiments were carried out to measure the solvent deuterium kinetic isotope effects more accurately and estimate the number of proton(s) in flight in the rate-determining transition state(s) (*35*). V_1/K_{Glu} was measured at pH(D) 7.0 in 100% H_2O, 20% D_2O, 40% D_2O, and 85% D_2O with glutamate as the variable substrate at fixed concentrations of NADPH (10 K_m) and AASA (5 K_m).

3-2-8. Effect of Solvent Viscosity

In order to determine whether the finite solvent deuterium isotope effect included an effect of increased solvent viscosity, 9 % glycerol (w/v) was used as the viscosogen, which generates the same relative viscosity as 100% D_2O at 25°C (*35*). For viscosity dependence studies with L-glutamate as a substrate, the *V* and *V*/*K* for L-glutamate were measured in the absence of glycerol and in the presence of 9% glycerol as a viscosogenic agent.

3-2-9. Primary Kinetic Deuterium Isotope Effects

The initial rate was measured as a function of L-glutamate with NADH(D) and α-AASA maintained at 0.7 mM (0.3K_m) and 10K_m, respectively. Saturation by NADH was not achieved, so the isotope effect on V/K_{Glu} was the only effect measured. All isotope effects were measured in triplicate, and the SEM is reported.

3-2-10. Data Analysis

Initial velocity data obtained in both reaction directions were fitted to eqs. 1 and 2 using the Enzfitter program from BIOSOFT, Cambridge, U.K., and programs developed by Cleland (*14*). Initial velocity data at pH 9.0 were fitted to eq. 3.

$$\upsilon = \frac{V\mathbf{A}}{K_a + \mathbf{A}} \tag{1}$$

$$\upsilon = \frac{V\mathbf{AB}}{K_{ia}K_b + K_b\mathbf{A} + K_a\mathbf{B} + \mathbf{AB}} \tag{2}$$

$$\upsilon = \frac{V\mathbf{AB}}{K_{ia}K_b + K_b\mathbf{A} + K_a\mathbf{B} + \mathbf{AB}\left(1 + \frac{\mathbf{B}}{K_{IB}}\right)} \quad (3)$$

In eqs 1, 2 and 3, υ and *V* are the observed initial rate and the maximum rate, respectively, **A** and **B** are substrate concentrations, K_a and K_b are Michaelis constants for substrates A and B, respectively, K_{ia} is the dissociation constant for the EA complex and K_{IB} is the substrate inhibition constant for B.

pH-rate profiles were generated by plotting log $V/\mathbf{E_t}$ and log $V/K\mathbf{E_t}$ values as a function of pH to assess data quality and to determine the appropriate rate equation for data fitting. pH rate-profiles that exhibited a slope of 1 at low pH and -1 at high pH were fitted using eq. 4, while those that exhibited a slope of 1 at low pH were fitted using eq. 5. pH-rate profiles with a slope of 1 at low pH and a slope of -2 at high pH were fitted by using eq. 6, or 7.

$$log\ y = log\left[C / \left(1 + \frac{\mathbf{H}}{K_1} + \frac{K_2}{\mathbf{H}}\right)\right] \quad (4)$$

$$log\ y = log\left[C / \left(1 + \frac{\mathbf{H}}{K_1}\right)\right] \quad (5)$$

$$log\ y = log\left[C / \left(1 + \frac{\mathbf{H}}{K_1} + \frac{K_2}{\mathbf{H}} + \frac{K_2K_3}{\mathbf{H}^2}\right)\right] \quad (6)$$

$$log\ y = log\left[C / \left(1 + \frac{\mathbf{H}}{K_1} + \frac{{K_0}^2}{\mathbf{H}^2}\right)\right] \quad (7)$$

In eqs 4-6, *y* is the observed value of the parameter (*V* or *V*/*K*) as a function of pH, *C* is the pH-independent value of *y*, **H** is the hydrogen ion concentration, $K_{1,}$ $K_{2,}$ and K_3 represent acid dissociation constants for functional groups on the reactant or enzyme required in a given protonation state for optimal binding and/or catalysis; K_0 is an average value for two acid dissociable groups.

The proton inventory data were fitted using the form of the Gross–Butler equation given in eq. 8 (*35*)

$$^{n}k = {}^{D_2O}k(1 - n + n\phi^{T})^{2} \quad (8)$$

In eq. 8, ^{n}k is the ratio of the rate constants (*V* or *V*/*K*) measured in different fractional concentrations of D_2O compared to 100% D_2O, ^{D2O}k is the solvent deuterium isotope effect, i.e., the ratio of the rate constants in 100% H_2O and 100% D_2O, *n* is the fractional concentration of D_2O, and ϕ^{T} is the fractionation factor for protons of import in the transition state.

3-3. Results

3-3-1. Initial velocity studies at pH 9.0

In order to determine whether the kinetic mechanism depends on pH, initial velocity patterns were obtained at pH 9.0. In the direction of glutamate formation the initial rate was measured as a function of saccharopine at different fixed concentrations of NADP. An intersecting pattern was obtained. Substrate inhibition

by saccharopine is observed that is uncompetitive vs. NADP. Data were fitted to eq. 3, and estimates of kinetic parameters are summarized in Table 3-1.

Product inhibition by NADPH is competitive vs. NADP and noncompetitive vs. saccharopine, consistent with addition of the cofactor to free enzyme. Glyoxylate is competitive vs. saccharopine and uncompetitive vs. NADP consistent with the ordered mechanism reported previously (*10*). Inhibition constants are summarized in Table 3-2.

3-3-2. pH Dependence of Kinetic Parameters

The pH dependence of kinetic parameters provides information on groups required in a given protonation state for optimum binding of reactant and/or catalysis (*17*). The pH dependence of kinetic parameters of the SR reaction was determined, and the results are shown in Figures 3-1 and 3-2. In the direction of saccharopine formation, V_1/E_t exhibits a slope of +1 at low pH with a pK_a of 5.7 and decreases at high pH with a pK_a of 7.9, Fig. 3-1A.

NADPH is the first reactant bound in an ordered mechanism, and $V_1/K_{NADPH}\mathbf{E_t}$ is the on-rate constant for NADPH binding to enzyme. The pH dependence of V_1/K_{NADPH} reflects groups important for binding the dinucleotide. The pH-rate profile has limiting slopes of +1 and -2, giving pK_a values of 6 on the acidic side, and an average pK_a of 8.2 on the basic side, Fig. 3-1B. The group with a pK_a of 6 likely reflects the 2'-phosphate of NADPH, which must be ionized for optimum binding (*36*)**.** The groups with an average pK_a of 8.2 likely represents an enzyme

group that must be protonated for optimum binding of the dinucleotide, probably interacting with the 2'-phosphate and the group observed in the $V_1/\mathbf{E_t}$ pH-rate profile, i.e., the protonation state of a catalytic group affects the binding of the nucleotide substrate. The $V_1/K\mathbf{E_t}$ for glutamate exhibits a slope of -2 at high pH, giving pK_as of 7.8 and 8.5 and a slope of 1 on the acid pH side with a pK_a of 5.6, Fig. 3-1C. The pK_a of 7.8 likely reflects the same enzyme side chain observed in the $V_1/\mathbf{E_t}$ pH-rate profile important for catalysis and/or binding and this will be considered in detail in the Discussion section. pK_a values are summarized in Table 3-3. Estimates of the pH-independent values of the kinetic parameters are as follows: $V_1/\mathbf{E_t}$, 1.9 ± 0.1 s^{-1},

Table 3-1: Kinetic Parameters for SR in the Direction of AASA Formation at pH 7.0 and 9.0

	pH 9	pH 7[a]
$V_2/\mathbf{E_t}$ (s^{-1})	13 ± 1	1.06 ± 0.02
$V_2/K_{NADP}\mathbf{E_t}$ ($M^{-1}s^{-1}$)	(8.5 ± 1.2) x 10^4	(5.67 ± 0.01) x 10^3
$V_2/K_{Sacc}\mathbf{E_t}$ ($M^{-1}s^{-1}$)	(1.7 ± 0.3) x 10^4	(1.6 ± 0.3) x 10^2
K_{NADP} (mM)	0.15 ± 0.01	0.187 ± 0.006
K_{Sacc} (mM)	0.77 ± 0.12	6.6 ± 0.2
K_{iNADP} (mM)	Undefined	0.020 ± 0.004
K_{ISacc} (mM)	12 ± 2	

[a] from ref. (*10*).

$V_1/K_{NADPH}\mathbf{E_t}$, (7.1 ± 0.5) x 10^4 $M^{-1}s^{-1}$, and $V_1/K_{Glu}\mathbf{E_t}$, (52 ± 5) $M^{-1}s^{-1}$.

In the direction of AASA formation, $V_2/\mathbf{E_t}$ decreases at low pH with a limiting slope of +1 giving pK_a value of 7.2, Fig. 3-2A. $V_2/K_{NADP}\mathbf{E_t}$ decreases at high and low pH with limiting slopes of -1 and +1, giving pK_a values of 10.6 and, 6.2 Fig. 3-2B. $V_2/K_{Sacc}\mathbf{E_t}$ also decreases at low and high pH giving pK_a values of 7.6 and 9.9, Fig. 3-2C. pK_a values are summarized in Table 3-3. The pH-independent values of kinetic parameters are as follows: $V_2/\mathbf{E_t}$, 7.8 ± 0.4 s^{-1}, $V_2/K_{NADP}\mathbf{E_t}$, (2.0 ± 0.2) x 10^4 $M^{-1}s^{-1}$, and $V_2/K_{Sacc}\mathbf{E_t}$, (2.9 ± 0.5) x 10^4 $M^{-1}s^{-1}$.

Table 3-2: Summary of Product and Dead End Inhibition Data for SR at pH 9.0 in the Direction of AASA Formation

Varied Substrate	Fixed substrate	Inhibitor	K_{is} (mM)	K_{ii} (mM)	Inhibition Pattern Observed
NADP	Saccharopine (K_m)	NADPH	0.027 ± 0.001	N/A	C
Saccharopine	NADP (K_m)	NADPH	0.12 ± 0.02	0.20 ± 0.03	NC
Saccharopine	NADP (K_m)	Glyoxylate	14 ± 2	N/A	C
NADP	Saccharopine (K_m)	Glyoxylate		15 ± 1	UC

N/A is not applicable.

3-3-3. Primary Kinetic Deuterium Isotope Effect with NADH a Slow Substrate

The primary deuterium kinetic isotope effects on V and V/K_{Glu}, obtained with NADPH(D) are 1 and 0.87 respectively, (*10*). In order to obtain an estimate of the rate of the catalytic steps with the natural substrates, the isotope effect on the hydride transfer step was measured with the slow substrate, NADH(D). An estimate of $V_1/K_{NADH}.\mathbf{E_t}$ was obtained by measuring the initial rate as a function of NADH concentration with AASA and glutamate fixed at $10K_m$. K_{NADH} is high and saturation was not attained. The $V_1/K_{NADH}\mathbf{E_t}$ is (24 ± 0.9) $M^{-1}s^{-1}$. The ratio of $V_1/K_{NADPH}\mathbf{E_t}$ and $V_1/K_{NADH}\mathbf{E_t}$ at pH 7.0 is (2.9 ± 0.2) x 10^4. The isotope effect on V_1/K_{Glu} at pH 7.0 is 1.9 ± 0.7.

Table 3-3: Summary of pK_a values for SR

Parameter	pK_1	pK_2	pK_3
	Forward Reaction		
V_1	5.7 ± 0.2	7.9 ± 0.1	
V_1/K_{NADPH}	6.0 ± 0.2	8.2 ± 0.1[a]	
V_1/K_{Glu}	5.6 ± 0.1	7.8 ± 0.1	8.5 ± 0.2
	Reverse Reaction		
V_2	7.2 ± 0.1		
V_2/K_{NADP}	6.2 ± 0.1	10.6 ± 0.1	
V_2/K_{Sacc}	7.6 ± 0.1	9.9 ± 0.2	

[a] **Average value.**

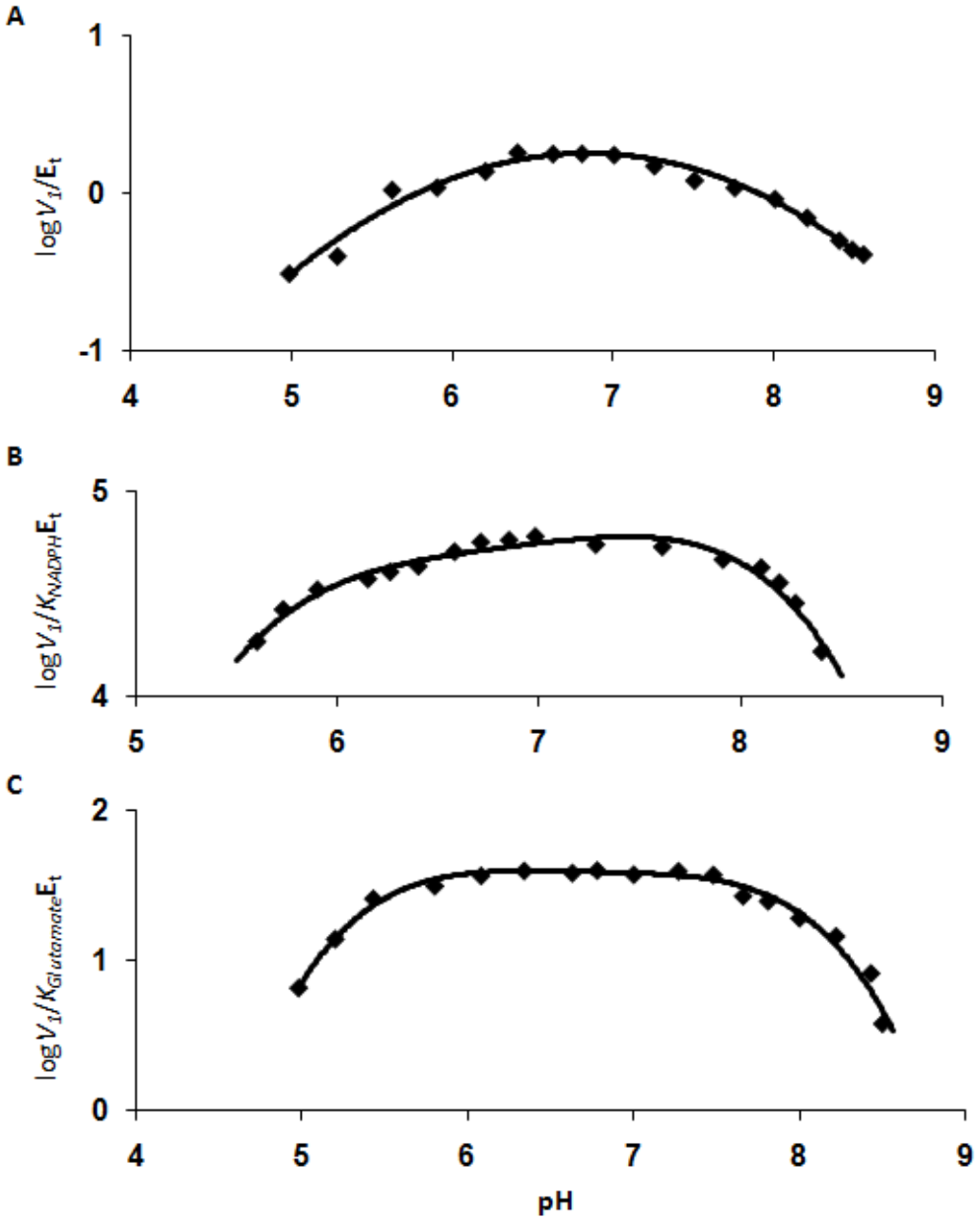

Figure 3-1: pH dependence of kinetic parameters in the direction of saccharopine formation. pH dependence of: A. V_1/E_t; B. $(V_1/K_{NADPH})E_t$; C. $(V_1/K_{Glu})E_t$. All data were obtained at 25°C. Points are experimental, while curves are based on a fit of the data to eq. 4 for (A), eq. 7 (B) or eq. 6 for (C).

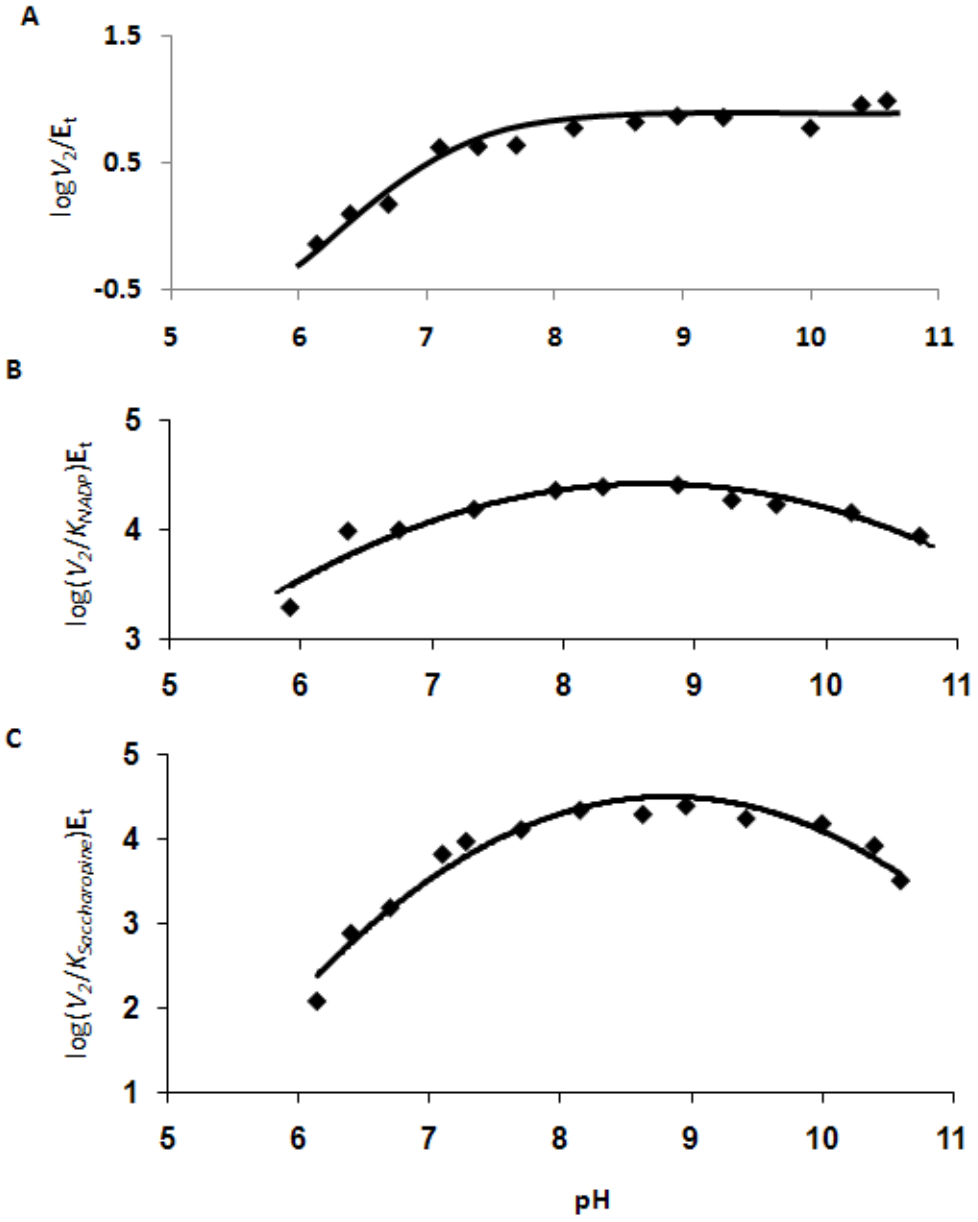

Figure 3-2: pH dependence of kinetic parameters in the direction of glutamate formation. pH dependence of: A. V_2/E_t; B. $(V_2/K_{NADP})E_t$; C. $(V_2/K_{Sacc})E_t$. All data were obtained at 25°C. Points are experimental, while curves are based on a fit of the data to eq. 5 (A) or 4 (B, C).

3-3-4. Effect of Solvent Deuterium and Viscosity

Initial rates were measured at saturating NADP, varying saccharopine over the pH(D) range 6.5-10.5, Fig. 3-3. Solvent isotope effects were calculated as the ratio of the pH(D) independent values of V_2 and V_2/K_{Sacc}. Equal values of 1.8 ± 0.1 were obtained for $^{D2O}V_2$ and $^{D2O}V_2/K_{Sacc}$.

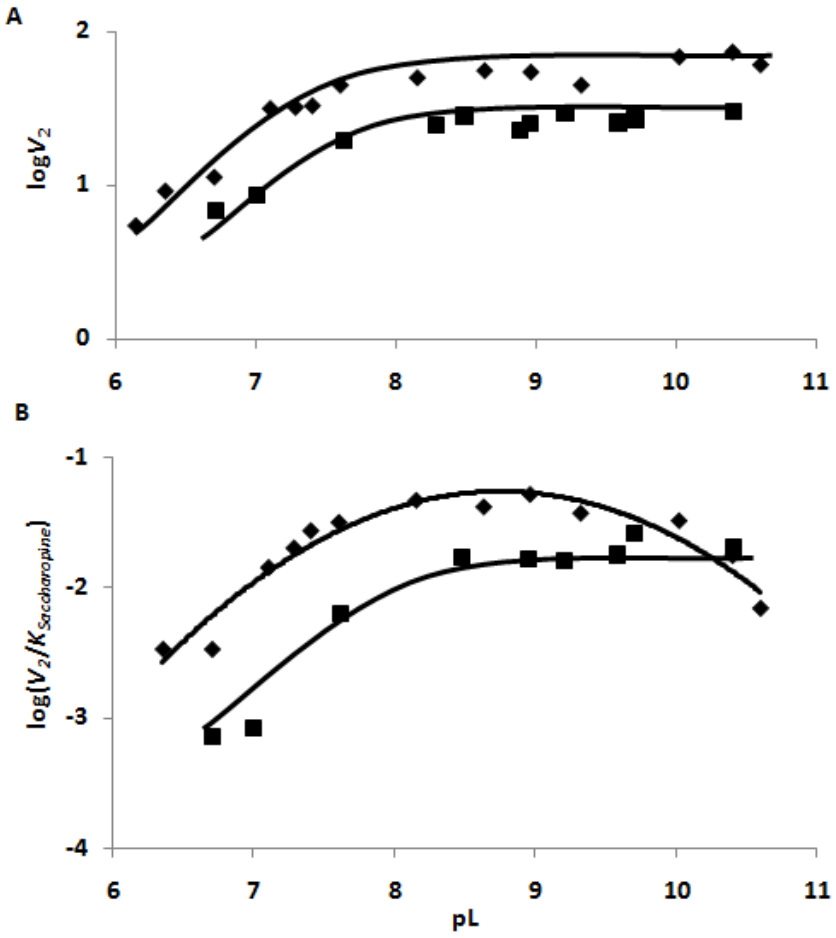

Figure 3-3: pH(D) dependence of V_2/E_t and $(V_2/K_{Sacc})E_t$ at 25 °C in the direction of glutamate formation. A. V_2/E_t vs. pL (pH or pD) in H_2O (♦) and in D_2O (■). B. $(V_2/K_{Sacc})E_t$ in H_2O (♦) and D_2O (■). Points are experimental, while curves are based on a fit of the data to eq. 5 (A) and eq. 4 (B).

Glycerol was used as a viscosogen for SR. The ratio of the values of V_1 and V_1/K_{Glu} determined in H_2O and at a relative viscosity of 1.24 are within error equal. Therefore, the values of the observed solvent isotope effects, $^{D2O}V_2$ and $^{D2O}(V_2/K_{sacc})$, result from a classical isotope effect and not from an effect of the increased viscosity of 100% D_2O.

3-3-5. Proton Inventory

A proton inventory is obtained from the change in V/K_{Glu} with the concentration of D_2O. At pH(D) 7.0, the proton inventory is shown in Figure 4. The proton inventory is nonlinear and can be best described as concave upward. A fit of the Gross-Butler equation to the data gives $^{D2O}k = 1.72 \pm 0.07$, within error equal to that estimated from the pH(D) profiles, and $\phi^T = 0.70 \pm 0.04$ for the two protons in the rate-determining transition state in the reaction catalyzed by SR in the direction of saccharopine formation.

3-4. Discussion

3-4-1. Initial Velocity Studies at pH 9.0

In the direction of saccharopine oxidative deamination, a double reciprocal plot of initial rate vs. saccharopine concentration at different fixed levels of NADP exhibits substrate inhibition by saccharopine that is uncompetitive vs. NADP. The substrate inhibition suggests binding of saccharopine to the E-NADPH complex which builds up in the steady state; K_{ISacc} is 12 mM. Substrate inhibition by

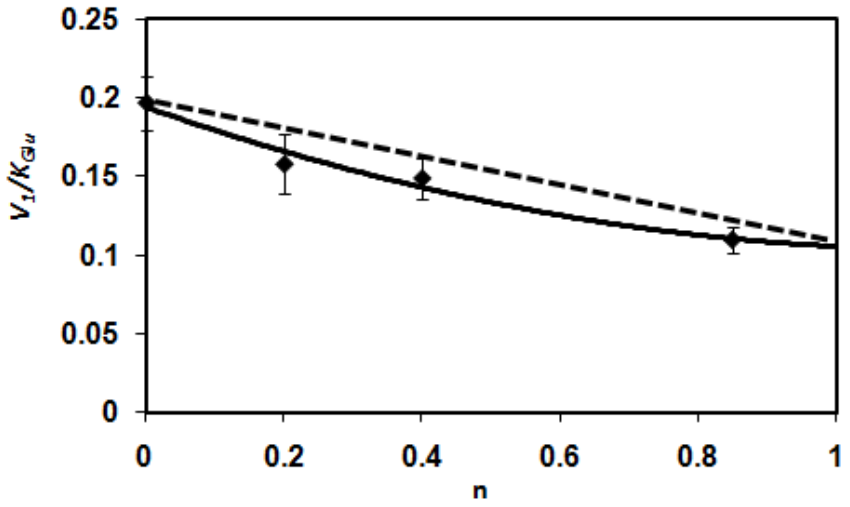

Figure 3-4: Proton Inventory. Dependence of (V_1/K_{Glu}) on the fraction of deuterium (n) in solvent. Velocities were measured at a pH(D)-independent value of 7.0 in 100% H_2O, 20% D_2O, 40% D_2O, and 85% D_2O. Points are experimental values, and the curve is drawn through predicted values. The dotted line is theoretical for a linear proton inventory.

saccharopine is complete since the initial rate tends to zero as the substrate concentration tends to infinity. Values of $V_2/K_{NADP}\mathbf{E_t}$ and $V_2/K_{sacc}\mathbf{E_t}$ are 8.5 x 10^4 $M^{-1}s^{-1}$ and 1.7 x 10^4 $M^{-1}s^{-1}$, lower than the diffusion limited rate constant of 10^8-10^9 $M^{-1}s^{-1}$, suggesting little, if any limitation by diffusion.

Product inhibition by NADPH is competitive vs. NADP and noncompetitive vs. saccharopine, suggesting NADP is the first substrate to add to enzyme followed by saccharopine, which adds to the E-NADP binary complex. In agreement, glyoxylate, a dead-end analog of saccharopine, is competitive against saccharopine and uncompetitive vs. NADP, indicating binding to the E-NADP complex. Overall, data are consistent with the ordered mechanism reported at pH 7.0 (*10*). As suggested above, the uncompetitive substrate inhibition by sacharopine suggests release of NADPH contributes to rate limitation at pH 9.0 in the direction of

glutamate formation. An estimate of the contribution can be obtained from the difference in pK_a values of $V_2/\mathbf{E_t}$ and $V_2/K_{Sacc}\mathbf{E_t}$. The pK_a observed for $V_2/K_{Sacc}\mathbf{E_t}$ is likely close to the intrinsic pK_a, for an enzyme side chain (see below, Interpretation of pH Dependence of Kinetic Parameters). The pK_a observed in the $V_2/\mathbf{E_t}$ pH-rate profile is perturbed to lower pH by about 0.4 pH units. The perturbation of the pK_a is dependent on the ratio of the net rate constant of the chemical steps to the rate constant for release of NADPH; app pK_a = pK_a -log (1+$k_{chem}/k_{offNADPH}$) (*15*). A value of 1.5 is estimated for $k_{chem}/k_{offNADPH;}$ suggesting the release of NADPH is 1.5 times slower than the rate of the chemical step. This would give a value of about 8 mM for the K_I for saccharopine substrate inhibition corrected to 100% E:NADPH.

3-4-2. Interpretation of Solvent Deuterium Kinetic Isotope Effects

Isotope effects were previously measured using NADPH(D) in the direction of saccharopine formation (*10*). A value near unity was observed for $^{D}V_1$, while an inverse effect of about 0.87 was observed for $^{D}(V_1/K_{Glu})$. Data were interpreted in terms of a slow release of products, including saccharopine. A primary deuterium isotope effect of 1.9 ± 0.7 is estimated on V_1/K_{Glu} using NADH(D). Although not well defined, a finite normal isotope effect is observed.

Solvent isotope effects probe proton transfer in chemical reactions. As a result, solvent isotope effects were measured for the SR reaction in the direction of AASA formation as the ratio of the pH(D) independent values in the pH(D) rate profiles. It is important to note that equilibrium solvent deuterium isotope effects are

observed on the pK_a values of acid dissociable groups of oxygen or nitrogen containing acids and bases that result in an increase in the pK_a by 0.4-0.6 pH units (*35*). As seen in Fig. 3, the expected shift in the pK_a is observed reflecting the equilibrium isotope effect, and in addition, the pH independent value is lower in D_2O than in H_2O, indicating a kinetic isotope effect. A normal effect of 1.8 is observed on V_2 and V_2/K_{Sacc}. The change in solvent viscosity that results from substitution of D_2O for H_2O can account for solvent isotope effects (*37, 38*). Kinetic parameters at increased viscosity are identical, within error, to those observed in H_2O, strongly suggesting the isotope effects are not a consequence of the change in solvent viscosity. The finite solvent isotope effect and concave upward proton inventory are consistent with the rate determining conformational change to open the site and release products. An estimate of the number of protons important to the overall reaction and the number of proton transfer steps that contribute to rate limitation can be obtained from the proton inventory method (*35*). If a single proton is transferred in the rate-limiting transition state, a plot of the rate constant versus atom fraction of deuterium (n) will be linear. If more than one proton is transferred in a single transition state, the plot will be concave upward, while if protons are transferred in multiple transition states, the plot will be concave downward. A concave upward proton inventory is observed for V_1/K_{Glu}, suggesting that more than one proton is transferred in a single transition state. The reaction catalyzed by SR involves two protons and these protons have identical fractionation factors, suggesting equal contributions to the transition state for both protons (Attempts to fit the data to other

forms of the Gross-Butler equation, e.g., allowing the fractionation factors for both protons to be independent, failed). Data suggest a proton transfer is involved in the rate-limiting step in the reaction. Given the results with NADPH(D), the step(s) must involve the conformational change to open the site and release products.

3-4-3. Interpretation of pH Dependence of Kinetic Parameters

The maximum rate, *V,* is obtained at saturating concentrations of all substrates, and the dominant enzyme form will depend on the location of the slow step(s). As suggested above, the slow step occurs after the chemical steps and accompanies product release. The *V*/*K* for a reactant is obtained at limiting concentrations of one of the reactants and saturating levels of all others, and free substrate and the enzyme form to which the substrate binds are dominant in the steady state. The *V* profile reflects groups required in a given protonation state for catalysis, while the *V*/*K* profile will reflect the protonation state of groups on reactant and/or enzyme responsible in a given protonation state for binding and/or catalysis (*17*). In an ordered mechanism, the *V*/*K* for all of the reactants with the exception of the last one to add is the on rate constant for binding reactant to enzyme, and its pH dependence will thus reflect groups important for binding.

In the direction of saccharopine formation, the free enzyme and NADPH predominate for the V_1/K_{NADPH} profile, while E-NADPH-AASA and glutamate predominate for the V_1/K_{Glu} profile. However, AASA adds in rapid equilibrium prior to glutamate, and as a result K_{AASA} is zero and thus a V_1/K_{AASA} profile was not

obtained. In the non-physiologic reaction direction, the free enzyme and NADP predominate for the V_2/K_{NADP} profile, while E-NADP and free saccharopine dominate for the V_2/K_{Sacc} profile, and the enzyme form that precedes the slow step(s) at saturating substrates dominates for the V_2 pH-rate profile.

The V_1/K_{NADPH} exhibits the requirement for a group with a pK_a of 6 that must be unprotonated and two groups with an average pK_a of 8.2 that must be protonated for optimum binding of NADPH. The V_2/K_{NADP} reflects the need for a group with a pK_a of 6.2 that must be unprotonated, and a second group with a pK_a of 10.6 required protonated for optimum binding of NADP. The ionization state of the 2'-phosphate of NADP(H) is often an important binding determinant for NADP-dependent enzymes, e.g., as seen for glutathione reductase (*39*). In agreement, the *V*/*K* for NADH is 10^4-fold lower than that of NADPH. The pK_a of the 2'-phosphate is 6.1 (*36*), within error identical to the pK_a of 6-6.2 observed in the V_1/K_{NADPH} and V_2/K_{NADP} pH-rate profiles. A group that must be protonated is observed in the pH-rate profile of V_2/K_{NADP}, with pK_a value of 10.6. An arginine (R34) is within hydrogen-bonding distance to the 2'-phosphate of the dinucleotide substrate, Fig. 5 (*6*, *9*). The group with a pK_a of 10.6 observed in the V_2/K_{NADP} pH-rate profile may reflect R34, which forms a salt bridge with the 2'-phosphate. One of the groups with an average pK_a of about 8.2 observed in the V_1/K_{NADPH} pH-rate profile that must be protonated is likely the same group seen in the V_1 and V_1/K_{Glu} pH-rate profiles, and this will be discussed below under *Proposed Chemical Mechanism*. The function of the second group with a pK_a of 8.2 is not known. If the pH-rate profile could be

extended to higher pH, the group with a pK_a of 10.6, thought to reflect R34, should also be observed.

The V_1/K_{Glu} profile exhibits the requirement for groups with pK_as of about 7.8 and 8.5 that must be protonated, and a group with a pK_a of 5.6 that must be unprotonated for optimum binding and catalysis. The group with a pK_a of 7.8 is also observed in the V_1 pH-rate profile, and likely reflects the catalytic general acid group, which protonates the carbonyl oxygen of AASA as the carbinolamine is formed upon attack by the α-amine of glutamate. In agreement, a group on enzyme with a pK_a of 7.2-7.6 is observed in the V_2 and V_2/K_{Sacc} pH-rate profiles that must be unprotonated for catalysis in the direction of glutamate formation. In the reverse reaction direction the group activates H_2O as it attacks the imine carbon formed upon oxidation of saccharopine and thus must be unprotonated. In the non-physiologic reaction direction (formation of glutamate), the observed pK_a in the V_2/K_{Sacc} pH-rate profile is 7.6, probably the intrinsic pK_a for the catalytic group, is perturbed to higher pH in the opposite direction (V_1/K_{Glu} pH-rate profile). It is possible that the group responsible is D125, which is in the vicinity of the saccharopine secondary amine in the structure of the E-NADPH-saccharopine complex of SR from *Magnaporthe grisea*, a closely related homolog of the *S. cerevisiae* SR (*6*). This residue is completely conserved in SR amino acid sequences from fungi including *S. cerevisiae* and human pathogenic fungi such as *Candida albicans* (*7*), *Aspergillus fumigatus* (*8*) and *Cryptococcus neoformans* (*7*).

The group with a pK_a of 5.6, observed in the V_1/K_{Glu} and V_1 pH-rate profiles

is likely a base required to accept a proton from the α-amine of glutamate prior to its nucleophilic attack on the semialdehyde carbonyl. One would also expect to see this group in the V_2/K_{Sacc} pH-rate profile if it could be extended to lower pH, since the same group is responsible for accepting a proton from the saccharopine secondary amine. The identity of this group is at present unknown.

The V_2/K_{Sacc} pH-rate profile exhibits a pK_a of 9.9, while the V_1/K_{Glu} pH-rate profile exhibits a pK_a 8.5. These groups are not observed in V_2 or V_1 pH-rate profiles, and thus reflect binding groups for saccharopine and glutamate, respectively. The pK_a value of the secondary amino group of saccharopine is 10.1 (*16*), while the pK_a of the α-amine of glutamate is about 9.5 (*36*). Thus, the additional binding groups likely reflect the substrate amine pK values, suggesting they must be protonated for optimum binding.

It is also possible that substrates bind with their amine unprotonated, and that they are in reverse protonation state with an enzyme group, i.e., although the pK_a is observed on the basic side, the group must be unprotonated for optimum binding, while the group observed on the acid side must be protonated (*15*). Data are not in agreement with this suggestion. Reverse protonation may work in the direction of saccharopine formation since pK_a values are observed on the acid and base sides of the V_1/K_{Glu} pH-rate profile and a general acid catalyst is required in this reaction direction. However, in the opposite reaction direction, reverse protonation states would require that the saccharopine secondary amine is unprotonated and the enzyme group is protonated. Since a general base is required in this reaction

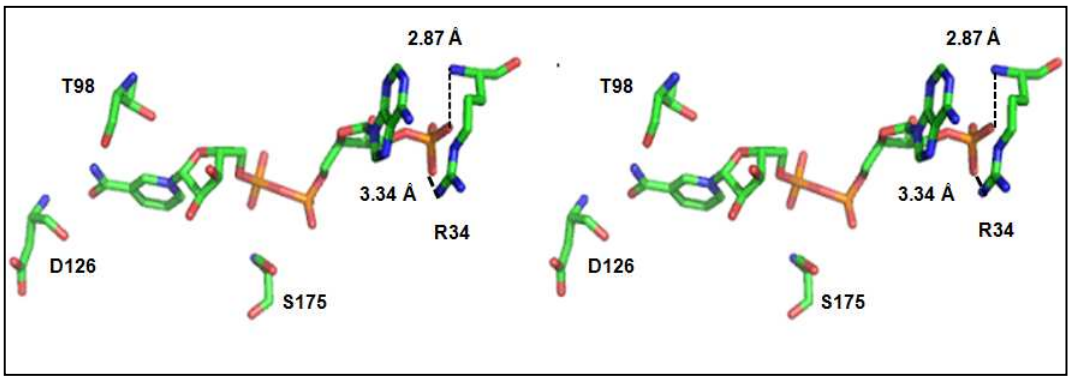

Figure 3-5: Stereo view of a close-up of the saccharopine reductase from *M. grisea* (PDB code 1E5Q) binding site for NADP(H). Residues that interact with the cofactor and their hydrogen-bonding distances are shown. The following color scheme is used: C, green, O, red, N, blue; and P, orange. This figure was generated using the PyMOL molecular visualization program (website: http:// pymol.Sourcefor ge.net/).

direction, data are not in agreement with reverse protonation states. Thus, the α-amine of glutamate and the secondary amine of saccharopine must be protonated for appropriate binding and catalysis and an enzyme group must act as a base to accept a proton prior to reaction. The only group observed on the acid side of the V_1/K_{Glu} pH-rate profile is the one with a pK_a of 5.6.

3-4-4. Proposed Chemical Mechanism of Saccharopine Reductase

On the basis of the pH-rate profiles, an acid-base chemical mechanism is proposed as shown in Scheme 3-1. The reaction begins with all reactants bound (I), which requires the α-amine of L-glutamate protonated (Fig. 3-6), and NADPH bound with its 2'-phosphate ion paired with R34 on enzyme (Fig. 3-5). As seen in Fig. 3-6, the α-carboxylates of L-glutamate and AASA are within hydrogen bond distance to arginine residues, while the γ-carboxylate of L-glutamate is within hydrogen bond

distance to a tyrosine and serine. An enzyme group with a pK_a of 5.6-5.7, B_2, accepts a proton from the α-amine of glutamate to generate the neutral amine that can act as a nucleophile (II). The α-amine of glutamate attacks the carbonyl of the semialdehyde to generate the carbinolamine, which is protonated by a second enzyme group with a pK_a of about 7.8-8, B_1, which may be D125 (III). The distance between the closest oxygen of D125 and the 2^o amine nitrogen of saccharopine is long enough (5.57 Å) to accommodate a water molecule. The protonation state of this group apparently affects the binding of NADPH, but not NADP, since it is observed in the V_1/K_{NADPH} pH-rate profile. The reason for the effect on NADPH binding is not obvious, but may reflect optimizing the conformation of the Michaelis complex.

A proton is accepted from the carbinolamine (III), to give the neutral carbinolamine (IV), which can then collapse, expelling water with a proton donated by B_1 (V). NADPH reduces the imine, generating the unprotonated secondary amine (VI), which is protonated by B_1 (VII), and saccharopine is released. On the basis of the finite solvent deuterium kinetic isotope effect, the release of saccharopine may be coupled to a conformational change accompanying proton transfer to the secondary amine nitrogen. The proposed mechanism is now being tested using site-directed mutagenesis. An important question is the identity of the general acid that accepts a proton from the α-amine of glutamate.

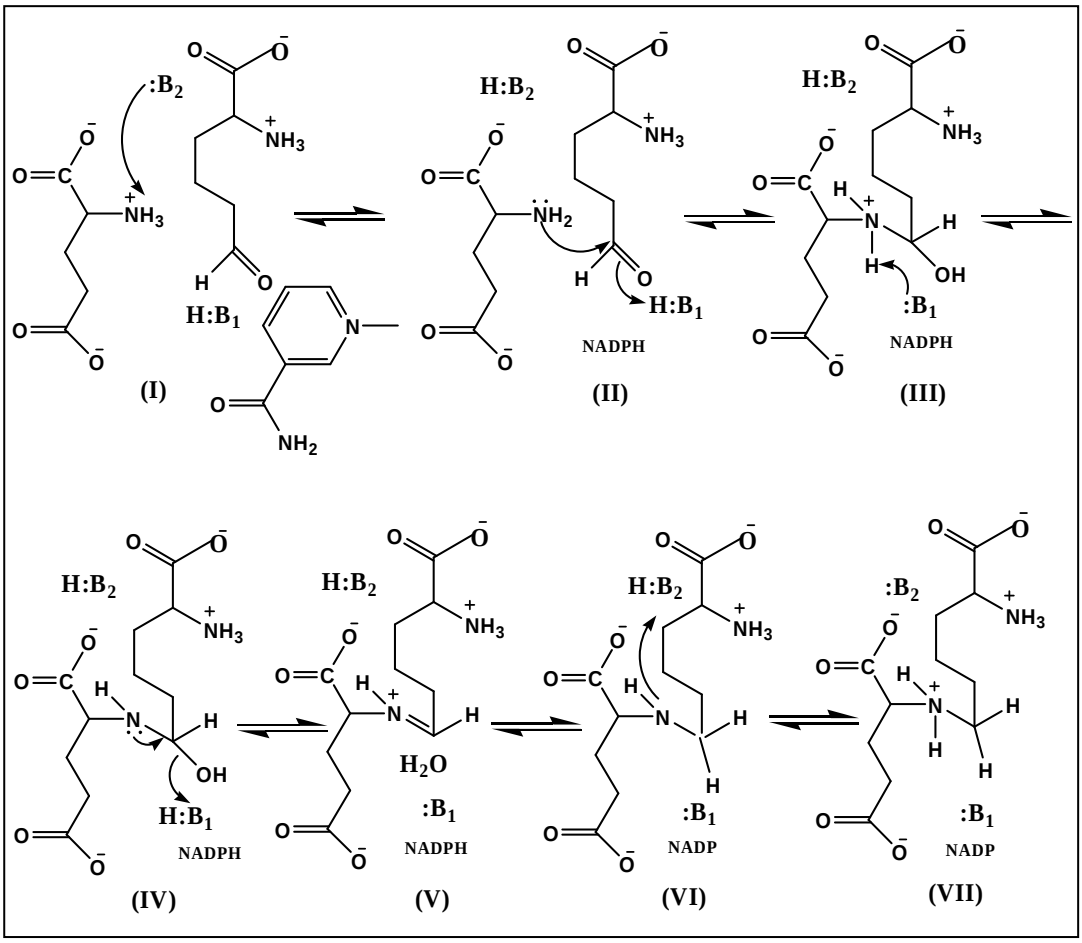

Scheme 3-1: Proposed Chemical Mechanism for Saccharopine Reductase. I, the central E-NADPH-AASA-glutamate complex formed upon binding of substrates; II, production of the neutral amine of glutamate, which acts as a nucleophile attacking the carbonyl of the semialdehyde; III, protonated carbinolamine intermediate; IV, neutral carbinolamine intermediate; V, the protonated imine intermediate; VI, neutral L-saccharopine formed upon hydride transfer from NADPH; and VI, protonated saccharopine.

3-4-5. Comparison to Other NAD(P)-dependent Oxidative Deaminases

The enzymes that are involved in pyridine nucleotide-dependent oxidative deamination reactions can be roughly divided into two classes, those that carry out the oxidative deamination of primary amines and those that function with secondary amines. Of the primary amine dehydrogenases, glutamate (*18-22*) and alanine (*19,*

23, *24*) dehydrogenases are well studied. However, the closest relative to SR is saccharopine dehydrogenase (SDH), which catalyzes the reaction following that catalyzed by SR and results in the formation of lysine and saccharopine. Indeed, the reaction chemistry is identical and occurs at a C-N bond adjacent to the C-N bond formed by SR (*1*). The SDH from *S. cerevisiae* was the only secondary amine dehydrogenase that has been characterized with respect to its chemical mechanism prior to this study (*16*, *25*-*27*). The mechanism of the closely related SDH will be considered first.

Saccharopine is a common substrate for the last two enzymes of the AAA pathway and as suggested above SR and SDH differ in their regio-chemistry. In spite of the two enzymes having virtually no identity in their primary, secondary, and tertiary structure (*9*, *34*), they catalyze the same reaction. Both enzymes utilize the same general acid-base catalytic strategy to catalyze their reaction. Beginning with saccharopine and NAD(P), the enzymes both utilize two bases to catalyze the reaction. In both cases the secondary amine of saccharopine must be protonated for optimum binding and reaction, as is true for the α-amine of glutamate (SR) and the ε-amine of lysine (SDH). A second base carries out most of the chemistry in both cases, i.e., beginning with sacchaopine, hydrolysis of the imine formed upon oxidation. The identity of the catalytic groups in SDH has not yet been determined, but there is no paucity of groups in the active site and in proximity to reactants that can serve in this capacity. On the other hand, there are no obvious candidates, other than D125, that can serve as a catalyst in the active site of SR. In addition, chemistry

contributes to rate limitation in SDH, while product release limits the SR reaction.

α-Amino acid dehydrogenases, such as glutamate and alanine dehydrogenase generate ammonia, a α-keto acid, and reduced pyridine dinucleotide as products of the oxidative deamination reaction (*28*). The glutamate dehydrogenases (GDH) from bovine liver and *Chlorella sorokiniana* have been studied, and an acid-base chemical mechanism has been proposed on the basis of pH-rate and pK_i profiles (*29*, *30*). Chemical mechanisms of other amine dehydrogenases, including alanine dehydrogenase from *Bacillus subtilis* (*31*), L-phenylalanine dehydrogenase from *Rhodococcus* sp. M4 (*32*), and leucine dehydrogenase from *Bacillus stearothermophilus* (*33*) have also been studied.

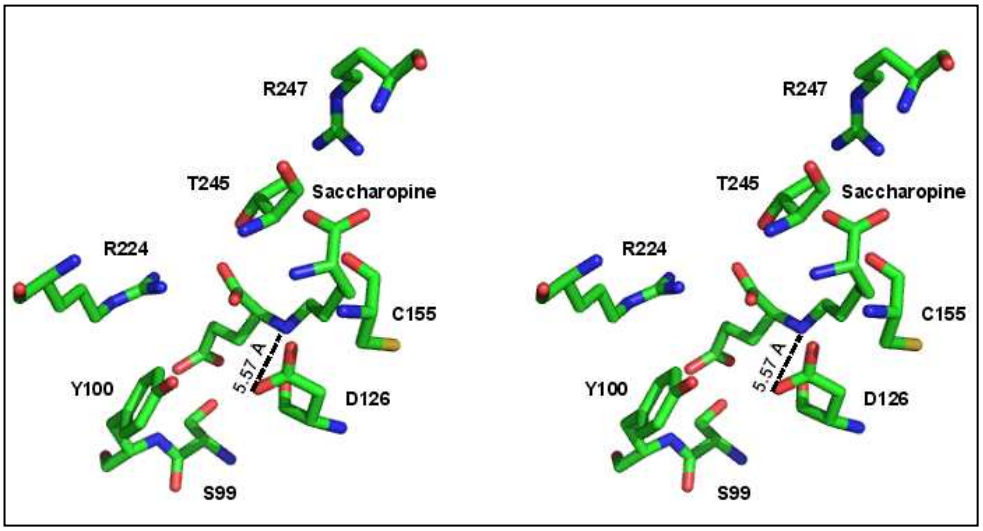

Figure 3-6: Stereo view of a close-up of the active site of saccharopine reductase from *M. grisea* (PDB code 1E5Q). Residues that interact with saccharopine and their hydrogen-bonding distances are shown. Colors are as in the legend to Fig. 3-5. This figure was generated using the PyMOL molecular visualization program.

The chemical mechanisms of the above primary amine dehydrogenases are very similar to one another. They all employ general acid-base catalysis and the chemical mechanisms are similar overall, and very similar to the strategy utilized by the secondary amine dehydrogenases. The main difference between the two classes of dehydrogenase is the protonation state of the α-amine of the substrate, glutamate or alanine. The secondary amine dehydrogenases bind saccharopine with its secondary amine protonated, while the primary amine dehydrogenases selectively bind reactant with a neutral amine (*29*, *31*). Oxidation generates the protonated imine, which is attacked by water, activated by an active site lysine. The same group then functions to generate the ammonia and ketone products. The neutral ammonia is then released, opposed to the protonated α-amine of glutamate or lysine in the secondary amine dehydrogenases. Another difference in the primary amine dehydrogenases is the identity of the acid-base catalyst. L-Glutamate (*29*) and phenylalanine (*32*) dehydrogenases utilizes a lysine as the base, while alanine dehydrogenase uses a histidine (*31*). The identity of the base may also differ in the secondary amine dehydrogenases, but this will have to await additional studies that are now in progress.

3-5. Acknowledgments

We thank Dr. William E. Karsten and Dr. Babak Andi for cloning the gene encoding SR from *S. cerevisiae*.

References

1. Xu, H., Andi, B., Qian, J., West, A. H., and Cook, P. F. (2006) The α-aminoadipate pathway for lysine biosynthesis in fungi, *Cell Biochem. Biophys. 46*, 43-64.

2. Broquist, H. P. (1971) Lysine biosynthesis (yeast), *Methods Enzymol. 17*, 112-129.

3. Ye, Z. H., and Bhattacharjee, J. K. (1988) Lysine biosynthesis pathway and biochemical blocks of lysine auxotrophs of *Schizosaccharomyces pombe*, *J. Bacteriol. 170*, 5968-5970.

4. Jaklitsch, W. M., and Kubicek, C. P. (1990) Homocitrate synthase from *Penicillium chrysogenum*. Localization, purification of the cytosolic isoenzyme, and sensitivity to lysine, *J. Biochem. 269*, 247-253.

5. Trupin, J. S., and Broquist, H. P. (1965) Saccharopine, an intermediate of the aminoadipic acid pathway of lysine biosynthesis. I. Studies in *Neurospora crassa*, *J. Biol. Chem. 240*, 2524-2530.

6. Johansson, E., Steffens, J. J., Lindqvist, Y., and Schneider, G. (2000) Crystal structure of saccharopine reductase from *Magnaporthe grisea*, an enzyme of the α-aminoadipate pathway of lysine biosynthesis, *Structure 8*, 1037-1047.

7. Garrad, R. C. and Bhattacharjee, J. K. (1992) Lysine biosynthesis in selected pathogenic fungi: characterization of lysine auxotrophs and the cloned *LYS1* gene of *Candida albicans*, *J. Bacteriol. 174*, 7379-7384.

8. Palmer, D. R., Balogh H., Ma, G., Zhou, X., Marko, M., and Kaminskyj, S. G. (2004) Synthesis and antifungal properties of compounds which target the alpha-aminoadipate pathway, *Pharmazie 59*, 93–98.

9. Andi, B., Cook, P. F., and West, A. H. (2006) Crystal structure of His-tagged saccharopine reductase from *Saccharomyces cereviciae* at 1.7Å resolution. *Arch. Biochem. Biophys. 46*, 243–254.

10. Vashishtha, A. K., West, A. H., and Cook, P. F. (2008) Overall kinetic mechanism of saccharopine dehydrogenase from *Saccharomyces cerevisiae*, *Biochemistry 47*, 5417-5423.

11. Storts, D. R., and Bhattacharjee, J. K. (1987) Purification and properties of saccharopine dehydrogenase (glutamate forming) in *Saccharomyces cerevisiae*

lysine biosynthetic pathway, *J. Bacteriol. 169*, 416-418.

12. Jones, E. E., and Broquist, H. P., (1966) Saccharopine, an intermediate of the aminoadipic acid pathway of lysine biosynthesis. III. Aminoadipic semialdehyde-glutamate reductase, *J. Biol. Chem. 241*, 3430-3434.

13. Schowen, K. B., and Schowen, R. L. (1982) Solvent isotope effects on enzyme systems, *Methods Enzymol. 87*, 551.

14. Cleland, W. W. (1979) Statistical analysis of enzyme kinetic data, *Methods Enzymol. 63*, 103-108.

15. Cook, P. F. and Cleland, W. W. (2008) *Enzyme Kinetics and Mechanism.* pp 325-364, Garland Publishing, Madison Ave., NY.

16. Xu, H., Alguindigue, S. S., West, A. H., and Cook, P. F. (2007) A Proposed Proton Shuttle Mechanism for Saccharopine Dehydrogenase from *Saccharomyces cerevisiae*, *Biochemistry 46*, 871-882.

17. Cleland, W. W. (1977) Determination the chemical mechanisms of enzyme-catalyzed reactions by kinetic studies, *Adv. Enzymol. Relat. Areas Mol. Biol. 45*, 273-387.

18. Cook, P. F. (1982) Kinetic studies to determine the mechanism of regulation of bovine liver glutamate dehydrogense by nucleotide effectors. *Biochemistry 21*, 113–116.

19. Weiss, P. M., Chen, C. Y., Cleland, W. W., and Cook, P. F. (1988) Use of primary deuterium and ^{15}N isotope effects to deduce the relative rates of steps in the mechanisms of alanine and glutamate dehydrognases. *Biochemistry 27*, 4814–4822.

20. Frieden, C. F. (1959) Glutamic dehydrogenase. The order of substrate addition in the enzymatic reaction. *J. Biol. Chem. 234*, 2891–2896.

21. Engel, P. C., and Dalziel, K. (1970) Kinetic studies of glutamate dehydrogenase. The reductive amination of 2-oxoglutarate. *Biochem. J. 118*, 409–419.

22. Colen, A. H., Prough, R. A., and Fisher, H. F. (1972) The mechanism of the glutamate dehydrogenase reaction. Evidence for random and rapid binding of substrate and coenzyme in the burst phase. *J. Biol. Chem. 247*, 7905–7909.

23. Ohshima, T., Sakane, M., Yamazaki, T., and Soda, K. (1990) Thermostable alanine dehydrogenase from thermophilic *Bacillus sphaericus* DSM 462.

Purification, characterization and kinetic mechanism. *Eur. J. Biochem. 191*, 715–720.

24. Grimshaw, C. E., and Cleland, W. W. (1981) Kinetic mechanism of *Bacillus subtilis* L-alanine dehydrogenase. *Biochemistry 20*, 5650–5655.

25. Fujioka, M., and Nakatani, Y. (1970) A kinetic study of the saccharopine dehydrogenase reaction. *Eur. J. Biochem. 16*, 180–186.

26. Fujioka, M., and Nakatani, Y. (1972) Saccharopine dehydrogenase, interaction with substrate analogues. *Eur. J. Biochem. 25*, 301–307.

27. Xu, H., West, A. H., and Cook, P. F. (2006) Overall kinetic mechanism of saccharopine dehydrogenase from *Saccharomyces cerevisiae*. *Biochemistry 45*, 12156–12166.

28. Brunhuber, N. M. W., and Blanchard, J. S. (1994) *Crit. Rev. Biochem. Mol. Biol. 29*, 415-467.

29. Rife, J. E., and Cleland, W. W. (1980) Determination of the chemical mechanism of glutamate dehydrogenase from pH studies. *Biochemistry 19*, 2328-2333.

30. Meredith, M. J., Gronostajski, R. M., and Schmidt, R. R. (1978) Physical and kinetic properties of the nicotinamide adenine dinucleotide-specific glutamate dehydrogenase purified from *Chlorella sorokiniana*. *Plant Phys. 61*, 967-974.

31. Grimshaw, C. E., Cook, P. F., and Cleland, W. W. (1981) Use of isotope effects and pH studies to determine the chemical mechanism of *Bacillus subtilis* L alanine dehydrogenase. *Biochemistry 20*, 5655-5661.

32. Brunhuber, N. M. W., Thoden, J. B., Blanchard, J. S. and Vanhooke, J. L. (2000) *Rhodococcus* L-phenylalanine dehydrogenase: kinetics, mechanism, and structural basis for catalytic specifity. *Biochemistry 39*, 9174-9187.

33. Sekimoto, T., MatsuyamaS, T., Fukui, T., and Tanizawa, K. (1993) Evidence for Lysine 80 as General Base Catalyst of Leucine Dehydrogenase. *J. Biol. Chem. 268*, 27039-27045.

34. Andi, B., Xu, H., Cook, P. F., and West, A. H. (2007) Crystal structures of ligand-bound saccharopine dehydrogenase from *Saccharomyces cerevisiae*. *Biochemistry 46*, 12512–12521.

35. Quinn, D. M., and Sutton, L. D. (1991) in *Enzyme Mechanism from Isotope Effects* (Cook, P. F., Ed.) pp 73–126, CRC Press, Boca Raton, FL.

36. Dawson, R. M. C., Elliott, D. C., Elliott, W. H., and Jones, K. H. (1991) *Data for Biochemical Research*, Oxford University Press, New York.

37. Karsten, W. E., Lai, C.-J, Gavva, S. R., and Cook, P. F. (1995) Inverse Solvent Deuterium Isotope Effects in the NAD-Malic Enzyme Reaction are the Result of the Viscosity Difference Between H_2O and D_2O: Implications for Solvent Deuterium Isotope Effect Studies. *J. Am. Chem. Soc. 117*, 5914-5918.

38. Lin, Y., Volkman, J., Nicholas, K. M., Yamamoto, T., Eguchi, T., Nimmo, S. L., West, A. H., and Cook, P. F. (2008) Chemical Mechanism of Homoisocitrate Dehydrogenase from *Saccharomyces cerevisiae*. *Biochemistry 47*, 4169-4180.

39. Wong, K. K., and Blanchard, J. S. (1989) Human erythrocyte glutathione reductase: pH dependence of kinetic parameters. *Biochemistry 28*, 3586-3589.

CHAPTER 4

Overall Discussion and Conclusion

Saccharopine reductase (SR) (EC 1.5.1.10) is the penultimate enzyme in the α-aminoadipate pathway encoded by *LYS9* gene in *S. cerevisiae.* Saccharopine reductase (SR) catalyzes the condensation of L-α-aminoadipic acid-δ-semialdehyde with L-glutamate to form an imine which is subsequently reduced by NADPH to give saccharopine. The last two enzymes in lysine biosynthesis pathway namely saccharopine reductase and saccharopine dehydrogenase (L-Lysine forming) use the same substrate saccharopine and catalyze oxidation of adjacent bonds in saacharopine. These two enzymes have very little sequence homology at the amino acid level so it is of interest to study how these enzymes catalyze similar reactions *i.e.* oxidation of adjacent bonds in saccharopine.

4.1. Kinetic Mechanism of Saccharopine Reductase.

Kinetic studies have been carried out for SR at pH 7.0 and a sequential kinetic mechanism has been proposed for SR on the basis of initial rate studies, product inhibition studies, dead end inhibition studies, and isotope effect studies, scheme 4-1. In the forward reaction direction, the mechanism involves the ordered addition of reduced nicotinamide adenine dinucleotide phosphate (NADPH) to the free enzyme followed by L-α-aminoadipate-δ-semialdehyde (L-AASA) which adds in rapid equilibrium prior to L-glutamate in the forward reaction direction. In the

reverse reaction direction, nicotinamide adenine dinucleotide phosphate (NADP) adds to the enzyme followed by addition of saccharopine.

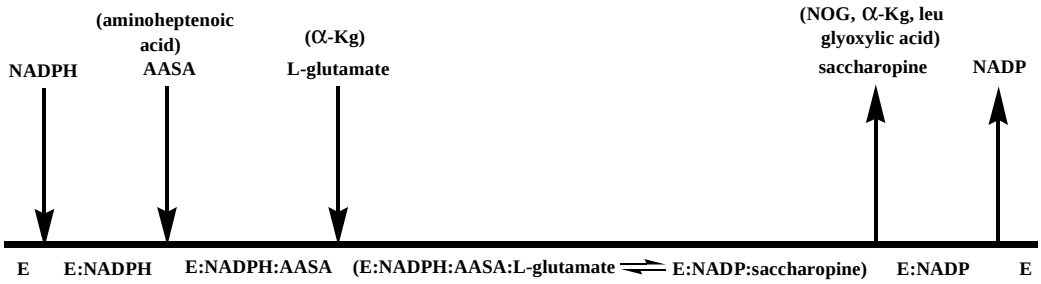

Scheme 4-1. Proposed Kinetic Mechanism for SR. Dead end analogues of the substrates are shown in parentheses.

Primary kinetic deuterium isotope effect studies show that $^{D}(V/K_{NADPH})$ is within error 1 corroborating the proposed mechanism. The inverse isotope effect observed for $^{D}(V/K_{glutamate})$ suggests the hydride transfer step is close to equilibrium in the steady state and step(s) after reduction of the imine limits the overall reaction, likely the conformational change to open the active site to release saccharopine (*1*). This proposition is also supported by the solvent isotope effect and proton inventory studies which suggest that protons are in flight in the rate determining steps along the reaction pathway.

A comparison of the kinetic mechanism of SR with other amine dehydrogenases has been discussed with emphasis on the comparison with saccharopine dehydrogenase. The kinetic mechanism of the two enzymes is very similar, with ordered addition of the dinucleotide and saccharopine and release of the reduced dinucleotide last. In the case of SR the addition of L-AASA and glutamate

are ordered, while α-Kg and lysine can add randomly to the E:NADPH binary complex for SDH (*1*, *2*, *3*).

4.2. Chemical Mechanism of Saccharopine Reductase.

pH-rate profiles and solvent isotope effect studies were carried out to probe optimum protonation states of functional groups on enzyme and substrates required for binding and catalysis. On the basis of pH-rate profiles and solvent isotope effect studies the chemical mechanism of SR has been proposed, Scheme 4-2. The mechanism involves binding of L-glutamate and AASA in protonated state along with NADPH to the enzyme. A general base B_2 accepts a proton from the primary amine of glutamate generating a nucleophile which attacks the carbonyl carbon of AASA. This is followed by the formation of the carbinolamine intermediate catalyzed by a general acid-base catalyst B_1. The next step involves the expulsion of a water molecule to give protonated imine which is reduced by NADPH to produce L-saccharopine. In the final step, the general acid B_2:H protonates the secondary amine of saccharopine resulting in the formation of protonated saccharopine (*4*). The proposed chemical mechanism of SR is very similar to that proposed for SDH (*7*). Both enzymes catalyze the oxidation of saccharopine bonds at adjascent positions and the proposed mechanisms of these enzymes are also very similar involving a major acid-base catalytic group which carried out most of the chemistry in the reaction and another gropu which is participates only in the final step of the reaction to protonate the secondary amine of saccharopine. The identity of the general acid-

base catalysts in both enzymes is presently under study.

Site directed mutagenesis has been carried out for SR to determine the identity of the general acid-base catalyst. Substrate bound active site structure of SR from *M. grisea* and multiple sequence alignment results show that the residues D125, C154 and Y99 are in position to act as the general acid-base catalyst. Kinetic

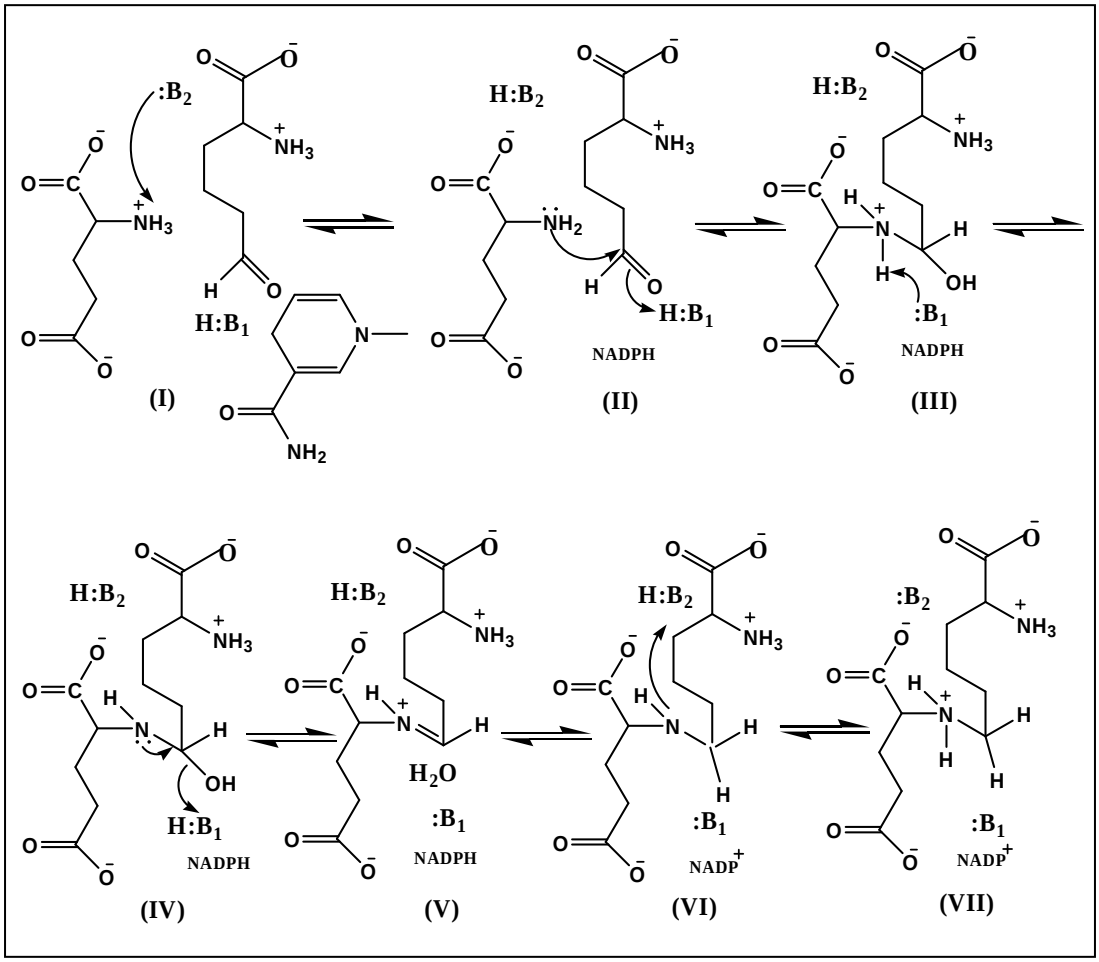

Scheme 4-2. Proposed Chemical Mechanism for Saccharopine Reductase. I, the central E-NADPH-AASA-glutamate complex formed upon binding of substrates; II, production of the neutral amine of glutamate, which acts as a nucleophile attacking the carbonyl of the semialdehyde; III, protonated carbinolamine intermediate; IV, neutral carbinolamine intermediate; V, the protonated imine intermediate; VI, neutral L-saccharopine formed upon hydride transfer from NADPH; and VI, protonated saccharopine.

parameters for these single mutant enzymes and of the double mutants D125A-C154S, D125A-Y99F and C154S-Y99F indicate that these residues are important for the reaction but the pH-rate profiles show that none of these residues act as the catalyst. Further studies need to be carried out to identify the residue which plays the catalytic role in the reaction catalyzed by SR. Despite the structural dissimilarities among these two enzymes, they show similarity in their order of addition of substrates and release of products with little variation. The chemical mechanisms of these enzymes are also strikingly similar suggesting that the imine dehydrogenases employ similar catalytic strategies to catalyze their reactions.

4.3. Future Studies

Kinetic and chemical mechanisms for SR have been proposed and described in this dissertation. The apo structure of SR from *S. cerevisiae* and a ternary E:NADPH:saccharopine complex of SR from *M. grisea* were solved to 2.0 and 2.1 Å, respectively (*5*, *6*). However, to date there is no substrate bound structure of SR from *S. cerevisiae* which is required to test the proposed chemical mechanism. Determination of ligand bound structures of SR would help to confirm the proposed chemical mechanism and would shed more light on the orientation and binding of the substrates in the active site.

Thus far, the identity of the general acid-base catalyst in the reaction is not known. Site directed mutagenesis studies show that D125, C154 and Y99 residues are important but do not play a catalytic role in the mechanism. The primary amino group of saccharopine is another candidate which is in a position to assist in the

reaction by anchimeric assistance and further studies are required to elucidate its role in the reaction mechanism. Thr245 residue is in hydrogen bonding distance to the amino group of saccharopine, hence site directed mutagenesis should be employed to elucidate the role of Thr245 residue in the reaction.

References

1. Vashishtha, A. K., West, A. H., and Cook, P. F. (2008) Overall kinetic mechanism of saccharopine dehydrogenase from *Saccharomyces cerevisiae*, *Biochemistry 47*, 5417-5423.

2. Fujioka, M., and Nakatani, Y. (1970) A kinetic study of the saccharopine dehydrogenase reaction, *Eur. J. Biochem. 16*, 180-186.

3. Xu, H., West, A. H., and Cook, P. F. (2006) Overall kinetic mechanism of saccharopine dehydrogenase from *Saccharomyces cerevisiae*, *Biochemistry 45*, 12156-12166.

4. Vashishtha, A. K., West, A. H., and Cook, P. F. (2009) Chemical Mechanism of Saccharopine Reductase from *Saccharomyces cerevisiae*, *Biochemistry 48*, 5899-5907.

5. Andi B., Cook P. F., West, A. H., (2006) Crystal structure of his-tagged saccharopine reductase from Saccharomyces cerevisiae at 1.7-Å resolution. *Cell Biochem. Biophys. 46*, 17-26.

6. Johansson, E., Steffens, J. J., Lindqvist, Y., and Schneider, G. (2000) Crystal structure of saccharopine reductase from *Magnaporthe grisea*, an enzyme of the α-aminoadipate pathway of lysine biosynthesis. *Structure 8*, 1037-1047.

7. Xu, H., West, A. H., and Cook, P. F. (2007) A proposed proton shuttle mechanism for saccharopine dehydrogenase from *Saccharomyces cerevisiae*. *Biochemistry 46*, 871-882.

Appendices

LIST OF SCHEMES

LIST OF ABBREVIATIONS

AAA	α-aminoadipic acid
AASA	α-aminoadipic acid-δ-semialdehyde
ADP	adenosine diphosphate
Amp	ampicillin
AMP	adenosine monophosphate
3-APADP	3-acetyl pyridine adenine dinucleotide phosphate
ATP	adenosine triphosphate
Bis-Tris	bis (2-hydroxyethyl) imino-tris (hydroxymethyl) methane
C	competitive
Ches	2-(*N*-cyclohexylamino)-ethanesulfonic acid
DAP	diaminopimelate
DCl	deuterium chloride
D_2O	deuterium oxide
EDTA	ethylenediaminetetraacetic acid
FAD	flavin adenine dinucleotide
$FADH_2$	flavin adenine dinucleotide (reduced form)
HCS	homocitrate synthase
Hepes	4-(2-hydroxyethyl)-1-piperazine-ethanesulfonic acid
IPTG	isopropyl-β-D-1-thiogalactopyranoside
kDa	kilodaltons
α-Kg	α-ketoglutarate

LB	Luria-bertani
Mes	2-(*N*-morpholino)-ethanesulfonic acid
Mops	3-(*N*-Morpholino)-propanesulfonic acid
NAADP$^+$	nicotinic acid adenine dinucleotide phosphate
NADP$^+$	nicotinamide adenine dinucleotide phosphate
NADPH	nicotinamide adenine dinucleotide phosphate (reduced form)
NaOD	sodium deuterioxide
NC	noncompetitive
Ni-NTA	nickel-nitrilotriacetic acid
NMN$^+$	nicotinamide mononucleotide
NMR	nuclear magnetic resonsnce
NOG	N-oxalylglycine
OAA	oxaloacetic acid
PDB	protein data bank
PIPOX	pipecolic acid oxidase
PMSF	phenylmethanesulfonyl fluoride
SDH	saccharopine dehydrogenase (L-Lys forming)
SDS	sodium dodecyl sulfate
SDS-PAGE	sodium dodecyl sulfate-polyacrylamide gel electrophoresis
SEM	standard error of the mean
SR	saccharopine reductase
Tris	tris-(hydroxymethyl) aminomethane

UC	uncompetitive
UV	ultraviolet

APPENDIX I

Role of D125, Y99F and C154S in the reaction of saccharopine reductase from *Saccharomyces cerevisiae*

I-1. Introduction

Recently, a chemical mechanism was proposed for saccharopine reductase from *Saccharomyces cerevisiae*, on the basis of pH dependence of the kinetic parameters, primary deuterium kinetic isotope effects and solvent kinetic deuterium isotope effects (Scheme I-1) (*1*). The reaction begins with all reactants bound which requires the α-amine of L-glutamate protonated and NADPH bound with its 2'-phosphate ion paired with R34 on enzyme. On the basis of the substrate bound ternary structure of SR from *M. grisea* (*2*), a plant pathogen, the α-carboxylates of L-glutamate and AASA are within hydrogen bond distance to arginine residues, while the γ-carboxylate of L-glutamate is within hydrogen bond distance to a tyrosine and serine. Two groups are involved in the acid-base chemistry of the reaction. An enzyme group with a pK_a of 5.6-5.7, accepts a proton from the α-amine of glutamate to generate the neutral amine that can act as a nucleophile (II). The α-amine of glutamate attacks the carbonyl of the semialdehyde to generate the carbinolamine, which is protonated by a second enzyme group with a pK_a of about 7.8-8, which may be D125 (III). A proton is accepted from the carbinolamine (III), to give the neutral carbinolamine (IV), which can then collapse, expelling water with a proton donated by B_1 (V). NADPH reduces the imine, generating the unprotonated secondary amine

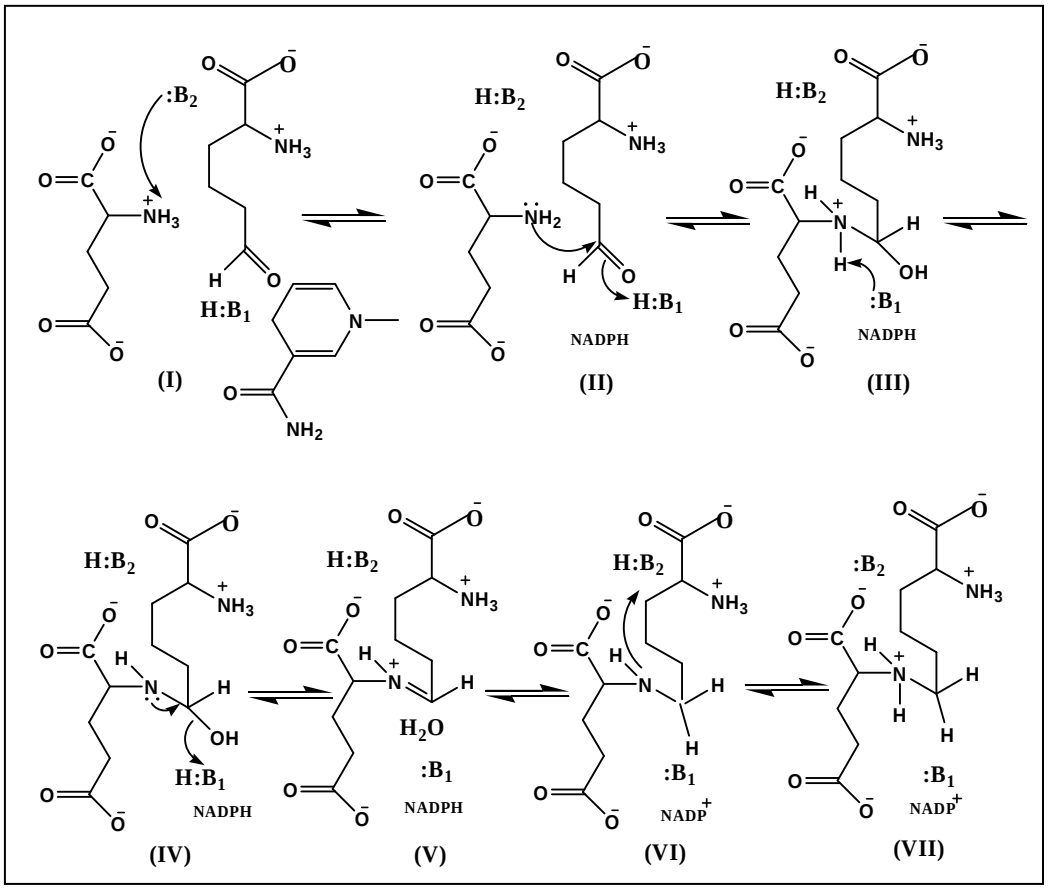

Scheme I-1. Proposed chemical mechanism of saccharopine reductase

(VI), which is protonated by B_1 (VII), and saccharopine is released.

Crystal structures of saccharopine reductase from *S. cerevisiae* and *M. grisea* have been reported (*3*, *2*). Structures of the *M. grisea* apo form and ternary, E-NADPH-saccharopine, complex of SR were solved to 2.0 and 2.1 Å, respectively. Structure of the *S. cerevisiae* apo form was solved to 2.1 Å while no structure has yet been solved for substrate bound SR from *S. cerevisiae*. SR from *Magnoportha grisea* shows 63% sequence identity and 78% sequence homology to the enzyme from *S. cerevisiae* in terms of sequence conservation. Comparison of the active site superimposed structure of SR from *Magnoportha grisea* and *S. cerevisiae* shows that

all the residues in the active site are completely conserved, Fig. I-1. A possible role as general base was proposed for D125, C154 and/or Y99, in accepting a proton from the water molecule to facilitate the hydrolysis of imine (IV and V in Scheme I-1). Multiple sequence alignment results show that Y99, D125 and C154 are highly conserved in SR from various organisms (see appendix IV) and are in a position to act as a general base in the reaction activating water molecule to attack the protonated imine intermediate. The distance between the closest oxygen of D125 and the 2^{o} amine nitrogen of saccharopine is long enough (5.57 Å) to accommodate a water molecule.

To date, the identity of the general acid-base catalyst of SR is unknown. In this study, site-directed mutagenesis was used to change three active site residues, and the resulting mutant enzymes were characterized using initial velocity studies, the pH dependence of the kinetic parameters, and isotope effects. Data combined with the available structures of SR from *S. cerevisiae* and *M. grisea* suggest that D125, C154 and Y99F residues are important in the reaction but none of these residues function as a general base to deprotonate the water molecule to facilitate the hydrolysis of imine. It is thus possible that sacchaorpine shows anchimeric assistance and the amino group of saccharopine acts as the general base to deprotonate the water molecule.

I-2. Materials and Methods

I-2-1. Chemicals and enzymes

L-Saccharopine and L-glutamic acid were from Sigma. β-NADPH and β-

NADP were purchased from USB. Mes, Mops, Ches and Hepes were obtained from

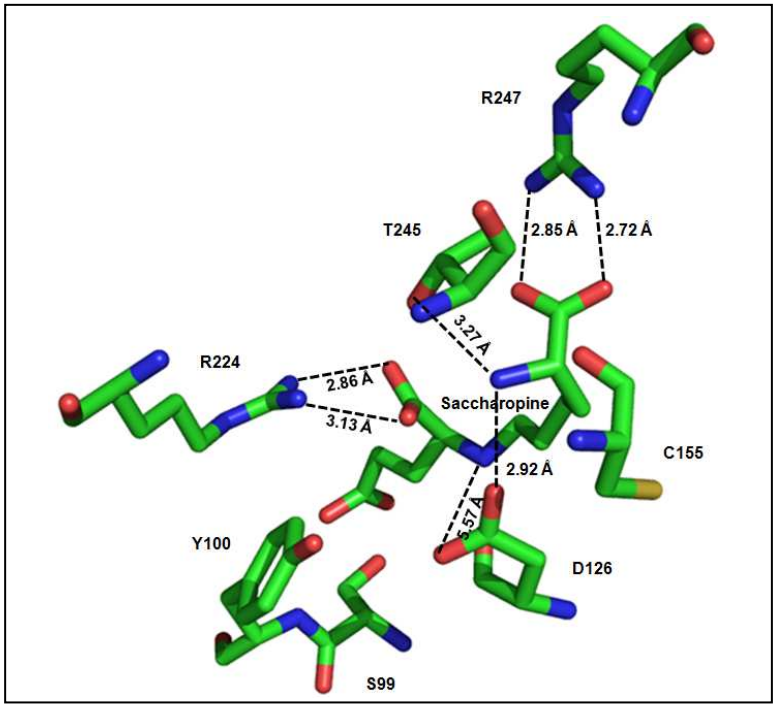

Fig. I-1: Close-up view of the active site of saccharopine reductase from *M. grisea* (PDB code 1E5Q). Residues that interact with saccharopine and their hydrogen-bonding distances are shown. The following color scheme is used: C, green, O, red, N, blue; and P, orange. This figure was generated using the PyMOL molecular visualization program (website: http:// pymol.Sourcefor ge.net/).

Research Organics. Deuterium oxide (99 atom % D) was purchased from Cambridge Isotope Laboratories, Inc. All other chemicals were of the highest grade available and were used as purchased.

Cell growth, expression of wt, and mutant enzymes purification were carried out as reported previously (*4*).

I-2-2. Generation of mutant enzymes

The D125A, C154S, Y99F, D125A-C154S, D125A-Y99F and C154S-Y99F mutant enzymes were prepared using the Quick Change site-directed mutagenesis kit

(Stratagene), in accordance with the recommendations of the manufacturer.

Aspartate 125 was mutated to alanine utilizing the following forward and reverse primers: $D125A_f$ (5′CGA AAT TGG GTT GGC TCC AGG TAT CGA CC3′) and $D125A_r$ (5′GGT CGA TAC CTG GAG CCA ACC CAA TTT CG3′). Cysteine 154 was mutated to serine utilizing the following forward and reverse primers: $C154S_f$ (5′CTT GTC ATA CTC TGG TGG TTT ACC3′) and $C154S_r$ (5′GGT AAA CCA CCA GAG TAT GAC AAG3′), while the tyrosine 99 to phenylalanine mutation utilized the following primers: $Y99F_f$ (5′CGT CAC TTC CTC TTT CAT CTC ACC TGC3′) and $Y99F_r$ (5′GCA GGT GAG ATG AAA GAG GAA GTG ACG3′). The point mutation codons are underlined. The entire mutant gene was sequenced for each mutant enzyme and the nucleotide sequences of the mutant enzymes were confirmed. Initial velocity studies, pH studies, solvent deuterium kinetic isotope effect studies and viscosity studies were carried out as described in chapter 2 and 3.

Initial velocity data at pH 7.0 and 9.0 for D125A, C154S, Y99F, D125A-C154S, and D125A-Y99F, and Y99F-C154S mutants were fitted to eq. 1 and 2.

$$\upsilon = \frac{V\mathbf{A}}{K_a + \mathbf{A}} \tag{1}$$

$$\upsilon = \frac{V\mathbf{AB}}{K_{ia}K_b + K_b\mathbf{A} + K_a\mathbf{B} + \mathbf{AB}} \tag{2}$$

pH rate-profiles that exhibited a slope of 1 at low pH and -1 at high pH were fitted using eq. 3, while those that exhibited a slope of 1 at low pH were fitted using eq. 4.

$$log\ y = log\left[C / \left(1 + \frac{\mathbf{H}}{K_1} + \frac{K_2}{\mathbf{H}} \right) \right] \quad (3)$$

$$log\ y = log\left[C / \left(1 + \frac{\mathbf{H}}{K_1} \right) \right] \quad (4)$$

I-3. Results

In order to obtain information concerning the identity of the acid-base catalysts in the proposed chemical mechanism of SR, initial velocity parameters were obtained for D125A, C154S, Y99F, D125A-Y99F, and D125A-C154S mutant enzymes and the pH dependence of kinetic parameters was determined.

I-3-1. Initial Velocity Studies at pH 7.0 and pH 9.0

In the forward reaction direction, initial rates were obtained by varying one substrate around its K_m and saturating with the others. In the direction of glutamate formation the initial rate was measured as a function of saccharopine at different fixed concentrations of NADP. Estimates of kinetic parameters for D125A, C154S, Y99F, and D125A-Y99F, D125A-C154S mutant enzymes are summarized in Table I-1. Kinetic parameters obtained in the reverse reaction direction are summarized in Table I-2.

I-3-2. pH Dependence of Kinetic Parameters

The pH dependence of kinetic parameters provides information on groups required in a given protonation state for optimum binding of reactant and/or catalysis

Table I-1. Summary of Kinetic Parameters for D125A, C154S, D125A-Y99F, and Y99F-C154S mutant enzymes in the Direction of Saccharopine Formation at pH 7.0.

	wt	D125A	C154S	D125A-Y99F	Y99F-C154S
$V_1/\mathbf{E_t}$ (s^{-1}) (Fold Decrease)	1.9 ± 0.1	0.1 ± 0.004 (19)	0.27 ± 0.02 (7)	0.08 ± 0.003 (24)	0.050 ± 0.004 (38)
$V_1/K_{NADPH}\mathbf{E_t}$ ($M^{-1}s^{-1}$) (Fold Decrease)	(7.3 ± 1.8) x 10^5	(2.3 ± 0.2) x 10^3 (317)	(1.7 ± 0.1) x 10^4 (43)	(5.83 ± 0.31) x 10^2 (1252)	(2.64 ± 0.18) x 10^2 (2765)
$V_1/K_{Glu}\mathbf{E_t}$ ($M^{-1}s^{-1}$) (Fold Decrease)	(2.9 ± 0.7) x 10^2	N/A	0.71 ± 0.14 (408)	6.25 ± 0.50 (46)	0.41 ± 0.08 (707)
K_{NADPH} (μM) (Fold Increase)	11.4 ± 2.6	43.6 ± 5.2 (4)	164 ± 25 (14)	146 ± 13 (13)	209 ± 35 (18)
K_{Glu} (mM) (Fold change)	28 ± 6	N/A	67 ± 2 (2.4)	2.64 ± 0.02 (11)	33 ± 9 (1.1)
K_{iAASA} (mM) (Fold Increase)	0.31 ± 0.071	1.26 ± 0.08 (4)	2.46 ± 0.02 (8)	7.35 ± 0.94 (24)	2.3 ± 0.3 (7.4)

Table I-2. Kinetic Parameters for D125A, C154S, Y99F, D125A-Y99F, D125A-C154S, and Y99F-C154S mutant enzymes in the Direction of glutamate Formation at pH 9.0

	Wt	D125A	C154S	Y99F	D125A-Y99F	D125A-C154S	Y99F-C154S
$V_2/\mathbf{E_t}$ (s^{-1}) (Fold Decrease)	13 ± 1	1.4 ± 0.1 (9)	0.12 ± 0.03 (112)	0.29 ± 0.01 (45)	0.043 ± 0.004 (302)	0.0028 ± 0.0005 (4643)	0.0014 ± 0.0004 (9285)
$V_2/K_{NADP}\mathbf{E_t}$ ($M^{-1}s^{-1}$) (Fold Decrease)	(8.5 ± 1.2) x 10^4	(6.0 ± 0.4) x 10^3 (14)	(2.1 ± 0.4) x 10^3 (41)	(3.3 ± 0.2) x 10^3 (26)	(1.2 ± 0.2) x 10^3 (72)	N/A	N/A
$V_2/K_{Sacc}\mathbf{E_t}$ ($M^{-1}s^{-1}$) (Fold Decrease)	(1.7 ± 0.3) x 10^4	(6.7 ± 0.2) x 10^3 (3)	105.6 ± 7.5 (161)	51.4 ± 1.9 (331)	32.5 ± 4.2 (523)	4.2 ± 0.7 (4086)	0.38 ± 0.02 (44737)
K_{NADP} (mM) (Fold Increase)	0.15 ± 0.01	0.071 ± 0.005 (2)	0.278 ± 0.056 (0.5)	0.745 ± 0.050 (5)	0.393 ± 0.064 (2.5)	N/A	N/A
K_{Sacc} (mM) (Fold Change)	0.77 ± 0.12	0.21 ± 0.04 (4)	18.3 ± 7.2 (24)	5.64 ± 0.53 (7)	2.1 ± 0.4 (3)	3.16 ± 1.14 (4)	32.4 ± 10.3 (42)

N/A is not applicable

(5). The pH dependence of kinetic parameters for the D125A, C154S, Y99F, and D125A-Y99F, and D125A-C154S mutant enzymes was determined, and the results are shown in Figures I-2 and I-3.

In the direction of AASA formation, $V_2/K_{Sacc}\mathbf{E_t}$ decreases at low and high pH for D125A, C154S, Y99F, and D125A-Y99F mutants. pK_a values along with the pH-independent values of kinetic parameters are summarized in Table I-3.

I-3-3. Effect of Solvent Deuterium and Viscosity

Initial rates were measured at saturating NADP, varying saccharopine over the pH(D) 9.0. Solvent isotope effects were calculated as the ratio of the pH(D) independent values of $V_2/K_{Sacc.}$ for D125A, C154S, and Y99F mutants enzymes. The values of solvent deuterium kinetic isotope effects for D125A, C154S, and Y99F mutants enzymes are 1.9 ± 0.6, 4.2 ± 0.7, and 1.9 ± 0.2 for $^{D2O}V_2/K_{Sacc}$.

Glycerol was used as a viscosogen for the mutant enzymes. The ratio of the values of $V_2/K_{Saccharopine}$ determined in H_2O and at a relative viscosity of 1.24 are within error equal. Therefore, the values of the observed solvent isotope effects, $^{D2O}(V_2/K_{sacc})$ for the mutants, result from a classical isotope effect and not from an effect of the increased viscosity of 100% D_2O.

I-4. Discussion

Initial velocity from Table I-1 suggests that the residues D125A, C154S, Y99F are important for the reaction as is indicated in the sharp decrease observed in V/E_t

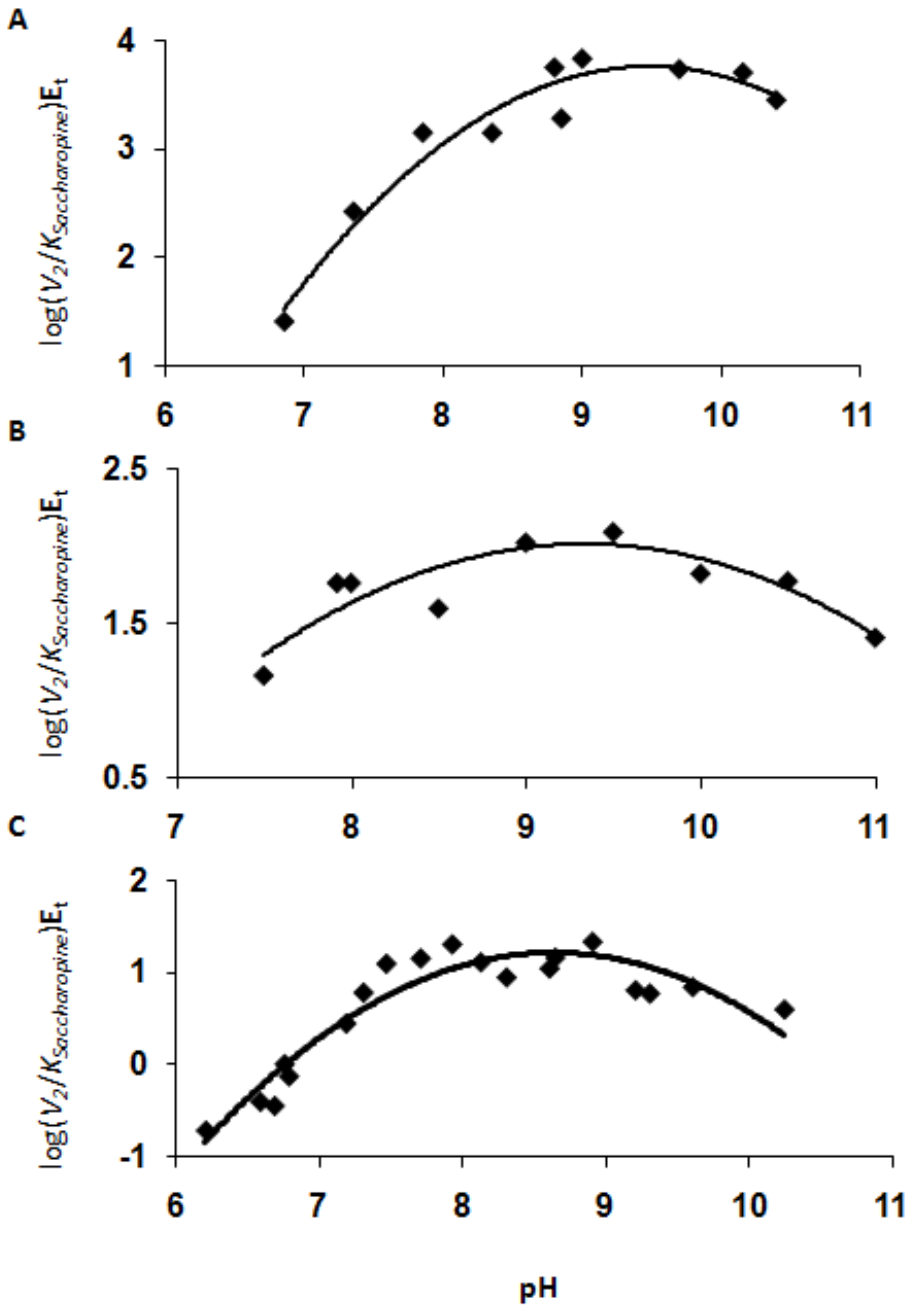

Figure I-2. pH dependence of kinetic parameters in the direction of glutamate formation for D125A, C154S, and Y99F mutant enzymes. pH dependence of: A. (V_2/K_{Sacc})E_t for D125A; B. (V_2/K_{Sacc})E_t for C154S; C. (V_2/K_{Sacc})E_t for Y99F. All data were obtained at 25°C. Points are experimental, while curves are based on a fit of the data to eq. 3.

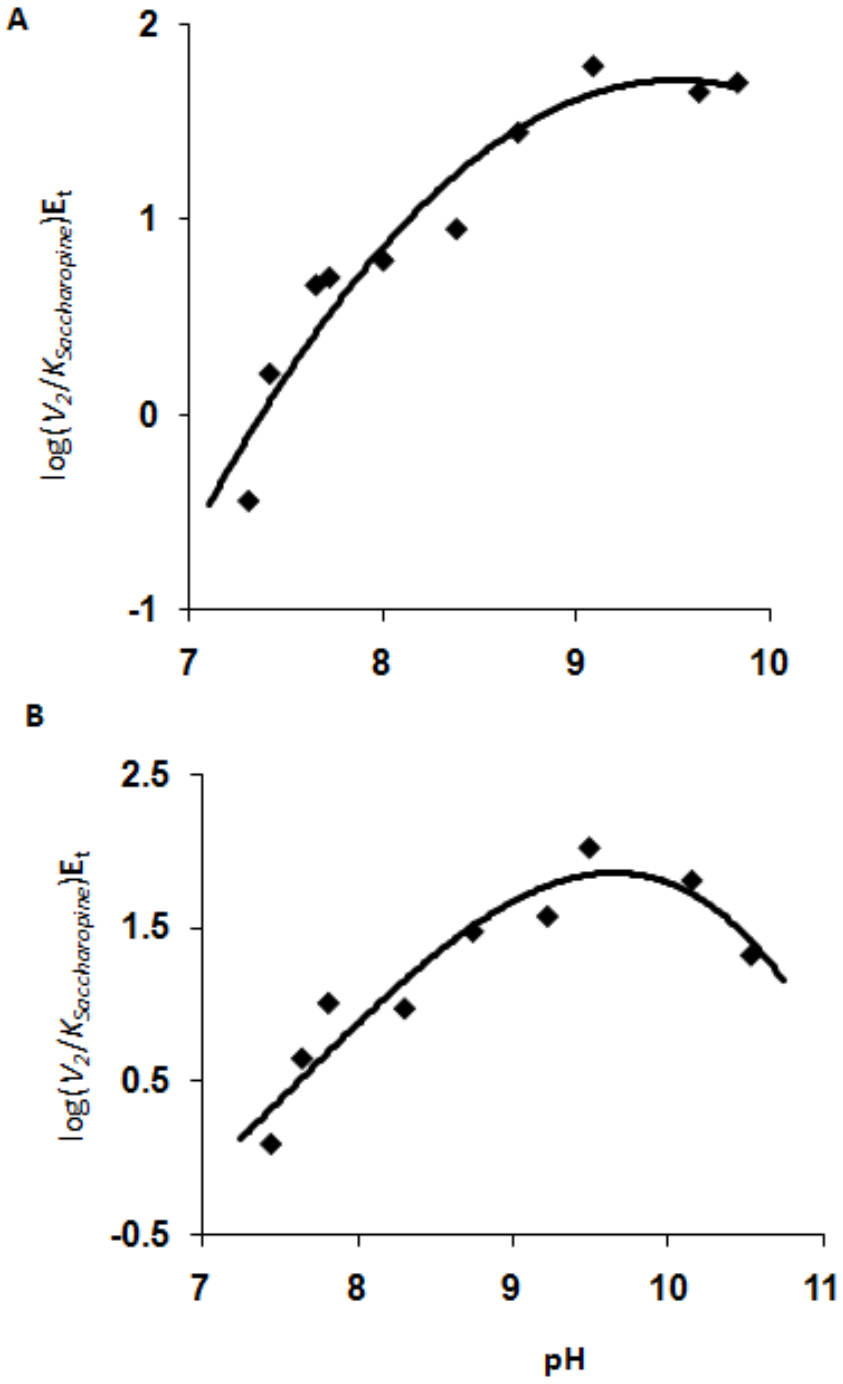

Figure I-3. pH dependence of kinetic parameters in the direction of glutamate formation for D125A-C154S, and D125A-Y99F mutant enzymes. pH dependence of: A. (V_2/K_{Sacc})E_t for D125A-C154S; B. (V_2/K_{Sacc})E_t for D125A-Y99F. All data were obtained at 25°C. Points are experimental, while curves are based on a fit of the data to eq. 4 (A) or 3 (B).

Table I-3. Summary of pK_a values for log $V_2/K_{Sacc}E_t$ profile for D125A, C154S, Y99F, and D125A-Y99F, and D125A-C154S mutant enzymes in the Direction of glutamate Formation.

Enzyme	pK_1	pK_2	pH Independent value ($M^{-1}s^{-1}$)
wt	7.6 ± 0.1	9.9 ± 0.2	(2.9 ± 0.5) x 10^4
D125A	8.8 ± 0.3	9.9 ± 0.3	(1.0 ± 0.3) x 10^4
C154S	8.1 ± 0.2	10.3 ± 0.2	73.7 ± 7.5
Y99F	7.1 ± 0.4	9.5 ± 0.3	11.1 ± 1.7
D125A-Y99F	9.3 ± 0.2	10.3 ± 0.5	85.5 ± 22.3
D125A-C154S	8.5 ± 0.2	N/A	56.1 ± 7.8

N/A is not applicable.

values for the mutants. The pH dependence of kinetic parameters for the D125A, C154S, Y99F, D125A-Y99F, and D125A-C154S mutant enzymes indicate that these residues do not play the role of general acid-base catalysts in the chemical mechanism of SR. Solvent isotope effects for D125A, and Y99F mutants are close to that of the wild type enzyme indicating that protons are in flight in the rate-determining step corroborating the proposed chemical mechanism. The solvent deuterium kinetic isotope effect for the C154S mutant is 4.2, higher than the corresponding isotope effect observed for the wild type enzyme. This value is close to the theoretical maximum value which can be obtained for the primary deuterium kinetic isotope effect suggesting that the proton transfer step is greatly rate limiting

for the C154S mutant. As proposed in the chemical mechanism of SR, this step is most likely the conformational change involving opening the active site and release of products.

Site directed mutagenesis studies showed that the residues D125, Y99F and C154 are important for the SR reaction but these residues do not act as the general acid-base catalysts in the chemical mechanism of SR. It is possible that the substrate itself provides anchimeric assistance to catalyze the reaction. Further studies need to be carried out to test this proposition by chemical modification of the primary amino group of saccharopine using formamidation and carrying dead-end inhibition studies using the formylated derivative. Alternate substrate studies should also be carried out in order to elucidate the role of the primary amino group of saccharopine.

References

1. Vashishtha, A. K., West, A. H., and Cook, P. F. (2009) Chemical mechanism of saccharopine reductase from *Saccharomyces cerevisiae*, *Biochemistry 48*, 5899-5907.

2. Johansson, E., Steffens, J. J., Lindqvist, Y., and Schneider, G. (2000) Crystal structure of saccharopine reductase from *Magnaporthe grisea*, an enzyme of the α-aminoadipate pathway of lysine biosynthesis, *Structure 8*, 1037-1047.

3. Andi, B., Cook, P. F., and West, A. H. (2006) Crystal structure of his-tagged saccharopine reductase from *Saccharomyces cereviciae* at 1.7Å resolution, *Arch. Biochim. Biophys. 46*, 243-254.

4. Vashishtha, A. K., West, A. H., and Cook, P. F. (2008) Overall kinetic mechanism of saccharopine dehydrogenase from *Saccharomyces cerevisiae*, *Biochemistry 47*, 5417-5423.

5. Cleland, W. W. (1977) Determination the chemical mechanisms of enzyme-catalyzed reactions by kinetic studies, *Adv. Enzymol. Relat. Areas Mol. Biol. 45*, 273-387.

APPENDIX II

Substrate specificity of saccharopine reductase

II-1. Introduction

Extensive inhibition studies have been carried out using analogs of saccharopine and nicotinamide adenine dinucleotide to gain information about the saccharopine and dinucleotide binding pocket and to determine the substrate specificity.

II-2. Materials and Methods

II-2-1. Chemicals

L-Saccharopine, L-glutamate, AMP, ADP, ADP-ribose, NMN, NAADP, 2′,3′-cyclic NADP, 2', 5' ADP, NAD3'P, thio-NAD, 3-APADP, thio-NADP, α-ketobutyrate, α-ketovalerate, glutarate, pyridine 2,4-dicarboxylate, pyridine 2, 3-dicarboxylate, pyridine 2,5-dicarboxylate, benzamidine, camphoric acid, L-pipecolinic acid, and isonicotinic acid were obtained from Sigma. *β*-NAD(P)H and *β*-NAD(P) were purchased from USB. Hepes, and Ches were from Research Organics, Inc. All other chemicals and reagents were used without further purification.

II-2-2. Alternate Substrate Studies

In order to check if we can substitute the dinucleotide with another substrate, reduced thio-NADP was used as an alternate substrate for NADPH in the forward

reaction direction at pH 7.0.

II-3. Results

II-3-1. Dead end inhibition studies Forward Reaction Direction

To gain information regarding the substrate binding pocket, and the reactant binding determinants, dead end inhibition experiments were carried out using a variety of inhibitory analogues in the forward reaction direction at pH 7.0 and in the reverse reaction direction at pH 9.0. Some of these compounds did not show any inhibition in the forward reaction direction at pH 7.0 and are summarized in Fig. II-2, Fig. II-3. Those compounds that acted as inhibitors in the forward reaction direction are summarized in Fig. II-1. The dead end inhibition constants for the dead end analogues of L-glutamate and AASA are summarized in Table II-1.

II-3-2. Dead end inhibition studies Reverse Reaction Direction

Dead-end analogues of L-saccharopine and NADP were employed in order to study the binding determinant. Analogues of NADP and L-saccharopine which showed inhibition are summarized in Table II-2 and Table II-3 along with their apparent K_i values.

II-3-3. Alternate Substrate Studies

In the forward reaction direction, thio-NADP was employed as a substitute for NADPH and the app K_m of thio-NADP was found to be 500 μM and saturation

was not achieved with thio-NADP.

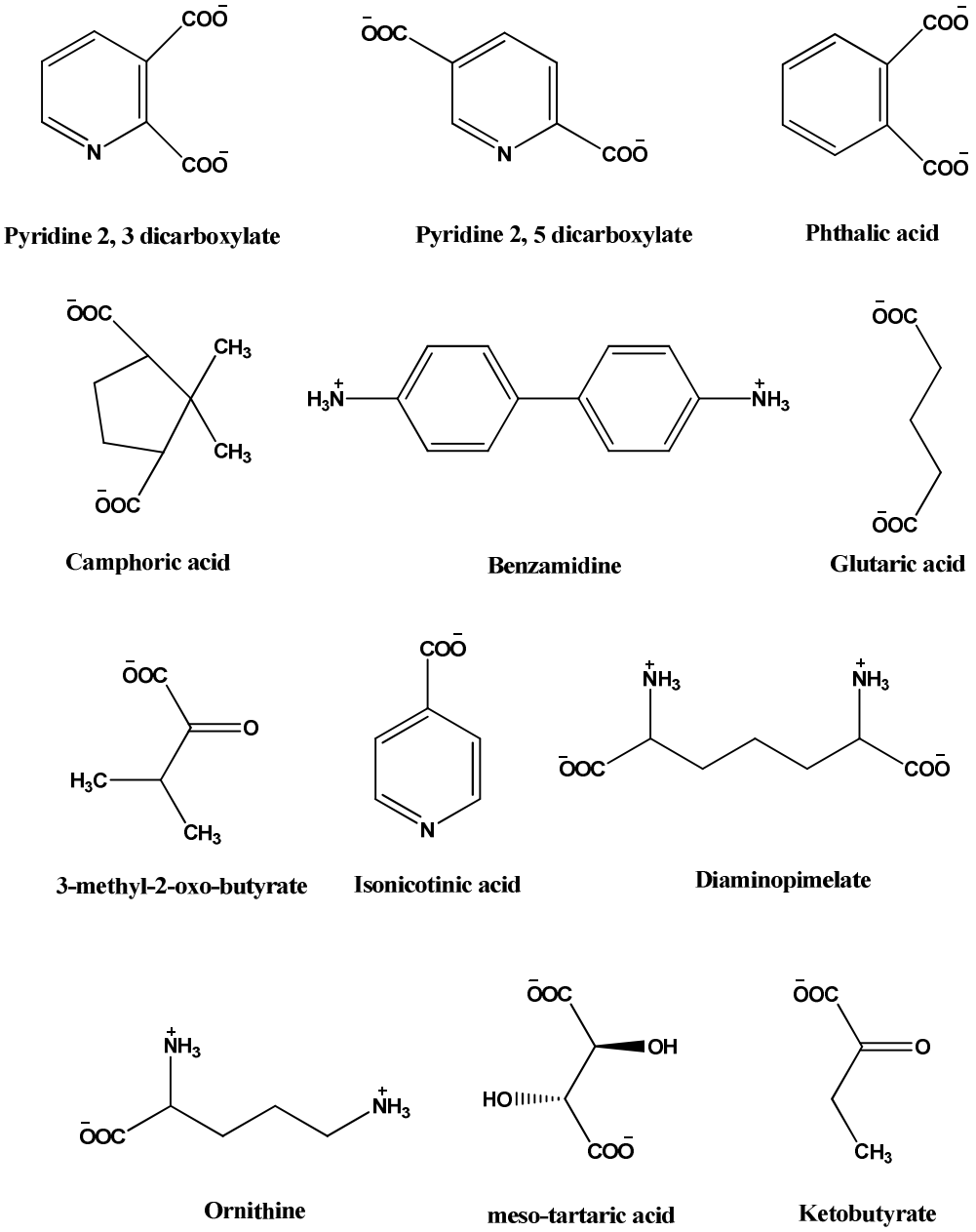

Fig. II-1. Structures of compounds which act as inhibitors for SR reaction at pH 7.0.

Table II-1. Summary of L-glutamate and AASA analogues inhibition studies in the forward reaction direction at pH 7.0

Inhibitor	Pattern vs. AASA	Pattern vs. L-glutamate
Pyridine 2, 4-dicarboxylic acid	NC K_m =26 ± 2.3 mM K_{ii} =75 ± 10 mM K_{is} =205 ± 65 mM	C K_m = 145 ± 30 mM K_I =116 ± 20 mM
Camphoric acid	NC K_m = 28 ± 1.7 mM K_{ii} = 72 ± 8 mM K_{is} = 63 ± 7.5 mM	NC K_m = 132 ± 10 mM K_{ii} = 62 ± 10 mM K_{is} = 55 ± 5 mM
Glutaric acid	NC K_m = 19 ± 1 mM K_{ii} = 10 ± 1 mM K_{is} = 46 ± 14 mM	C K_m = 58.4 ± 1.7 mM K_I = 12.5 ± 0.3 mM
Pipecolinic acid	C K_m = 14 ± 2 mM K_I = 23 ± 4 mM	NC K_m = 95 ± 9 mM K_{ii} = 34 ± 4 mM K_{is} = 93 ± 18 mM
Pyridine 2, 5-dicarboxylic acid	UC K_m = 18 ± 2 mM K_I = 13 ± 0.9 mM	C K_m = 38 ± 2 mM K_I = 23 ± 1 mM

II-4. Discussion

II-4-1. Dead end inhibition studies

The *app* K_i value of 3-APADP reduced form is almost the same as that for the substrate NADPH which means that 3-APADP reduced form binds as well as NADPH suggesting that most of the binding energy is coming from the ADP and the pyridine ring and hence the replacement of amide group with acetyl group does not result in much change in binding. The only difference between NADPH and 3-APADP reduced form is the replacement of amino group by methyl group. Net

Table II-2. Summary of app K_i values for L-Saccharopine analogues in the reverse reaction direction at pH 9.0

Inhibitor	app K_i
Glutaric acid	9 mM
Benzamidine	127 mM
Pyridine 2, 4 dicarboxylate	165 mM
Isonicotinic acid	70 mM

charge on both NADPH and 3-APADP reduced form is -4 which is required for binding. In AMP the nicotinamide portion is missing and the charge is reduced to -2 which affects the binding resulting in an increase in the *app* K_i value by 4 times indicating that the second phosphate is also required for proper binding in the active site. For ATP, the charge is -4 but instead of two phosphate groups we have three phosphate groups which might actually hinder the binding. Also, the nicotinamide portion is missing resulting in high value of the *app* K_i as compared to NADPH.

L-saccharopine and NADP analogues were used to probe the substrate binding site of SR. Glutaric acid has an *app*K_i value comparable to the true dead-end inhibition constants of ornithine, glyoxylic acid, and ketoglutarate, which are all competitive inhibitors vs. saccharopine (*1*). Pyridine 2, 4-dicarboxylic acid and isonicotinic acid have carboxylate groups which bind to SR but the binding of these compounds is poor as compared to the aliphatic dicarboxylic acid derivatives used before (*1*). The reason for poor binding of these analogues could be the presence of

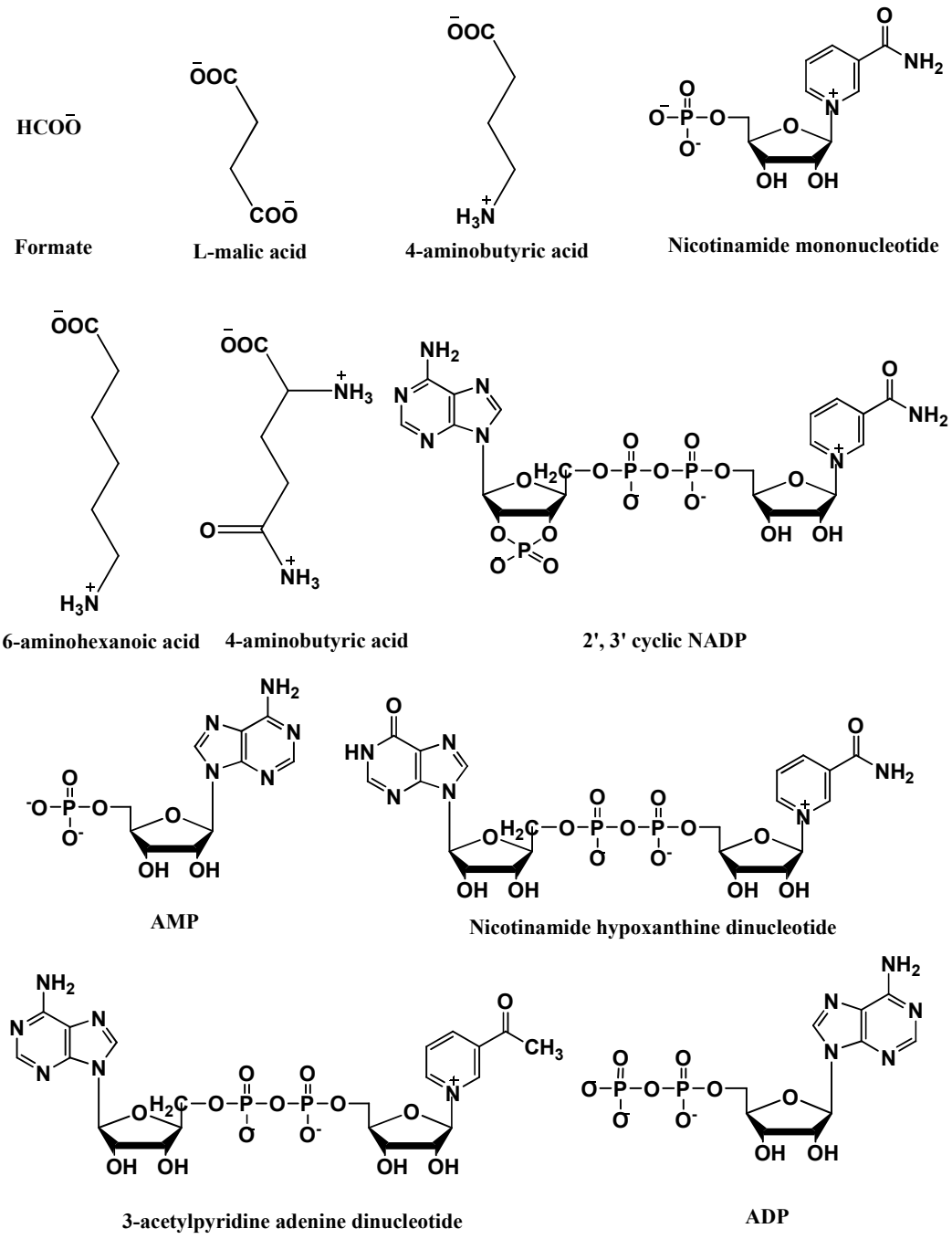

Fig. II-2. Structures of compounds which do not exhibit any binding to SR

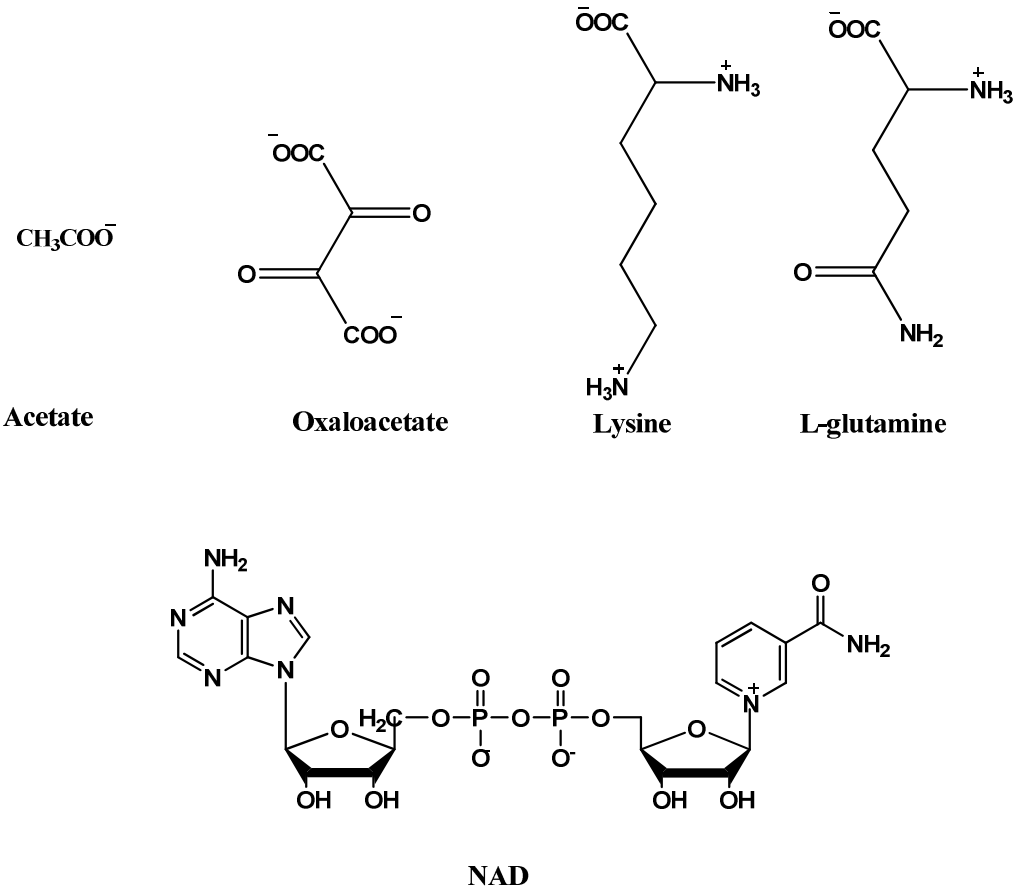

Fig. II-3. Structures of compounds which do not exhibit any binding to SR

Table II-3. Summary of app K_i values for NADPH/NADP analogues

Inhibitor	*app*K_i
ATP	200 μM
2', 3' cyclic NADP	44 μM
AMP	42 μM
3-APADP (reduced)	12 μM
β-NMN	15 mM
NAADP	45 μM
2', 5' ADP	2.5 mM
β-NAD3'P	6 mM
Thio-NAD	2 mM
3-APADP	0.5 mM

the bulky benzene ring in these inhibitors which could cause steric hindrance for binding in the active site. Another plausible explanation for high value of apparent inhibition constant for pyridine 2, 4-dicarboxylic acid could be that the two carboxylate groups are in a rigid non-optimal position and this might cause problems with binding SR.

II-4-2. Alternate Substrate Studies

Thio-NADPH is an analogue of NADPH in which the carbonyl group is replaced by a thio group. Thio-NADPH has a very high *app* K_m value as compared to NADPH and the possible reason could be the presence of a more polarizable sulphur atom in thio-NADPH as compared to NADPH. Also, sulphur is much bigger than oxygen and the electronegativity is considerably less. All these factors in combination could result in hindering the binding of thio-NADPH due to steric hindrance and prevention of hydrogen bonding to the residues in the active site of SR.

References

1. Vashishtha, A. K., West, A. H., and Cook, P. F. (2008) Overall kinetic mechanism of saccharopine dehydrogenase from *Saccharomyces cerevisiae*, *Biochemistry 47*, 5417-5423.

APPENDIX III

Activation studies on saccharopine reductase

III-1. Introduction

In order to carry out inhibition studies to elucidate the kinetic mechanism of SR, several saccharopine, AASA, and glutamate analogs were tested in both reaction directions. Some of these potential inhibitors turned out to be activators of the enzyme.

III-2. Materials and Methods

III-2-1. Chemicals

L-glutamic acid, adipic acid, 6-aminohexanoic acid, citric acid, malonic acid, oxamic acid, pyruvic acid, succinic acid, tartaric acid were from Sigma. β-NADPH and β-NADP were purchased from USB. Hepes was obtained from Research Organics. All chemicals were of the highest grade available and were used as purchased.

III-2-2. Activation studies at pH 7.0

The SR reaction was followed by monitoring the appearance or disappearance of NADPH at 340 nm ($\varepsilon_{340,}$ 6220 $M^{-1}cm^{-1}$) using a Beckman DU-640 spectrophotometer. All assays were carried out at 25 °C. Studies were carried out by measuring the initial velocity with fixed substrates equal to their respective K_m

values, and varying the concentration of the activator. The appK_{act} was then calculated from a plot of 1/υ vs. I.

III-2-3. Studies using amino adipic acid at pH 7.0

In order to obtain information regarding the effect of amino adipic acid on kinetic parameters, patterns were obtained using NADPH vs. AASA at fixed different concentrations of amino adipic acid.

III-3. Results and Discussion

The *app*K_{act} values for the activators are summarized in Table III-1 and the structures of these activators are summarized in Fig. III-1. Aminoadipic acid studies show that V_{max} is not greatly affected but the V/K_a value is affected (which represents the free enzyme form) hence aminoadipic acid binds to the free enzyme suggesting that there might be an allosteric site on the enzyme resulting in binding of aminoadipic acid to that site and affecting the V/K_a value while the V/K_b value is not affected, Table III-2.

The reason for the activation behavior of these compounds is not known, but it can be suggested that these compounds probably bind to the E:NADP binary form of the enzyme and accelerate the release of the products.

Table III-1. Summary of apparent activation constants in forward reaction direction at pH 7.0

Structure	$appK_{act}$	Fold Activation
Adipic acid	10 mM	1.5
6-aminohexanoic acid	8 mM	1.5
Citric acid	10 mM	1.9
Malonic acid	5 mM	1.8
Oxamic acid	8 mM	1.6
Pyruvic acid	5 mM	1.4
Succinic acid	8 mM	1.6
Tartaric acid	16 mM	1.5

Table III-2. Summary of kinetic parameters using amino adipic acid in forward reaction direction at pH 7.0

Adipate (mM)	0	10	20	40
K_{NADPH} (μM)	35 ± 6	39 ± 4	30 ± 4	24 ± 3
K_{IAASA} (mM)	5 ± 1	5.7 ± 0.6	5.4 ± 1	5.6 ± 0.8
V x 10^{-3} (mM min^{-1})	19 ± 2	20 ± 2	20 ± 4	20.5 ± 1.4
V/K_{NADPH} (min^{-1})	0.55 ± 0.01	0.53 ± 0.07	0.67 ± 0.01	0.85 ± 0.03
V/K_{IAASA} x 10^{-3} (min^{-1})	4.1 ± 1.3	3.6 ± 0.5	3.6 ± 0.9	3.6 ± 1.1

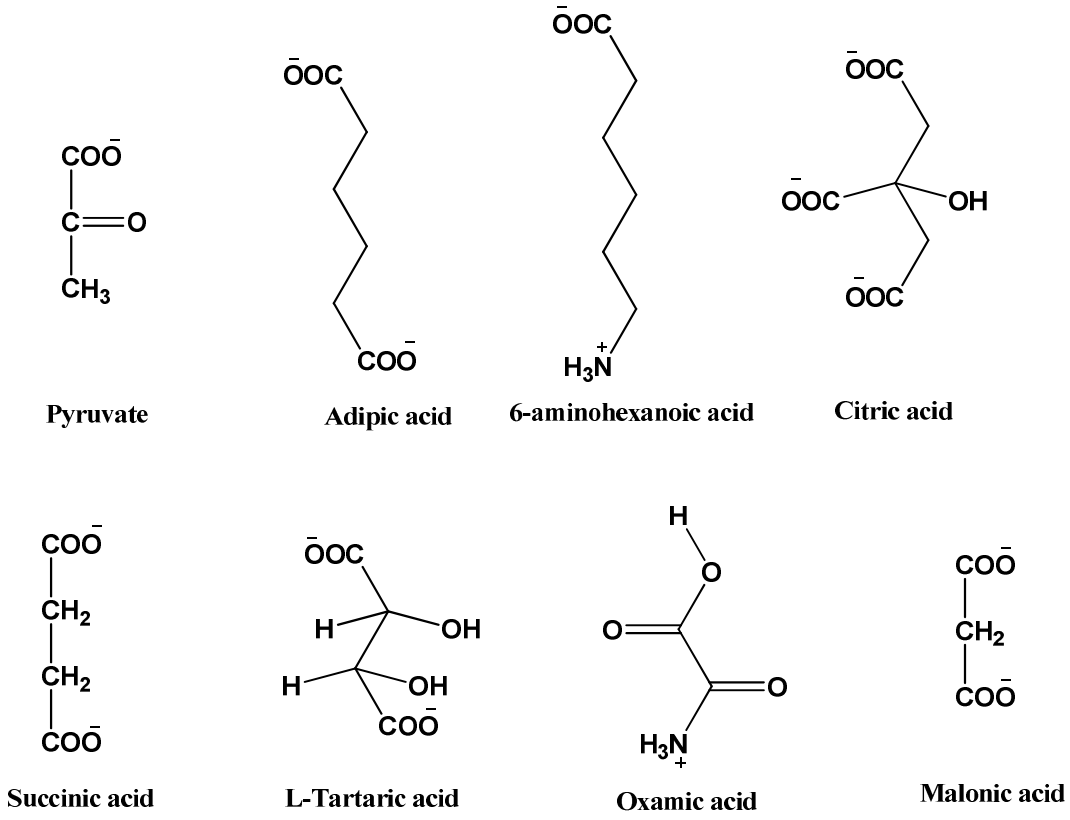

Fig. III-1. Structures of activators for the SR reaction at pH 7.0

APPENDIX IV

Multiple Sequence Alignments

IV-1. Results and Discussion

Multiple sequence alignments were carried out for saccharopine reductase (SR) from *Saccharomyces cerevisiae*, *Magnoporthe grisea*, *Schizosaccharomyces pombe*, *Aspergillus fumigatus*, *Candida albicans*, and *Cryptococcus neoformans* using CLUSTAL W sequence alignment[a] program.

```
S. cerevisiae      ------------------------------MGKNVLLLGSGFVAQPVIDT 20
M. grisea          ------------------------------MVKKVLLLGSGFVAKPTVDI 20
S. pombe           ------------------------------MATKSVLMLGSGFVTRPTLDV 21
A. fumigatus       -------------------------MVKQIAGSKVLLLGSGFVTKPTVEV 25
C. albicans        -------------------------------MPSILLLGSGFVAHPTLEY 19
C. neoformans      HEWLGGKIEQWKTGGAVAPDSLKQEKLRKGGKKKVLLLGSGLVAGPAVDV 500
                                                    .:*: ****:*: *.::

                                      34
S. cerevisiae      LAANDDINVTVACRTLANAQALAKP-SGSKAISLDVTDDSALDKVLADND 69
M. grisea          LSEQPDIEVTVACRTLSKAKELAG--DKAQAISLDVTDAAQLDEQVAKHD 68
S. pombe           LT-DSGIKVTVACRTLESAKKLSAGVQHSTPISLDVNDDAALDAEVAKHD 70
A. fumigatus       LT-KADVHVTVACRTLESAQKLCQGFPNTKAIALDVNDAAALDKALEQAD 74
C. albicans        LSRRKENNITVACRTLSKAEAFINGIPNSKAIALDVNDEAALEKAVSEHD 69
C. neoformans      FAARPDVHLIIASNNLAEGQSHIRGRPNVEAMALDVADDASMSEIVEEAD 550
                   ::     .: :*...* ..:          .::*** * : :.  : . *

                                                 9899
S. cerevisiae      VVISLIPYTFHPNVVKSAIRTKTDVVTSSYISPALRELEPEIVKAGITVM 119
M. grisea          LVISLIPYTFHVNVVKSAIKNKKNVVTTSYINPQLKALEKEIEEAGITVM 118
S. pombe           LVISLIPYTFHATVIKSAIRQKKHVVTTSYVSPAMMELDQAAKDAGITVM 120
A. fumigatus       LAISLIPYTFHALVIKSAIRTKKHVVTTSYVSPAMMELDEECKKAGITVM 124
C. albicans        LTISLIPYTYHATVMKAAIKHGKHVCTTSYVNPKMAELEEAAIKAGSICM 119
C. neoformans      IVVSLLPAPMHLRVAKHCLDHSRHLVTASYVSPELQALHSQAIEKDVIFL 600
                   :.:**:* . *  * *  .:   .: *:**:*    :*.    . .  :
```

```
                     125 129                          154
S. cerevisiae      NEIGLDPGIDHLYAVKTIDEVHRAGGKLKSFLSYCGGLPAPEDSDNPLGY 169
M. grisea          NEIGLDPGIDHLYAVKTIEEVHKAGGKIVSFLSYCGGLPAPENSDNPLGY 168
S. pombe           NEIGLDPGIDHLYAIKTIEGVHAAGGKIKTFLSYCGGLPAPESSDNPLGY 170
A. fumigatus       NEIGLDPGIDHLYAVKTISEVHAEGGKITSFLSYCGGLPAPECSDNPLGY 174
C. albicans        NEIGVDPGIDHLYAIKTIEEVHKAGGKIKSFLSYCGGLPAPEDSNNPLGY 169
C. neoformans      GECGLDPGIDSMAAMRILERAKREGKQVKSFVSWCGGLPELSASKVPLRY 650
                   .* *:***** : * :: :. .:* :: : *:*:*****  .*.** *

S. cerevisiae      KFSWSSRGVLLALRNSAKYWKDGKIETVSSEDLMAT-AKPYFIYPGYAFV 218
M. grisea          KFSWSSRGVLLALRNQAKYWLDGKVIDISSEDLMAS-AKPYFIYPGYALV 217
S. pombe           KFSWSSRGVLLALRNAASFYKDGKVTNVAGPELMAT-AKPYFIYPGFAFV 219
A. fumigatus       KFSWSSRGVLLALRNAAKFYQDGKEFSVAGPDLMAT-AKPYYIYPGYAFV 223
C. albicans        KFSWSSRGVLLALRNSAKFYENGKLVEIDGKDLMET-AKPYFIYPGYAFV 218
C. neoformans      KFSWSPKAVLTAAQNDASYKLEGKHVKIPGNELLARRFPEVKLWDGLPLE 700
                   *****.:.** *:* *.:  : **   : . :*:        :: * .:

                      223                  244 246
S. cerevisiae      CYPNRDSTLFKDLYHIPEAE---TVIRGTLRYQGFPEFVKALVDMGMLKD 265
M. grisea          CYPNRDSTTYKELYNIPEAQ---TVIRGTLRFQGFPEFIKVFVDLGFLKD 264
S. pombe           AYPNRDSTPYKERYQIPEAD---NIVRGTLRYQGFPQFIKVLVDIGFLSD 266
A. fumigatus       AYPNRDSCPYRERYQIPEAQ---TVIRGTLRYQGFPEMIKVLVDIGFLSD 270
C. albicans        CYPNRDSTVYQERYQIPEAE---TIIRGTLRYQGFPEFIHCLVDMGFLDE 265
C. neoformans      GLANRDSMPYAKKYGLGPAEGLTDLFRGTLRYQGFSSLLESFRLLGLLRS 750
                     .****  : . * :  *:    :.*****:***..::.: : *:* .

S. cerevisiae      DAN----EIFS---KPIAWNEALKQYLGAKSTSKEDLIAS-IDSKATWKD 307
M. grisea          EPM----EIFS---KPGPWNKALAELVGAKSSSEQDIIDK-INQLTKFKS 306
S. pombe           EEQ----PFLK---EAIPWKEATQKIVKASSASEQDIVST-IVSNATFES 308
A. fumigatus       EAK----DFLN---SPIPWKEATQKILGATSSDEKDLEWA-IASKTTFTD 312
C. albicans        TAQ----EYLSPEAPALPWKEVTARVIKAESSSEADLIKK-ISSIHKFKD 310
C. neoformans      DPLPGSP---------KSWTEFLSMTVERELGLSKGLKGEDVNSAVQDLV 791
                               .*.:    :     . .:    : .

S. cerevisiae       DEDRERILSGFAWLGLFSDAKITPR-------GNALDTLCARLEELMQYE 350
M. grisea           PEDQERILAGFRWLGLFSENQITPR-------GNPLDTLCATLEELMQYE 349
S. pombe            TEEQKRIVAGLKWLGIFSDKKITPR-------GNALDTLCATLEEKMQFE 351
A. fumigatus        NDSRNRLISGLRWIGLFSDEQITPR-------GNPLDTLCATLERKMQYG 355
C. albicans         EDDKKRILNGLKWLGMFSSKPVTPR-------GNPLDTLCATLEELMQYE 353
C. neoformans       GEGSKDVIRALKLFSLFPGSDTSLLPLPNLSTPSPIDFFAHLLSRKLAYL 841
                     :  : :: .:  :.:*.    :          ..:* :.  *.. : :

S. cerevisiae       DNERDMVVLQHKFGIEWADGTTETRTSTLVDYGKVGG---YSSMAATVGY 397
M. grisea           KGERDLVILQHKFGIEWANGTKETRTSTLVDYGDPNG---YSSMAKLVGV 396
S. pombe            EGERDLVMLQHKFEIENKDGSRETRTSSLCEYGAPIGSGGYSAMAKFVGV 401
A. fumigatus        PGERDMVMLQHKFGIEHKDGSKETRTSTLVEYGDPNG---YSAMAKTVGV 402
C. albicans         EGERDMLILQHKFEVETKEGKRQTRTCTLLDYGVPNG---YTSMAKLVGV 400
C. neoformans       PDERDTCLLHHSFTISTPSGDTQKVTASLRHMATPTQ----SSMSITVGK 887
                     .***  :*:*.* :.  .*  :. *.:* . .        ::*: **
```

```
S. cerevisiae       PVAIATKFVLDGTIKGPGLLAPYSPEINDPIMKELKDKYGIYLKEKTVA- 446
M. grisea           PCAVATKQILSGELSKKGLLAPMSSDINDSIMKELKDKYDIYLVEKTI-- 444
S. pombe            PCAVAVKFVLDGTISDRGVLAPMNSKINDPLMKELKEKYGIECKEKVVA- 450
A. fumigatus        PCGVAVKLVLDGTISQKGVLAPMTWDICEPLLKTLKEEYGIEMIEKTV-- 450
C. albicans         PCGVATQQILDGVINTPGVLAPNDMKLCGPLIDTLAKEG-IRLEEEIIDE 449
C. neoformans       TLAFAALRIADGEVKVRGVTGPYEPEVWAGVLSSLEGAGVVIEEKWH--- 934
                    . ..*  : . * :.  *: .*   .:   ::. *     :   :
```

[a]In the multiple sequence alignment, **.**, **:**, and * indicate that these corresponding residues are semi-conserved, conserved, and identical respectively.

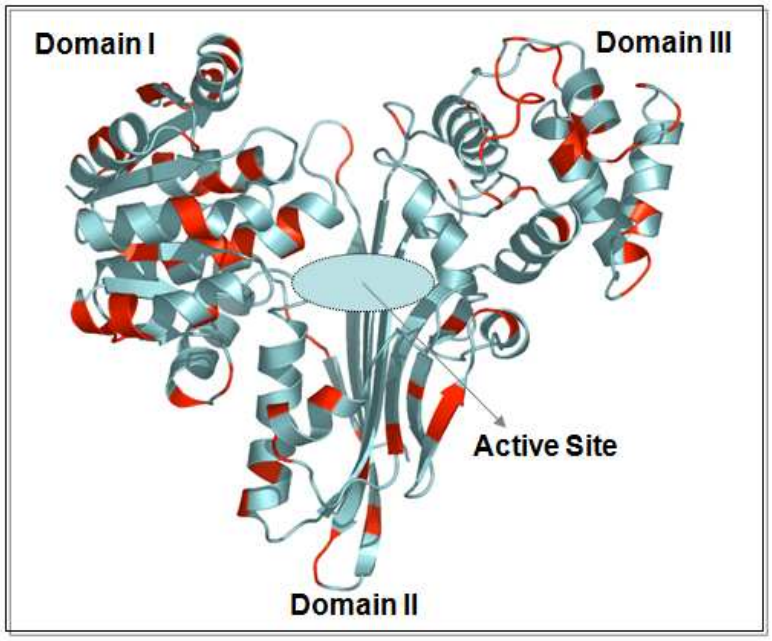

Fig. IV-1: Structure of SR from *S. cerevisiae*. The red regions represent the non-conserved amino acids relative to the structure from *M. grisea*

The multiple sequence alignment shows that the residues D125, C154 and Y99F in the saccharopine bound active site structure of saccharopine reductase from *M. grisea* are completely conserved in *S. cerevisiae*, *C. albicans*, *A. fumigatus*, *S. pombe*, and *C. neoformans* indicating that these residues are important in the reaction catalyzed by saccharopine reductase. These three residues are possible candidates for

the acid-base catalysts in the reaction and these are shown in bold in the alignment results along with R34 residue which is believed to bind to the 2' phosphate group of NADPH. The residues bound to the dinucleotide in the active site are also shown in bold along with other residues which are completely conserved in *S. cerevisiae, M. grisea, C. albicans, A. fumigatus, S. pombe,* and *C. neoformans*. The tertiary structure of SR from *S. cerevisiae* is shown in Fig. IV-1, the red regions in the figure show the non-conserved amino acid residues between *S. cerevisiae* and *M. grisea*. *Andi et al*. has reported that a total of 92 out of 446 amino acids (21%) are different. In domain I, 42 out of 176 residues differ, 24 out of 167 residues differ in domain II, and in domain III 26 out of 103 residues are different (*1*). Domain II shows the maximum number of conserved residues, suggesting that this domain plays an important role in substrate binding. All residues in the active site of SR involved in substrate binding are completely conserved in *S. cerevisiae, M. grisea, C. albicans, A. fumigatus, S. pombe,* and *C. neoformans*. The non conserved residues in SR from *S. cerevisiae* and *M. grisea* are not present in the active site.

References

1. Andi B., Cook P. F., West, A. H., (2006), Crystal structure of the his-tagged saccharopine reductase from Saccharomyces cerevisiae at 1.7-Å resolution. *Cell Biochem Biophys. 46,* 17-26.

APPENDIX V

Pipecolic acid oxidase and coupled assay of saccaropine reductase from *Saccharomyces cerevisiae*

V-1. Pipecolic Acid Oxidase

V-1-1. Introduction

L-Pipecolic acid oxidase (PIPOX) is a peroxisomal enzyme found in monkeys and humans that participates in lysine degradation via L-pipecolic acid (*1-6*). L-pipecolic acid is involved in the major lysine oxidation pathway in the brain (*7-9*). PIPOX belongs to the oxidoreductase class of enzymes. The reaction catalyzed by PIPOX involves the oxidation of pipecolic acid to produce α-aminoadipate-δ-semialdehyde (AASA) and the *in vitro* activity requires oxygen, which is reduced to hydrogen peroxide (*10*).

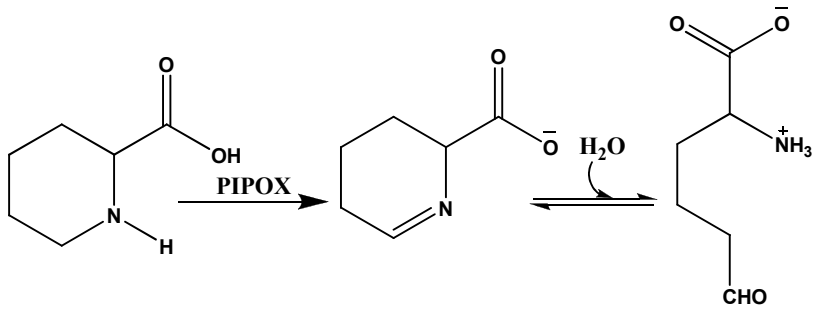

Pipecolic acid **Piperidine-6-carboxylic acid** **AASA**

Piperidine-6-carboxylic acid is the product of the first step of the reaction and under neutral conditions (pH 7-9), this product spontaneously undergoes ring opening to form AASA. The oxidation of pipecolic acid by pipecolic acid oxidase produces hydrogen peroxide by the reduction of oxygen, the final electron acceptor,

the enzyme activity is reduced significantly when nitrogen is bubbled through the reaction mixture (*10*).

V-1-2. Significance of L-Pipecolic acid oxidase

Two different pathways for lysine degradation exist in mammals, the saccharopine pathway and the pipecolic acid pathway, which leads to the formation of pipecolic acid via Δ^1-piperidine-2-carboxylate reductase (*11-15*). The saccharopine pathway is the primary route of degradation of lysine in most tissues with the exception of the brain, when the L-pipecolate pathway is most active (*14*). L-pipecolate oxidase (PIPOX) an enzyme in the L-pipecolate pathway localized in peroxisomes.

L-Pipecolic acid oxidase plays a significant role in the lysine degradation pathway in brain and liver in humans and the activity of this enzyme is reduced significantly in patients with disorders of peroxisomal biogenesis, such as Zellweger syndrome (an inborn genetic disorder) (*16, 17*) in which L-pipecolic acid, the substrate for PIPOX accumulates in the brain and liver, and these disorders present with severe neurological dysfunction and profound mental retardation and are associated with the loss of most peroxisomal metabolic functions (*18*). Zellweger syndrome is associated with the complete loss of PIPOX activity.

V-1-3. Expression, purification, and characterization

In *Penicillium chrysogenum,* PIPOX is induced by pipecolic acid and the

induction is prevented in the presence of ammonia, suggesting that ammonium prevents the uptake of pipecolic acid, as occurs with other amino acids in *P. chrysogenum* (*19*). The molecular weight of the enzyme from *Rhodotorula glutinis* has been reported to be approximately 43, 000 Da and it consists of a single subunit. PIPOX purified from Rhesus monkey liver is a yellow monomer, has a molecular weight of 46,000 by sodium dodecyl sulfate polyacrylamide gel electrophoresis, while using gel filtration it was calculated to be about 28,000 Da and a PI of 8.9 (*16*). In *R. glutinis,* lysine biosynthesis occurs through the AAA pathway (20). The pathway for the conversion of pipecolic acid to lysine has been elucidated only in *R. glutinis.* In *Aspergillus nidulans* (*1*), *Euglena gracilis* (*21*), and *R. glutinis*, pipecolic acid plays a nutritional role in the biosynthesis of lysine but not in *S. cerevisiae*. PIPOX has also been reported in *P. chrysogenum* (*19*). In *Metarhizium anisopliae* and *Rhizoctonia leguminicola,* pipecolic acid is formed by catabolism of lysine and is an intermediate in the biosynthesis of alkaloid compounds (*22–24*). In *R. glutinis* the enzyme is heat labile and pH optimum for the reaction is 8.5.

The pipecolic acid oxidase reaction produces AASA, which is converted enzymatically to saccharopine and lysine (*25*). In *Pseudomonas putida*, pipecolic acid is used as a carbon and nitrogen source (*26*). Aspen and Meister, using ^{14}C- and ^{15}N-labeled α-aminoadipic acid and [^{14}C] lysine, showed that in *Aspergillus nidulan*s the carbon chain of α-aminoadipic was the major precursor of pipecolic acid and not lysine, and the nitrogen atom of α-aminoadipic acid becomes the nitrogen atom of pipecolic acid (*1*). Using saccharopine reductase mutants, it was shown that pipecolic

acid enters the lysine pathway at the level of the α-aminoadipic acid-δ-semialdehyde since, saccharopine reductase catalyzes the conversion of α-aminoadipic acid-δ-semialdehyde to L-sacharopine which is then converted to L-lysine by saccharopine dehydrogenase.

Human L-pipecolate oxidase is cloned and the protein contains an ADP-βαβ-binding fold compatible with its identity as a flavoprotein. The human PIPOX has a KAHL sequence at the carboxy terminus which suggests that PIPOX is a typical peroxisomal protein (*15*). PIPOX has also been purified from rabbit kidney and it was shown that besides L-pipecolic acid, it can also utilize sarcosine, and L-proline as substrates. The enzyme is also called sarcosine oxidase since the maximal velocity was obtained with sarcosine as a substrate but the catalytic efficiency of the enzyme is highest with L-pipecolate (*15*).

Kinzel *et al.*, has reported that the enzyme does not require any external cofactor and the partially purified enzyme does not support the presence of any enzyme-bound metal or flavin group, while Mihalik *et al.*, reported that the enzyme contains a covalently bound flavin (*10*, *14*). The absorption spectrum of L-pipecolic acid oxidase is typical of a flavoprotein with dual maxima around 340-380 and 450 nm. The shoulder around 480 nm suggests the presence of a tightly bound flavin. Ruber *et al.* (*27*) has shown that the protein is indeed a flavoprotein and the FAD binding site is present at the N-terminus containing a conserved histidine at position 49 which is believed to be the covalent attachment site of FAD (*28*). A cysteine residue is also present in human PIPOX (C319) and this residue is conserved among

other oxidases and is believed to be the covalent attachment site for FAD in oxidases rather than histidine 49. If this is the case, then the histidine residue may play a role in flavinylation (*16*).

PIPOX is inhibited by the sulfhydryl agents p-chloromercuribenzoate and mercuric chloride. Metal chelating agents such as α, α′-dipyridyl, EDTA, and 1, 10-phenanthroline do not affect the enzyme activity, while the metal-complexing compounds (*29*) cyanide and sodium azide slightly inhibit the enzyme. Hydroxylamine (1 mM) results in a 15% inhibition of the enzyme activity (*7*).

V-2. Materials and Methods

V-2-1. Chemicals

L-pipecolic acid, L-glutamic acid, were from Sigma. *β*-NADPH[1], *β*-NADP, and LB broth were purchased from USB. Amylose affinity resin was from New England Biolabs. Isopropyl-*β*-D-1-thiogalactopyranoside was from Invitrogen, while ampicillin was from Fisher Biotechnologies, and HEPES was obtained from Research Organics. All chemicals were of the highest grade available and were used as purchased.

V-2-2. Cell growth, expression, and protein purification

pMal–PIPOX plasmid was a gift from Dr. Ronald Wanders (Amsterdam). The vector containing the insert was transformed into BL21*(DE-3) RIL *E. coli* cells using heat shock at 42 °C, followed by growth on ampicillin plates. Colonies were

picked and cells were grown overnight at 37 °C in LB media containing 100 μg/mL ampicillin. The cells were induced using 1mM IPTG at an A_{600} of 0.7-0.9, and allowed to grow overnight. After centrifugation at 4000*g*, the harvested cells were suspended in 20 mM Tris-HCl, pH 7.5, 1 mM EDTA, 10 mM β-mercaptoethanol and 200 mM NaCl. For protein purification, PMSF (1 mM) was added to the cell suspension followed by cell disruption using a MISONIX Sonicator XL. Sonication was carried out on ice for 1 min using a pulse on time of 15 s followed by a 30 s rest period. The cell debris was removed by centrifugation at 20,400*g* for 15 min, and the supernatant was loaded onto an amylose column, washed with equilibrating buffer, and then eluted using buffer containing equilibrating buffer with 10 mM maltose.

V-2-3. Determination of PIPOX activity using NMR spectroscopy

In order to determine the activity of PIPOX, NMR spectroscopy was used to monitor the appearance of the aldehyde peak around 9.8 ppm which is not present in the spectra of L-pipecolic acid. NMR spectra were obtained on a Varian Mercury VX-300 MHz spectrometer with a Varian 4-nuclei autoswitchable PFG probe. ^{1}H NMR spectra were collected in D_2O using the PRESAT pulse sequence supplied by Varian, Inc. The spectra were collected with a sweep width of 4803.1 Hz, eight transients, and an acquisition time of 3.411 s and processed with 108K data points resulting in a 1.0 Hz digital resolution. No peaks were obtained around 9.8 ppm. Upon addition of PIPOX to the mixture, a single peak corresponding to the aldehyde group appeared around 9.8 ppm. A blank was used to check the appearance of the

peak at 9.8 ppm. The blank contained PIPOX and D_2O in place of the substrate and no peaks around 9.8 ppm were seen.

V-2-4. Time Course Study for AASA Formation

To determine the time course for the formation of AASA, the reaction mixture after addition of PIPOX was monitored every 5 minutes for the peak at 9.8 ppm. The peaks at 9.8 ppm were integrated and the integrals were plotted against time, Fig. V-1. The plot shows an initial busrt and buildup of AASA followed by a steady phase in which the concentration of PIPOX is stabilized and upon taking the NMR spectra after two days, no peak around 9.8 ppm is observed indicating that AASA is unstable and is lost over time. When PIPOX was assayed for activity as a function of time, it was observed that PIPOX looses activity over time when kept at 4 °C. Attempts to stabilize the enzyme using 20 % glycerol at -20 °C were successful.

V-2-5. Enzyme assay

The SR reaction was followed in the forward reaction direction by monitoring the disappearance of NADPH at 340 nm ($\varepsilon_{340,}$ 6220 $M^{-1}cm^{-1}$) using a Beckman DU-640 spectrophotometer. All assays were carried out at 25 °C. A typical assay in 500 μL contained 100 mM HEPES, pH 7.0, and appropriate concentrations of substrates along with FAD which acts as the oxidizing agent and catalase which is used to decompose the hydrogen peroxide produced as a result of the PIPOX reaction.

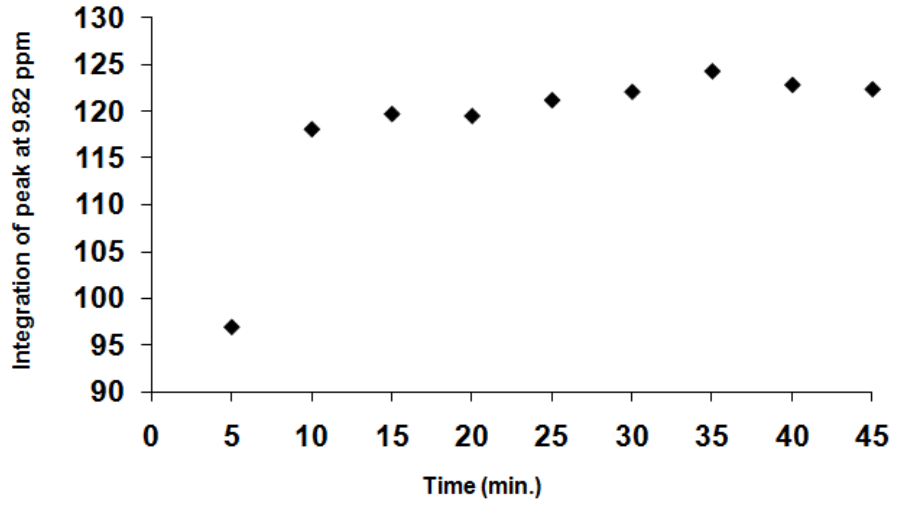

Fig. V-1. Time course for formation of AASA at pH 7.0. The spectra were collected on a Varian Mercury VX-300 MHz spectrometer every 5 minutes to monitor the appearance of the aldehyde peak around 9.8 ppm. The aldehyde peaks were integrated and the integrals were plotted against time.

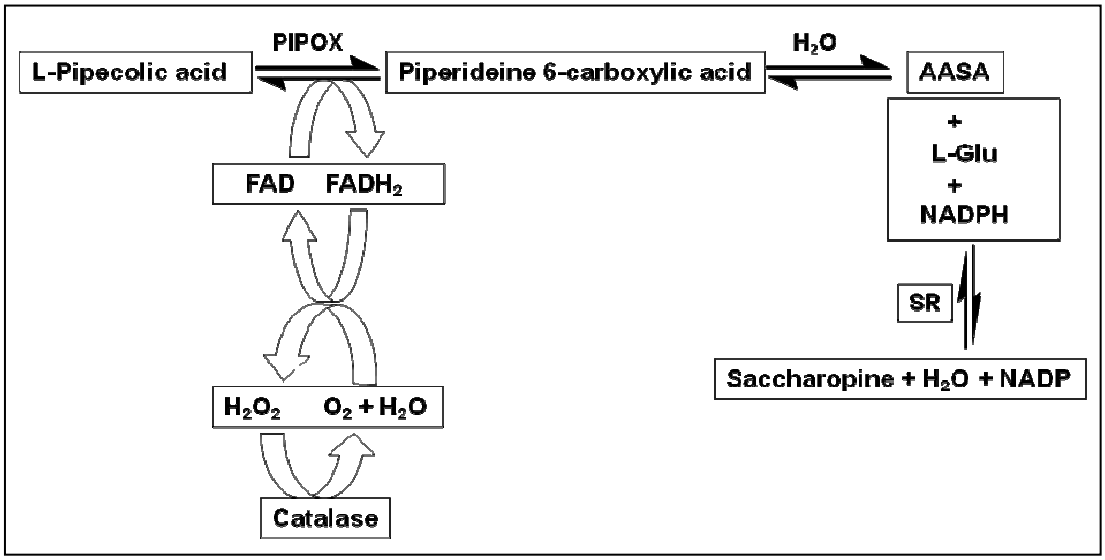

Fig. V-2: Coupled reaction scheme employed to study the saccharopine reductase reaction in the forward reaction direction. Pipecolic acid is converted to piperidine-6-carboxylic acid using PIPOX which spontaneously hydrolyses in the presence of water to give AASA which is used in a coupled reaction along with L-glutamate and NADPH to produce L-saccharopine. The reaction is studies at 340 nm measuring the rate of disappearance of NADPH.

Reaction was initiated by adding 10 μL of appropriately diluted saccharopine reductase in 100 mM HEPES, pH 7.0. All enzyme dilutions were made fresh for each set of experiments. The coupled assay scheme is shown in Fig. V-2.

V-3. Results and Discussion

The transformation of pMal–PIPOX plasmid in BL21*(DE-3) RIL *E. coli* cells was successful and the enzyme expressed but the expression was not very good. PIPOX was purified using an Amylose affinity resin and the SDS-PAGE showed that the protein is not 100% pure and contains several other proteins in elute. Activity assays were performed using PIPOX and L-pipecolic acid and the formation of AASA was monitored using NMR spectroscopy. The appearance of peak around 9.8 ppm confirmed the formation of AASA and this result is corroborated by the controls employed to study the reaction. PIPOX was found to be unstable when stored at 4 °C. Attempts to stabilize the enzyme using 20 % glycerol at -20 °C were successful. AASA was found to be stable over a short period of time which was enough to perform the coupled assay for SR but the prolonged storage resulted in a loss of the compound. Coupled assay was performed using PIPOX to generate the AASA *in situ* and coupling this reaction to the SR reaction resulting in the formation of L-sacharopine. Several attempts were made to optimize the conditions for the coupled assay but unfortunately, the coupled assay did not work. In order for the coupled assay to work, the reaction conditions need to be optimized.

References

1. Aspen, A. J., and A. Meister. (1962) Conversion of α-aminoadipic acid to L-pipecolic acid by *Aspergillus nidulans*. *Biochemistry 1*, 606-612.

2. Baginsky, M. L., and Rodwell, V. W. (1967) Metabolism of pipecolic acid in a *Pseudomonas* species pipecolate oxidase and dehydrogenase, *J. Bacteriol. 94*,1034-1039.

3. Broquist, H. P. (1971) Lysine biosynthesis (yeast). *Methods Enzymol. 17*, 112-129.

4. Davis, B. J. (1964) Disc electrophoresis. Method and application to human serum proteins. *Ann. N.Y. Acad. Sci. 121*, 404-427.

5. Determann, R., and Michael, W. (1966) The correlation between molecular weight and elution behavior in the gel chromatography of protein. *J. Chromatogr. 25*, 303-313.

6. Durham, D. R., and Perry, J. J. (1978) Purification and characterization of a heme-containing amine dehydrogenase from *Pseudomonas putida. J. Bacteriol. 134*, 837-843.

7. Chang, Y. F. (1978) Lysine metabolism in the rat brain: The pipecolic acid-forming pathway. *J. Neurochem. 30*, 347-354.

8. Hutzler, J., and Dancis, J. (1968) conversion of lysine to saccharopine by human tissues. *Biochim. Biophys. Acta 158*, 62-69.

9. Chang, Y. F. (1982) Lysine metabolism in the human and the monkey: Demonstration of pipecolic acid formation in the brain and other organs. *Neurochem. Res. 7*, 577-588.

10. Kinzel, J. J. and Bhattacharjee, J. K. (1982) Lysine biosynthesis in *Rhodotorula glutinis*: properties of pipecolic acid oxidase. *J. Bacteriol. 151*, 1073-1077.

11. Boulanger, P. and Osteux, R. (1956) Action of L-amino acid dehydrogenase from turkey liver on basic amino acids, *Biochimica et Biophysica Acta 21*, 552-561.

12. Rothsein, M. and Miller, L. L. (1954) The conversion of lysine to pipecolic acid in the rat. *J. Biol. Chem. 211,* 851-865.

13. Meister, A., Radhakrishnan, A. N. and Buckley, S.D. (1957) Enzymatic synthesis of L-pipecolic acid and L-proline. *J. Biol. Chem. 229,* 789-800.

14. Ghosh, P. and Chang, Y. F. Am. Soc. Biochem. Molec. Biol. Am. Soc. Cell Biol. Joint Meeting San Francisco, CA, Jan. 29, (1989), Abstract 3597.

15. Mihalik, S. J. and Rhead, W. J. (1989) L-pipecolic acid oxidation in the rabbit and cynomolgus monkey. Evidence for differing organellar locations and cofactor requirements in each species. *J. Biol. Chem. 264*, 2509-2517.

16. Wanders, R. J. A., Romeyn, G. J., van Roermund, C. W. T., Schutgens, R. B. H., van den Bosch, H., and Tager, J. M. (1988) Identification of L-pipecolic acid oxidase in human liver and its deficiency in zellweger syndrome. *Biochem. Biophys. Res. Commun. 154*, 33-38.

17. Mihalik, S. J., Moser, H., Watkins, P. A., Poulos, A., Danks, D. M., and Rhead, W. J. (1989) Peroxisomal L-pipecolic acid oxidation is deficient in liver from zellweger syndrome patients. *Pediatr. Res. 25*, 548-552.

18. Lazarow, P. B., and Moser, H. W. (1989) in *The Metabolic Basis of Inherited Disease* (Schriver, C. R., Beaudet, A. L., Sly, W. S., and Valle, D., eds) 6th Ed., pp. 1479-1509, McGraw-Hill, New York.

19. Banuelos, O., J. Casqueiro, S. Gutierrez, J. Riano, and J. F. Martin. (2000) The specific transport system for lysine is fully inhibited by ammonium in *Penicillium chrysogenum*: an ammonium insensitive system allows uptake in carbon starved cells. *Antonie Leeuwenhoek 77*, 91–100.

20. Broquist, H. P. (1971) Lysine biosynthesis (yeast). *Methods Enzymol.17,* 112-129.

21. Rothstein, M., and E. M. Saffran. (1963) Lysine biosynthesis in algae. *Arch. Biochem. Biophys. 101*, 373-377.

22. Sim, K. L., and D. Perry. (1997) Analysis of swainsonine and its early metabolic precursors in cultures of *Metarhizium anisopliae*. *J. Glycoconjugate 14*, 661–668.

23. Wickwire, B. M., Harris, C. M., Harris, T. M. and Broquist, H. P. (1990) Pipecolic acid biosynthesis in *Rhizoctonia leguminicola*. I. The lysine

saccharopine, delta L-piperideine-6-carboxylic acid pathway. *J. Biol. Chem. 265*, 14742–14747.

24. Wickwire, B. M., C. Wagner, and H. P. Broquist. (1990) Pipecolic acid biosynthesis in *Rhizoctonia leguminicola*. II. Saccharopine oxidase: a unique flavin enzyme involved in pipecolic acid biosynthesis. *J. Biol. Chem*. *265*, 14748–14753.

25. Kinzel, J. J., and Bhattacharjee, J. K. (1979) Role of pipecolic acid in the biosynthesis of lysine in *Rhodotorula glutinis*. *J. Bacteriol. 138*, 410-417.

26. Payton, C. W., and Chang, Y. F. (1982) δ1-piperideine-2-carboxylate reductase of *Pseudomonas putida*. *J. Bacteriol. 149*, 864-871.

27. Reuber, B. E., Karl, C., Reimann, S. A., Mihalik, S. J., and Dodt, G. (1997) Cloning and functional expression of a mammalian gene for a peroxisomal sarcosine oxidase. *J. Biol. Chem. 272*, 6766–6776.

28. Wagner, M. A., Khanna, P., and Jorns, M. S. (1999) Structure of the flavocoenzyme of two homologous amine oxidases: monomeric sarcosine oxidase and *N*-methyltryptophan oxidase. *Biochemistry 38*, 5588–5595.

29. Durham, D. R., and J. J. Perry. (1978) Purification and characterization of a heme-containing amine dehydrogenase from *Pseudomonas putida*. *J. Bacteriol*. *134*, 837-843.